Elsevier Editorial System(tm) for Journal of African Earth Sciences

Manuscript Draft

Manuscript Number: AES6331R4

Title: Thermal history and basin evolution of the Moatize - Minjova Coal Basin (N'Condédzi sub-basin, Mozambique) constrained by organic maturation levels

Article Type: Research Paper

Keywords: Karoo, Mozambique, Organic maturation, Permian - Triassic, Reworked palynomorphs, Moatize - Minjova Coal Basin, Vitrinite Reflectance

Corresponding Author: Miss Francesca Galasso, MSc

Corresponding Author's Institution: University of Zurich

First Author: Francesca Galasso, MSc

Order of Authors: Francesca Galasso, MSc; Paulo Fernandes, Ph.D; Giovanni Montesi, MSc; Joao Marques; Amalia Spina, Ph.D; Zelia Pereira, Ph.D

Abstract: Kerogen concentrates obtained from Lopingian (Late Permian) to Upper Triassic mudrock lithologies of seven coal exploration boreholes, drilled in the Moatize - Minjova Coal Basin (N'Condédzi sub-basin, Mozambique), were studied by means of vitrinite reflectance (VR), spore fluorescence and spore colour, in order to constrain the thermal history and basin evolution by organic maturation levels. VR increases with depth, indicating organic maturation related to sediment burial for most of the boreholes. Modelled VR data indicate a regional palaeogeothermal gradient between 35 and 40°C/km. Lower Jurassic doleritic intrusions observed in three boreholes had only local thermal effects without affecting the regional palaeogeothermal gradient. Two boreholes located near the basin margin show high palaeogeothermal gradients suggesting thermal processes other than heating due to burial were involved. These processes may have involved hot diagenetic fluids circulating through fault zones and/or permeable lithologies, locally elevating geothermal gradients. Circulation of these fluids was induced by lithostatic pressure due to rapid rates of sedimentation. These high sedimentation rates lead to the accumulation of a thick succession (over 2000 m) of Lopingian (Late Permian) to Upper Triassic siliciclastic sediments. All the organic maturation indices measured and the age of the successions indicate that organic maturation occurred during or after Late Triassic times. However, the presence of reworked Permian palynomorphs into Upper Triassic sediments and the absence of Middle Triassic sediments indicate an exhumation and erosion of Permian strata in Middle Triassic times. The organic maturation levels of the reworked palynomorph population are considerably higher than the indigenous Upper Triassic population, indicating that they attained higher burial temperatures prior to being reworked.

Research Data Related to this Submission

There are no linked research data sets for this submission. The following reason is given:
All the data used in this research are available, in the article as tables and the protocols and methodologies used are also described in the article.

Thermal history and basin evolution of the Moatize - Minjova Coal Basin (N'Condédzi sub-basin, Mozambique) constrained by organic maturation levels

Francesca Galasso[1,2]*, Paulo Fernandes[2], Giovanni Montesi[1], João Marques[3], Amalia Spina[1], Zélia Pereira[4]

1. Department of Physics and Geology, University of Perugia.Via Pascoli, 06123 Perugia, Italy

2. Centro de Investigação Marinha e Ambiental (CIMA), Universidade do Algarve, Campus de Gambelas, 8005-139 Faro, Portugal

3. Gondwana Empreendimentos e Consultorias, Limitada, Rua B, no. 233, Bairro da COOP, Caixa Postal 832, Maputo, Mozambique

4. Laboratório Nacional de Energia e Geologia (LNEG), Rua da Amieira, Apartado 1089, 4466-901 S. Mamede Infesta, Portugal

* Corresponding author: francescagalasso1992@gmail.com

Abstract

Kerogen concentrates obtained from Lopingian (Late Permian) to Upper Triassic mudrock lithologies of seven coal exploration boreholes, drilled in the Moatize – Minjova Coal Basin (N'Condédzi sub-basin, Mozambique), were studied by means of vitrinite reflectance (VR), spore fluorescence and spore colour, in order to constrain the thermal history and basin evolution by organic maturation levels. VR increases with depth, indicating organic maturation related to sediment burial for most of the boreholes. Modelled VR data indicate a

regional palaeogeothermal gradient between 35 and 40ºC/km. Lower Jurassic doleritic intrusions observed in three boreholes had only local thermal effects without affecting the regional palaeogeothermal gradient. Two boreholes located near the basin margin show high palaeogeothermal gradients suggesting thermal processes other than heating due to burial were involved. These processes may have involved hot diagenetic fluids circulating through fault zones and/or permeable lithologies, locally elevating geothermal gradients. Circulation of these fluids was induced by lithostatic pressure due to rapid rates of sedimentation. These high sedimentation rates lead to the accumulation of a thick succession (over 2000 m) of Lopingian (Late Permian) to Upper Triassic siliciclastic sediments. All the organic maturation indices measured and the age of the successions indicate that organic maturation occurred during or after Late Triassic times. However, the presence of reworked Permian palynomorphs into Upper Triassic sediments and the absence of Middle Triassic sediments indicate an exhumation and erosion of Permian strata in Middle Triassic times. The organic maturation levels of the reworked palynomorph population are considerably higher than the indigenous Upper Triassic population, indicating that they attained higher burial temperatures prior to being reworked.

Keywords: Karoo, Mozambique, Organic maturation, Permian – Triassic, Reworked palynomorphs, Moatize – Minjova Coal Basin, Vitrinite Reflectance

1. Introduction

The Karoo Supergroup (KSG) of Southeastern Africa comprises sedimentary and volcanic rock units that span a time interval of Late Carboniferous to Early Jurassic, and which attained a considerable thickness (more than 7000 m) in some basins (Johnson et al., 1996; Cairncross, 2001; Catuneanu et al., 2005). Regardless of tectonic processes related to individual basin formation and subsequent geological development the stratigraphy of the KSG is very consistent across all basins where it is preserved (Johnson et al., 1996; Catuneanu et al., 2005, Hancox, 2016). The sedimentary successions reflect major palaeogeographical and climatic changes during the development of the Karoo basins (Catuneanu et al., 2005; Götz and Ruckwied, 2014; Götz et al., 2017). In central-west Mozambique, sediments of the KSG are well represented in various basins situated along the Zambezi River valley in the Tete Province (GTK Consortium, 2006) (Fig. 1). In these basins the KSG, normally, rests unconformably over crystalline Precambrian basement rocks, and the base of the stratigraphic succession consists of conglomerates and mudrocks of the Dwyka Group (Pennsylvanian to Cisuralian) comparable to the Main Karoo Basin of South Africa. These conglomerates were, deposited by waning and waxing of glaciers of the Late Palaeozoic glaciations of Gondwana (Visser, 1989, Isbell et al., 2008). The northward drift of Gondwana to lower latitudes during the Permian, caused more temperate climate conditions to establish throughout this paleocontinent. Glaciation was terminated by late Palaeozoic times and in basins located north of the Main Karoo Basin (South Africa), sedimentation mostly took place in continental environments characterized by river systems and freshwater lakes (Cairncross, 2001; Kreuser and Woldu, 2010; Götz and Ruckwied, 2014). The sedimentary record of these times corresponds to the siliciclastic-dominated, coal-bearing lithologies of the Cisuralian to Guadalupian Ecca Group (Cairncross, 2001; Catuneanu et al., 2005, Hancox, 2016). At present, the existence of widespread coal seams interbedded in the Ecca Group stratigraphic

sequence, represents an important natural resource and asset for Mozambique's economy (Vasconcelos, 2000, 2013). Overlying the Ecca Group are siliciclastic-dominated stratigraphic sequences belonging to the Beaufort Group (Lopingian - Middle Triassic) and the Stormberg Group (Late Triassic - Early Jurassic). The sediments of these two groups were deposited by major river systems or aeolian processes in desert environments under hot and arid climatic conditions (Johnson et al., 1996; Catuneanu et al., 2005). The contact between the Beaufort Group and the overlying Stormberg Group corresponds to a hiatus that spans most of the Middle Triassic (Catuneanu et al., 2005). The KSG is capped by the Lower Jurassic volcanic rocks (*ca.* 183 Ma) of the Drakensberg Group, which are related to the Karoo - Ferrar Large Igneous Province and pre-date the break-up of Gondwana (Duncan et al., 1997).

Thermal history analysis is an essential part of any study of sedimentary basins and their hydrocarbon source rock potential. There are several optical methods that can be used to estimate maximum temperatures attained by strata during subsidence and interpret their thermal history (Price, 1983). Vitrinite reflectance (VR) is an optical method considered to be a reliable indicator of the organic matter maturity levels of sedimentary rocks (Hunt, 1996; Robert, 1988; Tissot and Welte, 1978). Since maturity levels are largely related to temperature, VR is also a good indicator of peak (palaeo-) temperatures, which accounts for its widespread use in basin analysis (Middleton, 1982; Corcoran and Clayton, 2001; Fernandes et al., 2012, 2013, 2015; Mariño et al., 2015). Other optical methods, such as spore colour (TAI) and spore fluorescence provide a rapid evaluation of organic maturation levels, complementing the information attained by VR (Van Gijzel, 1979; McPhilemy, 1988; Suárez-Ruiz et al., 2012). Fernandes et al. (2015) studied the thermal history of the Lopingian KSG sediments of the Moatize – Minjova Coal Basin combining VR and Apatite Fission Track Analysis (AFTA) of two boreholes located in the Moatize sub-basin (Fig. 1). These authors

concluded that maturation levels corresponded to a coal rank of medium rank B and A coals (1.3 - 1.7%*Ro*). Maturation levels increase linearly downhole in the two studied boreholes, indicating that burial with a constant geothermal gradient was the main process controlling peak temperature. The thermal model for the history of the basin proposed by Fernandes et al. (2015), indicates that peak burial temperatures were attained shortly (3 - 10 Ma) after deposition in Lower Triassic times. The thermal model also indicates two episodes of cooling and exhumation: a first period of rapid cooling between 240 and 230 Ma (Middle– Late Triassic boundary) implying 2500 - 3000 m of denudation; and a second period, also of rapid cooling, from 6 Ma (late Miocene) onwards implying 1000 - 1500 m of denudation.

In the present work, a detailed account of the organic maturation levels assessed by different optical methods (VR, spore colour and spore fluorescence) of seven boreholes drilled for coal exploration is described. The boreholes are located in the N'Condédzi sub-basin of the Moatize – Minjova Coal Basin (Figs. 1 and 2). This study allowed the evaluation of the maturity of organic matter and the thermal history of the KSG sedimentary succession in the N'Condédzi region, and helps to constrain the tectonic model for the development of the Karoo Basin in this region.

2. Geological setting of the Moatize – Minjova Coal Basin in the N'Condédzi sub-basin

Differences in the stratigraphy, tectonic setting and geographic position of KSG outcrops along the Zambezi river valley in Mozambique, allow their division into three different coal-bearing basins, which are, from west to east, the Chicôa – Mecúcoè, Sanângoè – Mefidézi and the Moatize – Minjova Coal Basins, respectively (Lächelt, 2004; GTK Consortium, 2006) (Fig. 1). These basins are part of a network of rift related basins that formed north of the South African Main Karoo Basin, during the Permian to Lower Jurassic time interval. The

Zambezi River valley basins developed during brittle reactivation of high strain zones (e.g. the Sanângoé and Mzarabani shear zones) (Fig. 1) of the Zambezi Belt. This mobile belt formed between the Congo and Kalahari Cratons during the Pan-African Orogeny (620 – 530 Ma) (Carvalho, 1977; Afonso, 1984; Pinna et al., 1993; Jamal, 2005; GTK Consortium, 2006; Norconsult Consortium, 2007; Grantham et al., 2008; Viola et al., 2008). The tectonic fault-related reactivation started in the Cisuralian (early Permian) by the initiation of strike-slip faulting under a transtensional stress regime that formed extensional basins with a graben to half graben geometry (Carvalho, 1977; Hankel, 1994; Lächelt, 2004; Catuneanu et al., 2005; GTK Consortium, 2006).

The boreholes used in this study were drilled in the N'Condédzi sub-basin of the Moatize-Minjova Coal Basin, which is approximately 50 km long and 25 km wide, and is located *ca*. 70 km northeast of Tete City (Figs 1 and 2). Its margins are faulted against the Mesoproterozoic Tete Suite (Gabbro-Anorthosite) to the SW and the Mesoproterozoic gneiss and granite rocks of the Furancungo Suite to the N by the WNW –ESE trending Mwanza Fault.

The complete Karoo stratigraphic succession of the Moatize - Minjova Coal Basin is thicker than 800 m (Real, 1966; Thonnard, 1971/1972; Afonso, 1975; Vasconcelos, 1995; Mugabe, 1999; Lächelt, 2004; GTK Consortium, 2006), whereas in the N'Condédzi sub-basin Lakshminarayana (2015), a Lower Karoo succession with a thickness of more than 900 m is reported. The base of the succession consists of the tillites of the Vúzi Formation, which overly unconformably Precambrian basement rocks. However, the type section for this formation was defined in the area of the Mucanha and Vúzi Rivers (Carvalho, 1977) belonging to the Chicôa-Mecúcoè Basin, located upstream in the Zambezi River valley (Fig.

1). In the Mucanha-Vúzi area, the Vúzi Formation consists of 10 m-thick ill-bedded matrix supported red conglomerates that are conformably overlain by 10 m-thick mud supported grey-black conglomerates. Due to the lack of conclusive evidences of glacial action (transport and deposition), such as, striations on surfaces of the basement rocks and on surfaces of the clasts in the conglomerates, and dropstones and varve-like sedimentary rhythms, Carvalho (1977) interpreted these conglomerates, not as glacial deposits, but probably as coarse alluvial fans. These coarse clastic beds were probably deposited at the base of, and adjacent to, fault scraps, where the topographic relief was created by vertical fault movements coeval to the formation of the Karoo rift basins. Recently, a *ca.* 130 m thick succession of the Vúzi Formation, cropping out in the Murrongódzi River, was described in the Moatize - Minjova Basin by Achimo et al. (2014). The bulk of the succession consists of ill-sorted matrix-supported conglomerates showing typical features of glacial to sub-glacial transport and deposition, interpreted as being formed by the advance and retreat of ice caps over lakes and fluvio-glacial plains. From the description of the Vúzi Formation in the different Karoo basins of the Zambezi River valley, it is evident that it was deposited in a variety of sedimentary environments and tectonic conditions, which require further research in order to ascertain the relations between different processes and, possibly, the age and *tempus* of the accumulation of the sediments.

The coal-bearing Moatize Formation conformably overlies the Vúzi (Tillite) Formation and consists of interbedded carbonaceous mudstones, siltstones, sandstones and coal beds interpreted as fluvial and lacustrine sediments deposited under wet temperate climatic conditions. In the Moatize region, the formation attains a thickness of *ca*. 300 - 400 m (Real, 1966; Afonso, 1976; GTK Consortium, 2006) and has six main coal seams, which are known locally as “Carbonaceous Complexes.” These “Complexes” consist of interbedded plant-rich

carbonaceous mudstones and coal beds of variable thickness. Palaeoassemblages (plant macrofossils and palynomorphs) suggest Cisuralian-Guadalupian (Early to Middle Permian) age for the upper part of the Moatize Formation, correlated with the Middle-Late Permian age Ecca Group of the Main Karoo Basin in South Africa (Daber, 1984). However, recent palynological revision of the upper part of the Moatize Formation that was penetrated by two coal exploration boreholes (DW123 and DW132) indicates that this part of the Moatize Formation reaches the latest Permian, with the Permian-Triassic boundary identified at *ca.* 42 m depth in borehole DW132 (Pereira et al. 2016).

The Moatize (Sandstone) Formation is overlain by a thick sequence (*ca.* 4 km) of siliciclastic rocks divided into two stratigraphic units, the Matinde (Marl-Sandstone) Formation at the base, and the Cádzi (Sandstone) Formation at the top (GTK Consortium, 2006). Both formations were deposited in fluvial to possibly desert environments, recording the transition from seasonal temperate to hot arid climatic conditions. Due to the lack of biostratigraphic markers in both formations, the Matinde Formation is correlated to the Middle-Upper Ecca Group of the Main Karoo Basin of South Africa (Silva et al., 1967), whereas the Cádzi Formation is correlated with the Beaufort Group of the same basin. With the exception of few 1 - 3 m thick doleritic dykes and sills that intrude the sedimentary formations, the volcano-sedimentary lithologies of Lower Jurassic age that capped the KSG, and are correlated with the Stormberg Volcanics of the Main Karoo Basin, are not well represented in the Moatize-Minjova Coal Basin (Vasconcelos, 1995).

Lakshminarayana (2015) compared the stratigraphic succession of the KSG in the N'Condédzi sub-basin with the succession described for the Moatize sub-basin. The Vúzi Formation rests unconformably on gabbros and anorthosites of the Mesoproterozoic Tete

Suite. The Vúzi Formation consists of clast-supported conglomerates interbedded with sandstones, siltstones and carbonaceous shales forming thinning and fining upward cycles. The top part of the Vúzi Formation is characterized by a sequence known as the *Transitional Assemblage* consisting of sandstones, interbedded with carbonaceous shales and coal beds. This formation is *ca*. 60 – 140 m thick. The succeeding Moatize Formation attains a maximum of 900 m thick in the N'Condédzi sub-basin and consists of interbedded meter thick coal seam, sandstones, siltstones and carbonaceous shales. No new biostratigraphic information was provided by Lakshminarayana (2015) on the age of the Vúzi and Moatize formations in this sub-basin and, therefore, this author correlated these formations with the Pennsylvanian (Late Carboniferous) to Cisuralian (early Permian) Dwyka Group and the Permian Ecca Group, respectively.

3. Materials

The samples analysed in this study were obtained from seven coal exploration boreholes drilled in the N'Condédzi sub-basin (Fig. 2). Black carbonaceous shales, black shales, grey mudstones and grey siltstones, were the main lithologies sampled for organic maturation studies. Coal was not sampled because it was not present in the cores during the sampling. The coal seams were sampled earlier by the exploration companies that owned the mining rights of the area, and shipped to laboratories to assess its quality. The boreholes studied were chosen in order to represent all the stratigraphic units of the KSG present in the N'Condédzi sub-basin. Five of the boreholes studied intersected the basement at different depths, representing the coal bearing units that characterize the lower units of the stratigraphy (Moatize Formation), whereas two boreholes penetrated the *ca*. 500 m thick successions consisting mainly of red bed lithologies that represent the upper stratigraphic units (Matinde and Cádzi formations) of the KSG in sub-basin. One hundred and seventy two samples of the

lithologies indicated were processed for organic maturity analysis and palynology studies. One hundred and one samples yielded organic material suitable for these studies, however, seventy-one samples from boreholes A1TR-018, A1TM-039, TGDH(C)005 and CIMT-014 were barren.

3.1. Borehole ZSA-32

This borehole is located near the southern margin of the Karoo outcrop in the N'Condédzi sub-basin (Fig. 2). It has a total depth of 220 m, and penetrated at its base a 5 m thick sequence of the basement rocks of the Tete Suite, consisting of gabbros (Fig. 3). The latter lithologies are unconformably overlain by a 3 m thick bed of clast-supported conglomerates intercalated with very thin beds red siltstones and mudstones, positioned immediately above the unconformity. These red lithologies caused the red staining of the altered gabbros below the unconformity. These two features, red stain of the basement and red lithologies, are more compatible with deposition under oxidizing sub-aerial conditions, rather than glacial to peri-glacial environments of the Dwyka time. The succession in the borehole interval from 209 m to 180 m, consists of black carbonaceous shales capped by a 2 m thick coal bed. This is followed by an interval from 180 m to 62 m, characterized by coarse to medium grained sandstones interbedded with shales and siltstones and some coal beds. A 10 m thick coal bed caps the latter borehole interval. The upper part of the borehole from 50 m to the top of the borehole consists of sandstones interbedded with siltstones and shales. The succession in this borehole is also intruded by several doleritic sills (Fig. 3).

3.2. Borehole A1TR-018

Borehole A1TR-018 was drilled to a total depth of *ca*. 91 m, and penetrated Karoo sediments overlying crystalline basement rocks represented by gabbros of the Tete Suite at *ca*. 85 m

depth (Fig. 4). This borehole is located only 1 km (direction) from the outcrop, which includes the contact between the Tete Suite and Karoo Supergroup in the N'Condédzi sub-basin (Fig. 2). A 1 m clast-supported conglomerate bed unconformably overlies the Precambrian basement. The conglomerate grades upward into a 4 m thick bed of carbonaceous shales, followed upwards by *ca.* 6 m thick sandstone-siltstone dominated interval and a 4 m thick clast-supported conglomerate interval interbedded with very thin beds of shale. The upper part of the core consists of a 70 m sequence dominated by sandstones and siltstones beds interbedded with thin to very thin beds of shales, followed upward by a 10 m thick shale dominated interval.

3.3. Borehole TGDH(C)005

This borehole was drilled in a small outcrop area of the Karoo Supergroup surrounded by the Mesoproterozoic Tete Suite (Fig. 2). It has a total depth of *ca*. 230 m and penetrated, an 11 m thick sequence of basement rocks consisting of anorthosites (Fig. 5) at the base. These are unconformably overlain by about 38 m of coarse- to medium-grained sandstone and siltstone beds interbedded with thin to very thin beds of shales belonging to the KSG. This situation indicates the absence of the conglomerate beds that usually characterize the base of the KSG, in the Moatize and in other Karoo basins, suggesting that the base of Karoo Supergroup is diachronous in this sub-basin. The latter sandstone-siltstone interval is followed by approximately 70 m of dominantly siltstones and shales with thin beds of coal concentrated in the 162 – 168 m and 110 – 123 m depth intervals. In the interval between 98 m and 68 m, coarse- to medium-grained sandstone beds are interbedded with very thin beds of siltstones and shales. The interval from 68 m depth up to the top of the core consists of shales, carbonaceous shales and several thin beds of coal, typical of barcode coals.

3.5. Borehole A1TM-085

This borehole has a total depth of ca. 727 m and penetrated a 2 m thick sequence of basement rocks consisting of anorthosites belonging to the Tete Suite at its base (Fig. 6). The basement rocks are unconformably overlain by about 55 m of clast to matrix support conglomerates interbedded with siltstones, sandstones, and shales. Approximately 160 m of dominantly shales, carbonaceous shales, siltstones and thin beds of coals follow the latter conglomerate dominant interval. A coarser-grained interval consisting of siltstones, medium- to coarse-grained sandstones and thin beds of shales are positioned between approximately 415 m and 282 m depth. From 282 m to 18 m depth the succession consists of shales, carbonaceous shales and several thin beds of coal. The top, 18 m of this core consists of coarse- to medium-grained sandstones. The succession in this core is intruded by dolerite sills concentrated in the depth interval between 340 m and 90 m. The sill thickness is 1 – 2 m on average but at approximately 160 m, a conspicuous 12 m thick doleritic sill occurs that caused sufficient heating to affect the VR results (section 5).

3.4. Borehole CIMT-014

This borehole has a total depth of 500 m and mostly consists of siliciclastic red bed lithologies (Fig. 7). The top of the Mesoproterozoic basement was not penetrated. From the base to 470 m, the succession changes in both lithology and sedimentary features. This basal 30 m thick succession consists of medium- to coarse-grained grey sandstones interbedded with laminated grey siltstones and carbonaceous shales, the red sediment colours, which is characteristic for most of the core is absent in this basal interval. Two prominent coarse-grained sandstone dominant intervals are present, the first between 310 m and ca. 470 m, and the second between 210 m and 260 m depth. These intervals consist of coarse-grained (sometimes

conglomeratic) to medium-grained red sandstones interbedded with red to brown mudstones and siltstones. The interval from 310 m and 260 m depth of the is characterized by fine-grained lithologies dominated by red mudstones interbedded with thin beds of grey mudstones and brown siltstones, with few beds of coarse-to medium-grained red sandstones. Another fine-grained dominated interval with the same lithological features is found between 210 m depth and the top of the borehole.

3.6. Borehole A1TM-039

This borehole was drilled to total depth of *ca*. 600 m, and consists mainly of red siliciclastic lithologies (Fig. 8). This succession exhibits many lithological similarities with borehole CIMT-014. However, it differs by a higher dominance of coarse-grained siliciclastic rocks. Accordingly, from the base to 470 m depth, the succession is dominated by red to brown siltstone beds interbedded with red mudstones and few thin beds of grey mudstones and red sandstones, whereas the interval between 470 m and 350 m is characterized by thick, red to purple sandstone beds. Between 350 m and the top of the core, the succession consists of thick beds of coarse- to medium-grained red sandstones intercalated with thick beds of brown siltstones and red mudstones.

3.7. Borehole A1TM-058

With a total depth of 1000 m, borehole A1TM-058 (Fig. 9) is the deepest of all the boreholes studied, consisting mainly of fine-grained siliciclastic lithologies (shales and siltstones). At its base a 4 m sequence of gabbros – anorthosites belonging to the Tete Suite was penetrated. The latter lithologies are unconformably overlain by red siltstones, fine-grained sandstones, and red mudstones that grade upwards immediately into black carbonaceous shales interbedded with two intervals of clast- to matrix-supported conglomerates up to *ca*. 930 m

depth. The top of the basement rocks is red stained and the features of the lithologies above the unconformity, also suggest sub-aerial sedimentary conditions and the probable formation of soils, rather than sedimentation under glacial to peri-glacial conditions prevalent during the deposition of the Dwyka type lithologies. The interval between 930 m and 750 m in the succession is characterized by a cyclic repetition of siltstone and sandstone interbedded with shales. This is followed by a very thick interval from 750 m to 190 m, consisting mainly of black carbonaceous shales, shales, siltstones and coal beds. The latter interval also included more coarse-grained lithologies, consisting of sandstones and siltstones especially between 610 m and 490 m depth. From 190 m depth to the top of the core, the succession consists of coarse- to medium-grained grey sandstones alternating with laminated siltstones, carbonaceous shale and thin beds of coal. The occurrence of several doleritic sills is characteristic for the succession of this borehole.

4. Organic matter extraction techniques and methods of organic maturation assessment

One hundred and seventy two mudrock core samples were used for thermal maturity analysis using the laboratory facilities of CIMA, Universidade do Algarve. Twenty grams of mudrock were crushed and placed in a 50 mL Falcon tube. To the crushed rocks was added a few drops of HCl to test for carbonates. Since all the samples proved to be devoid of carbonates, the crushed mudrock samples were treated with HF (40%) until all the silicates were dissolved. Then the organic residue obtained was rinsed and decanted several times using distilled water until the organic residue was fully neutralized. Afterwards, the samples were sieved using a 15µm mesh sieve. For spore fluorescence, spore colour and palynological analysis, the organic residues were mounted on palynological slides using acrylic resin Elvacite®.

4.1. Vitrinite Reflectance

The obtained organic residues were mounted and polished after the method by Hillier and Marshall (1988). Mean random vitrinite reflectance in oil immersion (%*Ro*) was the vitrinite reflectance (VR) parameter chosen for thermal maturity assessment, because the methodology adopted accounts non-oriented vitrinite particles. For vitrinite identification and measurement several criteria were taken into account following the guidelines recommended by the ASTM D7708-14 (2014), ISO 7404-5 (2009) and the International Committee for Coal and Organic Petrology (1998). VR measurements on all samples was performed at the University of the Algarve, Portugal, using an Olympus BX 51 microscope equipped with a black and white Olympus XC-50 digital camera. The greyscale (8-bit) digital images of vitrinite particles were analysed using the graphical tool VITRINITE, which runs within the Mirone Suite and calibrates the scale of 256 grey levels with standards of known reflectivity (Fernandes *et al.*, 2015). The reflectance values of the standards used were: 0.00 %, 0.428 %, 0.595 %, 0.897 %, 1.314 %, 1.715 %, 3.15% and 5.37 %. VR was measured in non-polarized incident light with a wavelength of 546 nm and immersion oil with a refractive index of 1.518 at a room temperature of 20ºC. Figure 11 shows some photographs of vitrinite grains which reflectance values was measured for this study. One hundred random reflectance values were measured across the polished thin sections and their arithmetic mean and standard deviation were calculated (Table 1). The arithmetic mean was considered to be the true $\%R_O$ for the sample.

As described in Section 3, the stratigraphic sections of three of the boreholes studied (ZSA-32, A1TM-058 and A1TM-085) were intruded by doleritic sills. Some of the samples of these three boreholes, close to the intrusion walls, have high vitrinite reflectance values (Table 2). The high vitrinite reflectance values measured for these samples, are attributed to the

localized heat effect of the igneous intrusion in the aureoles and not to burial heat (see Section 7. Discussion). Hence, the vitrinite reflectance measured in the later samples (Table 2) were not included neither in the calculation of burial palaeotemperatures and palaeogeothermal gradients, nor in the estimation of eroded covers (see Section 6. Interpretation of organic maturation results). However, the vitrinite reflectance values of the heat affected were important for the thermal history discussion of the studied region.

4.2. Spore fluorescence and spore colour

Qualitative spore fluorescence and spore colour are two optical parameters of thermal maturity of organic maturation, useful for evaluating maturation levels of low-rank rocks until the end of the oil window (1.35 - 1.5%*Ro*) (Van Gijzel, 1979; McPhilemy, 1988; Suárez-Ruiz et al., 2012). When correlated with the quantitative VR method, spore fluorescence and colour parameters can provide additional support for the thermal maturity of the rocks. Maturation causes a gradual shift in organic matter fluorescence colours (red shift) from the shorter to the longer wavelengths, that is, blue and green to yellow, orange and finally red. Of all the macerals of the liptinite group, sporinite is the one that shows the most consistent changes in fluorescence colour spectra and intensity with increasing maturation. Under fluorescence excitation, it changes colour from green through yellow to orange and finally red, with increasing maturity to the top of the oil-window, after which it no longer fluoresces. A phenomenon frequently noticed in fluorescent palynomorphs is the fading effect (van Gijzel, 1979). The fading effect is due to a photochemical modification of the fluorescing organic matter during prolonged blue light exposure, (30 minutes to 2 hours or more). During this lengthy exposure the intensity of fluorescence may increase or decrease; if it increases, the fading is said to be positive, conversely, if it diminishes is negative. In other words, the

emitted fluorescence spectrum may move either towards higher wavelengths (red band) or towards shorter wavelengths (green band), the fading is said to be positive in the first case and negative in the second.

The analysis of qualitative spore fluorescence colours was undertaken in the University of the Algarve using an Olympus BX 51 microscope equipped with a metal halide lamp fluorescence unit; XCite Series 120Q and with a violet and Blue +12 filter block that generates a wavelength band of 390 - 490 nm. This system was allowed to stabilize for 5 min before any observation of the fluorescence of palynomorphs was attempted. Suitable spore species with smooth and medium thick exine, such as *Densoisporites* spp., were subjected to 5 minutes of excitation, after which their fluorescence colours were recorded. The same spores were exposed for a further thirty minutes to record any fading effects. The terminology used for describing fluorescence colours was blue (B), green (G), yellow (Y), dark yellow (DY), orange (O), dark orange (DO) and red (R).

Spore exine colour has long been suggested by palynologists as a method to assess the thermal maturity of sedimentary rocks, because they observed that, with increasing burial depth, spore colour changes from light to dark and that the change is progressive and irreversible (Correia, 1971; Staplin, 1982). In this study, spore colour was recorded using the Phillips Petroleum Colour Standard version no. 2 (Pearson, 1984), which is an adaptation of Staplin's Thermal Alteration Index (TAI) chart, because it includes more shades for the same colour index. The spore colour index for the samples was given by the colour of the dominant and lightest spores observed and compared with the Phillips Petroleum Colour Standard chart. The results of spore colour determination are presented together with VR measurements and spore fluorescence colours for each sample (Table 1). Figures 3 to 10 show the main features

of spore colour and spore fluorescence in the boreholes studied. Spore colours were recorded for acamerate, azonate trilete or monolete spores with a smooth exine of medium thickness, such as *Densoisporites* spp. and *Laevigatosporites* spp., which occurs throughout the section of both boreholes studied by (Pereira et al., 2016).

As mentioned above, both spore fluorescence and spore colour are qualitative methods for assessing organic maturation. The visual evaluation of the fluorescence colours and the colours the palynomorph walls is subjective, depending on the experience of the operator and lacking, therefore, the objectivity of VR. The lack of universally accepted standards of organic maturation, as VR, is another drawback of these two methods. Moreover, it has been reported (Mendonça Filho et al., 2010), that the acid treatment used to obtain kerogen concentrates (HCl and HF maceration) affects the fluorescence spectra of liptinites, shifting it to higher wavelengths (red-shift), when compared with the fluorescence spectra of whole rock samples. Despite these problems, spore fluorescence and spore colour, used together with VR are still important parameters of organic maturation, especially for low and medium rank rocks.

5. Organic Maturation and Palynological Results

Data of the thermal maturity analyses, both quantitative (VR) and qualitative (spore fluorescence and TAI), are shown in Table 1 and in VR profiles of the studied boreholes, which illustrate the change of the organic maturation indicators with burial depth (Figs. 3 to 9).

5.1. Borehole ZSA-32

Thirteen samples were processed from ZSA-32 and they were all suitable for organic maturation studies, whereas only three samples of the thirteen were suitable for palynological

studies. The VR values measured show a linear increase with depth in the borehole, ranging from 1.21%*Ro* at the top to 1.31%*Ro* at the bottom (Fig. 3). Spore fluorescence colours change intensity from orange at the top, to dark orange at the bottom of the borehole, indicating palaeotemperatures close to the fluorescence extinction. TAI values also change from 3 to 3/3+ with increasing depth. Six samples were affected by heating by dolerite intrusions and have TAI colours of 4-/4 or 5. In general, TAI and fluorescence of the samples not affected by the intrusions indicate a thermal maturity at the onset of the oil-window, and VR values indicate a coal rank of medium rank B (ISO 11760, 2018).

Palynological analysis of ZSA-32 samples revealed an assemblage characterized by bisaccate taeniate pollen grain such as *Lueckisporites virkkiae*, *Lunatisporites pellucidus*, *Guttulapollenites hannonicus* and monolete spores such as *Laevigatosporites colliensis*. These assemblages indicate a Lopingian (late Permian) age for the entire succession of this core (Montesi, 2016).

5.2. Borehole A1TR-018

Twenty-two samples from A1TR-018 were studied for palynology and organic maturation, but after laboratory processing, only six samples were suitable for maturation studies and thirteen samples yielded palynomorphs. VR values measured from the *ca*. 80 m thick succession of this borehole increase downhole, from 1.51%*Ro* at the top to 1.72%*Ro* at the bottom at depth of *ca*. 70 m (Fig. 4). Spore colours showed consistent TAI values of 3+/4- throughout the succession, which is fully consistent with the VR values measured. The thermal maturity obtained from this core indicates that the sedimentary succession straddles in the wet and dry gas zone of hydrocarbon generation. In terms of coal rank, VR values indicate a medium rank A (ISO 11760, 2018). All the samples studied for palynology yielded an assemblage characterized by rare trilete spores and colpate pollen grains, abundant

monossaccate and rare to common bissaccate (taeniate and non-taeniate) pollen. This assemblage shows similarity to the one described by Pereira *et al*. (2014) from the borehole ETA 72 located in the Muarádzi sub-basin (Fig. 1) and, therefore, is interpreted to be of Kungurian / Roadian age with *Alisporites* sp., *Cycadopites* sp., *Florinites* spp., *Potoniesporites* sp., *Striatopodocarpites cancellatus, S. fusus Protohaploxypinus* sp. and *Vittatina* sp.

5.3. Borehole TGDH(C)005

Twenty five samples were processed for both thermal maturity and palynological analysis but just twenty and twelve samples from borehole TGDH(C)005 were studied for palynology and organic maturation, respectively. The lowest maturation levels in this part of the Moatize – Minjova Basin were detected in this borehole. VR values range from 0.97%*Ro* at ca. 20 m depth to 1.15%*Ro* at 206 m depth. VR increases linearly with depth with a good correlation coefficient of $R^2 = 0.92$ (Fig. 5). In terms of hydrocarbon generation the entire succession in this borehole lies within the oil-window. Consistent TAI values of 2 were recorded for this borehole, with the exception of one sample from the bottom of the borehole with a TAI value of 2+. All samples show positive fluorescence with yellow to dark yellow colours (Fig. 10). Fluorescent samples also show a positive fading effect. The maturation levels measured straddle the boundary between medium rank C and B coals (ISO 11760, 2018) in terms of coal rank. The microfloristic assemblage recorded in this borehole show affinities with the assemblage described by Pereira et al. (2016) from borehole DW 123 located in the Muarádzi sub-basin (Fig. 1), that indicates a Lopingian age based on the presence of the key species, as *Lueckisporites virkkiae*, *Guttulapollenites hannonicus, Polypodiisporites* sp., *Thymospora* sp., and *Weylandites lucifer*.

5.4. Borehole A1TM-085

Ten samples were processed for both maturity and palynological studies, being all suitable for these studies. VR values measured increase downhole from 1.43%*Ro* at 138 m depth to 1.56%*Ro* at 731 m depth (Fig. 6). The VR profile shows a linear increase in reflectance with depth of burial, defining a gradient with a correlation coefficient of $R^2 = 0.83$. Maturation levels indicated by VR fall in the wet gas zone for all the samples of this borehole. TAI values of 3+/4- were obtained from most of the samples that contained suitable spores. However, in three samples between depths *ca*. 455 m and 222 m, spores with a TAI of 3/3+ were recorded, showing also feint fluorescence with brown to dark orange colours, indicating a position close to the spore fluorescence extinction level. Below 454 m depth, no palynomorphs fluoresce. In this borehole, the cut-off of fluorescence correlates with VR of ca. 1.49%*Ro*. According to Taylor et al. 1998 all fluorescence disappeared during the second coalification jump, which is between 1.2 % *Ro* and 1.6% *Ro*, therefore not all spores fluorescence coincide with 1.35%*Ro* taken as the end of oil-window. Fluorescent samples also showed a negative fading effect. The maturation levels measured correspond to a coal rank of medium rank A (ISO 11760, 2018). As in borehole A1TM-058, this borehole also shows effects of conductive heating related to the intrusion of doleritic sills in a sample at *ca*. 187 m depth.

Palynological studies performed on samples from this borehole highlighted an assemblage similar to the one found in borehole TGDH(C)005 indicating a Lopingian age with *Calamospora* sp., *Horriditriletes* sp, *Krauselisporites rallus, Osmundacidites senectus* and *Guttulapollenites hannonicus* and *Weylandites lucifer* for the whole succession penetrated by this borehole.

5.5. Borehole CIMT-014

As mentioned in the borehole descriptions, most of the lithologies penetrated by borehole CIMT-014 consist of red beds (mudstones, siltstones and sandstones), which are not suitable for organic maturation and palynological studies due to the oxic conditions that prevailed during deposition.

Fifty samples were processed for both maturity and palynological studies for CIMT-014 borehole. However, the majority of samples were barren with only 10 samples for palynology and 4 samples for maturation proving to be suitable for these studies. In borehole CIMT-014, a VR value of 1.07%*Ro* was measured from sample MQ111 at *ca*. 132 m depth. In general, VR increases downhole and a VR value of 1.47%*Ro* was measured for sample MQ147 near the bottom of the borehole (Fig. 7). However, the most important information regarding the maturation and thermal history of this borehole came from spore colour (TAI) and fluorescence. The observation of these two optical organic maturation indicators revealed two different palynomorph populations, in terms of both age and organic maturation level. All samples investigated contain an indigenous palynomorph population but samples MQ127, MQ115 and MQ111 also includes a reworked palynomorph population (Fig. 12). It is noteworthy that reworked vitrinite populations were not identified in these last three samples. TAI values of 2 and 3+/4- were recorded for the indigenous palynomorph population from *ca*. 132 m depth and at the bottom of the CIMT-014 borehole, respectively. Fluorescence intensity and colour also change downhole for the indigenous palynomorph population, from bright yellow colour in sample MQ111 to dark orange colour in sample MQ147. The reworked palynomorph population is absent in sample MQ147, but in the other three samples it is common, making up to 30 – 40% of all palynomorphs. The TAI values of the reworked palynomorphs are always 3+/4- and spore fluorescence is either orange colour or the spores do not fluoresce (Table 1). Non-fluorescent spores are more abundant in samples MQ111 and

MQ115 (Fig. 12). The organic maturation levels indicated by VR indicate that this borehole falls within the late oil-window, with sample MQ147 (at the bottom of the borehole) indicating a position at the beginning of the wet-gas generation zone. VR values also indicate a coal rank of medium rank B (ISO 11760, 2018) for most of the sedimentary succession in this borehole.

The palynological assemblage found in sample MQ111 suggest an Upper Triassic (Carnian) age, based on the presence of the spores ~~-~~*Anapiculatisporites spiniger/Carnisporites anteriscus, Densoisporites* spp., *Dictyophyllidites* sp., *Limatulasporites* limatulus, *Lophotriletes novicus, Lundbladispora* spp., *Nevesisporites fossulatus, Retitriletes* sp., *Striatella seebergensis* and *Uvaesporites* sp. and the pollen grains of *Camerosporites secatus*, *Cycadopites* sp., and *Samaropollenites speciosus,* that typifies to these ages (César and Colombi, 2016; Dawit, 2014; Paterson et al., 2018). The assemblages found in samples MQ115, MQ127 strongly suggests a Lower Triassic age, containing the spores *Aratrisporites* sp., *Densoisporites nejburgi, D. playfordii Lundbladispora* spp. and *Playfordiaspora cancellosa* and the pollen grains *Alisporites nuthallensis*, *Lunatisporites pellucidus, Falcisporites stabilis* , and *Platysaccus queenslandi*. The assemblages of these two samples are characterized by *Alisporites nuthallensis*, *Lunatisporites pellucidus, Densoisporites playfordii, Falcisporites stabilis* and *Lundbladispora obsoleta*, *Platysaccus queenslandii*, *Uvaesporites* sp. and *Carnisporites* sp. that typifies to these ages (Dawit, 2014). Between samples MQ111 and MQ115, separated vertical in the borehole by only *ca*. 15 m no palynomorphs were recorded in three samples located in this interval, suggesting an important hiatus, since no Middle Triassic palynomorphs were identified. Samples MQ111, MQ115 and MQ127 also have a considerable amount of reworked palynomorphs of Lopingian (Permian age) as for instance *Polypodiisporites* sp., *Thymospora* sp. The Permian-Triassic boundary is tentatively placed at *ca*. 489 m depth according to the scheme described by Pereira et al.

(2016) from borehole DW132, where the Permian-Triassic boundary was identified at *ca.* 42 m depth.

5.6. Borehole A1TM-039

For A1TM-039 borehole, twenty samples were processed, but only two samples were suitable for organic maturation studies and three yielded palynomorphs suitable for palynological analysis. VR values measured are 1.15%*Ro* (MQ231) and 1.17%*Ro* (MQ233) and the indigenous palynomorphs population shows yellow fluorescence colours and TAI values of 2+ (Fig. 8). The reworked palynomorph population either shows no fluorescence or dull dark orange colours and TAI values of 3+/4- (Table 1). The maturation levels suggested by the VR results and the indigenous palynomorph population indicate a position within the oil-window and a coal rank of medium rank B (ISO 11760, 2018), whereas the maturation levels of the reworked population indicate a position at the end of the oil-window and at the beginning of the wet-gas generation zone.

The three productive samples studied are located near the bottom of the borehole and contain an assemblage assigned to Carnian age (Upper Triassic) age. The palynoassemblage included the pollen grains *Alisporites nuthallensis, Enzonalasporites vigens, Platysaccus queenslandi* and *Samaropollenites speciosus* and the spores *Aratrisporites* sp.*, Anapiculatisporites spiniger/Carnisporites anteriscus*, *Densoisporites* spp., *Lundbladispora* spp.*, Playfordiaspora cancellosa, Striatella seebergensis* and *Uvaesporites* sp. A second assemblage comprising reworked palynomorphs was also identified in the same samples. The reworded assemblage is assign to a Permian age due to the presence of*, Alisporites parvus, Cyclogranisporites gondwanensis, Polypodiisporites* sp.*, Thymospora* sp.*,* described as key species for this age in other Karoo basins.

5.7. Borehole A1TM-058

The twenty-nine samples processed were all suitable for maturity studies, whereas, only twelve samples were suitable for palynological studies. In borehole A1TM-058, VR values increase downhole from 1.19%*Ro* at 23.5 m depth to 1.51%*Ro* at 970 m depth, with a clear linear VR *vs.* depth relationship (Fig. 9). The boundary between the base of the oil-window and the wet gas zone, indicated by the VR profile, occurs at *ca*. 500 m depth, with VR values ranging from 1.31 to 1.36%*Ro*. Samples above 490 m depth show positive fluorescence with orange to dark orange colours (Fig. 10), whereas for samples below that depth, no palynomorphs (spores and pollen) were observed to fluoresce. The depth of fluorescence extinction in this borehole correlates with VR values between 1.31 and 1.33%*Ro*. Spore colour increases from a TAI of 3/3+ at the top of the borehole to values of 3+/4- at the bottom of the borehole. TAI values of 3+/4- were recorded for spores at the horizon of fluorescence extinction. All thermal maturity indices recorded correspond to medium rank B and A coals in terms of coal rank (ISO 11760, 2018). In this borehole, VR measured from samples between the depth intervals of 68 to 180 m and 610 to 625 m, yielded anomalously high values, that do not lie on the VR vs. depth profile (Fig. 9). These samples are positioned close to the margins of several doleritic intrusions that were intersected by the borehole. Therefore, the VR values from these samples were not included in the calculation of the VR profile, since they were interpreted as the result of post burial igneous activity, most likely related to the Jurassic Karoo - Ferrar Large Igneous Province (*op. cit.* Duncan et al., 1997). Palynological studies performed in this borehole, shows a palynoassemblages similar to the assemblage studied in the borehole A1TM-085. Present are the diagnostic species *Guttu~~l~~lapollenites hannonicus*, *Klausipollenites schaubergeri, Luecki~~e~~sporites virkkiae*, *Osmundacidites senectus*, *Polypodiisporites* sp., *Protohaploxypinus microcorpus*, *Thymospora* sp. and *Weylandites lucifer*, that indicates a Lopingian age (Late Permian). The assemblages investigated are also

very similar and correlate with those described for the borehole DW 123, Muarádzi sub-basin (see Fig. 1) (Pereira et al., 2016).

6. Interpretation of Organic Maturation Results

6.1. Palaeogeothermal gradient estimates

Except for boreholes CIMT-014 and A1TM-039, the thermal maturity obtained from the non-heat affected samples (Table 1), indicates a clear relationship between maturity and depth of the sedimentary beds despite the different techniques used (Figs. 3 to 10). This type of relation suggests that burial was the main factor controlling organic maturation. However, organic maturation profiles indicate that the boreholes located in close proximity to the southern basin boundary have less steep gradient indicating higher geothermal gradients at those locations. In order to investigate this aspect further, palaeotemperatures were calculated using Barker's (1988) empirical equation T(°C)= 104ln(%*Ro*)+148, where T(°C) is the maximum palaeotemperature attained by the sedimentary rock that yielded vitrinite particles with a measured VR of %*Ro*.

The palaeotemperatures calculated by this equation are shown in the Table 1. These were then used to estimate palaeogeothermal gradients (Fig. 13) and the amount the rock cover eroded in the N'Condédzi sub-basin of the Moatize - Minjova Coal Basin.

The palaeogeothermal gradients calculated vary significantly from a maximum of *ca*. 300°C/km in borehole A1TM-018 to a minimum of ca. 35°C/km in borehole A1TM-085. Palaeogeothermal gradients were not calculated for boreholes CIMT-014 and A1TM-039 due to insufficient numbers of samples studied.

Notably, the higher palaeogeothermal gradients were from the boreholes located near the basin margin and in the small isolated occurrence of the Karoo Supergroup where borehole TGDH(C)005 was drilled. Anomalously high VR values were measured in boreholes A1TM-085, A1TM-058 and ZSA-32 through several depth intervals that were interpreted as the results of conductive heating associated with Jurassic age doleritic intrusions. These anomalous VR values were not included in the construction of palaeogeothermal gradients.

However, there is no evidence that boreholes that have the highest calculated palaeogeothermal gradients were affected by igneous intrusion and, therefore, another thermal event was responsible for such high geothermal gradients. The calculated palaeogeothermal gradients of 35-40°C/km is considered to be the regional geothermal gradients for the N'Condédzi sub-basin of the Moatize - Minjova Coal Basin, and is similar to the 40°C/km geothermal gradient calculated by Fernandes et al. (2015) for the Muarádzi sub-basin of the same basin.

The calculated palaeogeothermal gradients are characteristic of extensional continental rift basins (Fernandes et al. 2015). However, the higher geothermal gradients calculated for the boreholes near the basin boundary, suggest that high heat flux rather than the regional geothermal gradient was responsible for locally elevated the geothermal gradients. A likely cause for this high palaeogeothermal gradient is the circulation of hot fluids associated with fault zones and permeable beds (sandstones).

6.2. Eroded cover estimates

The calculated palaeogeothermal gradients were used to estimate the amount of eroded sedimentary cover in sedimentary basins where rocks have already attained maximum

temperatures. The eroded sedimentary cover refers to the thickness of sedimentary section necessary to account for the measured VR results. In the boreholes studied, the shallowest samples, from 11 to 138 m depth, reached peak palaeotemperature of 185-190°C. The method used to calculate the eroded cover is after Bray et al. (1992). Applying this methodology to the estimates of exhumation in the study area suggests a maximum of *ca*. 5300 m and a minimum of 550 m. This range can be explained by different palaeogeothermal gradients used in calculations for these boreholes. Since the highest palaeogeothermal gradients are considered abnormal and related to high temperature fluid flow through fault zones and permeable lithologies, the amount of post-late Permian exhumation is between 4.3-5.3 km; values slightly higher than the 2.5 – 3 km calculated by Fernandes et al. (2015).

Thick sedimentary sections are found in other external rift-related Karoo basins in Eastern Africa, which are geometrically related to the Moatize Minjova Basin (Cairncross, 2001; Catuneanu et al. 2005). For example, Banks et al. (1995) reported at 8 km thick Permian-Triassic sedimentary section preserved in the Karoo rift basin of the Luargwa Valley in Zambia.

7. Discussion

The VR values measured from the N'Condédzi sub-basin, range from 1.3-1.7%*Ro*, indicating a coal rank of medium rank B and A coals (ISO 11760, 2018), and are similar to those reported by Fernandes et al. (2015) of dispersed organic matter, and Vasconcelos (1995) of coals, for the Moatize sub-basin (Fig. 1). In terms of zones of hydrocarbon generation, boreholes ZSA-32, A1TM-039 and TGDH(C)005 are within or at the end of the oil-window, boreholes A1TR-018 and A1TM-085 are within the wet gas generative zone, and boreholes

A1TM-058 and CIMT-014 span the base of oil window at depths of *ca*. 600 m depth and 400 m, respectively.

The linear increase of VR with depth observed in the boreholes indicates an organic matter maturation process related to burial. The calculated regional palaeogeothermal gradient for the N'Condédzi sub-basin is 35-40°C/km. The doleritic intrusions observed in three boreholes (A1TM-058, A1TM-085 and ZSA-32), had only local thermal effects and only increased VR for the samples in the contact aureoles. If the igneous episode, responsible for the doleritic intrusions, had a major effect on the regional organic matter maturity, a homogenisation of all maturity indicators will be expected for the sedimentary successions of these boreholes, this was not observed and supports our argument for the local thermal effects of the intrusions. However, boreholes TGDH(C)005 and A1TR-018 do not show evidence of igneous intrusions and have higher palaeogeothermal gradients suggesting that a thermal process other than burial heating, was responsible for these abnormal gradients. The close proximity of these boreholes to the southern fault-bounded basin margin suggests that hot fluids circulating through permeable lithologies (sandstones) and faults zones, as a likely processes capable of elevate the regional palaeogeothermal gradients in these parts of the basin margin (Fig. 14). The origin of the hot fluids may have been connate waters that moved through the sedimentary pile due to lithostatic pressure during fault-induced subsidence, or may have a deeper origin resulting from metamorphic dewatering reactions(?). The flow of hot fluids, expelled from the basal beds of the basin by lithostatic pressure, through permeable lithologies and fracture zones, allowed the advective and convective transmission of heat, which heated up the sedimentary successions located near the southern basin margin (Fig. 14). The rock successions in these zones were in equilibrium with the temperature of the hot fluids that overprinted the initial thermal maturity caused by burial heat only.

The initiation of fluid flow due to lithostatic pressure in this basin is probably due to the high sedimentation rates consequence of fault-induced subsidence, leading to the accumulation of the thick succession of sediments. In borehole A1TM-058, *ca*. 1 km of Lopingian age sediments are preserved and Lakshminarayana (2015) reported a Lower Karoo succession with more than 900 m thickness. Boreholes A1TM-039 and CIMT-014 encompass a *ca*. 500 – 600 m sedimentary succession of mostly Lower to Middle/Upper Triassic age, demonstrating the continuation of high sedimentation rates throughout Triassic times in this basin. An additional cause for the initiation of fluid flow is the structural geometry of the basin. The N'Condédzi sub-basin is half-graben, where the main fault, the Mwanza Fault, was formed by tectonic reactivation of the Sanângoe Shear Zone (Fig. 1). The Mwanza Fault was probably active since the early Permian and lead to the accumulation of a thick pile of sediments adjacent to the fault zone. Due to the half-graben geometry, the thicknesses of the sedimentary successions were considerably less near the southern margin of the basin. For example, borehole TGDH(C)005 located in the isolated occurrence of Karroo Supergroup sediments within the Tete Suite contains *ca.* 230 m of Lopingian aged strata, whereas borehole A1TM-058 includes a *ca*. 1 km succession of the same age.

Using the regional palaeogeothermal gradient calculated from VR, 4 to 5 km of cover was eroded after Lopingian times in the depocentre of this basin, whereas near the S-SW basin margin, the estimated eroded cover is significantly less from *ca*. 544 m to *ca.* 2.4 km. However, these estimates may be inaccurate, as they do not take account of the palaeogeothermal gradient probably having been elevated by hot fluids flowing through fault zone at the basin margin.

The maturation data and the age of the successions of boreholes A1TM-058, A1TM-085, TGDH(C)005, ZSA-32 and A1TR-018, indicate that the timing of organic matter maturation, when peak temperatures were attained, is prior to Lower Triassic times. This can be better constrained by taking into account the cooling episode that occurred between 240 and 230 Ma in the Moatize - Minjova Basin (Fernandes et al., 2015). The latter study also indicated that peak burial temperatures and consequently organic maturation levels, were attained shortly after deposition (3 - 10 Ma), implying high subsidence rates during Lopingian to Lower Triassic time in this region. In borehole CIMT-014~~5~~ palynological results indicate that Lower Triassic and the Upper Triassic (Carnian) rocks, samples MQ115 and MQ111, respectively (section 5.5 and Fig. 7), are only vertically separated in the borehole by a 15 m thick section of coarse clastic sedimentary rocks. Although, the samples processed in the borehole interval, between these two samples, for organic maturation and palynology were barren, it is unlike that Middle Triassic rocks are condensed in this 15 m thick section. This suggests that the N'Condédzi sub-basin was affected by the same Middle Triassic erosion event described by Fernandes *et al*. (2015) for the Moatize - Minjova Basin in the region of the Muarádzi sub-basin (Fig. 1). Also, the presence of common reworked palynomorphs of Permian age in Upper Triassic (Carnian) sediments in boreholes A1TM-039 and CIMT-014 indicates exhumation and erosion of Permian aged Karoo sedimentary rocks during Middle Triassic times in the neighbouring Karoo basins, *e.g*. in the Moatize and Muarádzi sub-basins (Lopes et al., 2014; Pereira et al., 2016; Götz, et al., 2018) (Fig. 1). Furthermore, the spore fluorescence colours and TAI values recorded from the reworked Permian age palynomorphs in boreholes CIMT-014 and A1TM-039, are considerably higher than those of the indigenous Triassic palynomorphs. Therefore, the Upper Triassic sedimentary rocks never attained higher temperatures than those indicated by the reworked palynomorph population. Unconformities between the late Permian and the Lower Triassic sedimentary successions are described in

several Karoo rift basins located to the north of the Main Karoo Basin of South Africa (Catuneanu et al., 2005 and references herein). In the Ruhuhu, Selous and Tanga basins of southern Tanzania this unconformity is well documented and corresponds, for example, to the unconformity between the Lopingian Usili Formation and the Lower Triassic Manda Formation. In Zambia it is the unconformity between the Lopingian Upper Madumabisa Formation and the overlying Lower Triassic Escarpment Grit, and in Madagascar, in the Morondova Basin, it is the unconformity between the Lower Sakamena Formation and the overlying Middle to Upper Sakamena Formation. However, the effects of this Middle Triassic erosion event on the organic maturation and thermal history of the N'Condédzi sub-basin are still uncertain. This is due to the similarity of VR values measured for the Lower and Upper Triassic samples in boreholes CIMT-014 and A1TM-039, together with the impossibility of constructing VR profiles for these two boreholes (see sections 5.5, 5.6 and 6.1), capable of identifying distinct palaeogeothermal gradients, below and above the Middle Triassic erosion event. Accordingly, the organic maturation results attained in this study indicate that the effects of the Upper Triassic reburial on the organic maturation, as a distinct thermal event of this sub-basin were not detected, suggesting that a single episode of burial under a sedimentary cover that ended in Upper Triassic – Lower Jurassic(?) times, was responsible for the organic maturation levels measured. The similar VR results, for example, between the Carnian age samples (MQ231 1.15% *Ro* and MQ233 1.17%*Ro*) in borehole A1TM-039 and the same age sample (MQ111_1.11%*Ro*) in borehole CIMT-014, separated vertically *ca.* 470 m (both boreholes were drilled on a ground surface at *ca*. 300 m above sea level), could be due to different burial cover thicknesses. In this case, borehole A1TM-039 was located in an area of the sedimentary basin that was buried under a thicker sedimentary cover (a depocentre area) than borehole CIMT-014.

Organic maturation levels measured for the N'Condédzi sub-basin suggest a complex thermal history (Fig. 14). The VR profiles of the boreholes studied indicate a maturation process related to burial heat. Though, the high palaeogeothermal gradients observed near the South margin of this basin, suggest the flow of hot fluids through permeable lithologies and fractures with discharge points located near the South boundary of this basin. The flow of hot fluids was due, most probably, to compaction-driven fluid flow. The movement of major extensional faults in the N'Condédzi sub-basin led to high fault-induced subsidence rates. The sediment accommodation space created by these processes was matched also by high sedimentation rates during Permian to Lower Triassic times, which increased considerably compaction pressures and may have originated hot overpressure fluids that initiated the fluid flow through the permeable lithologies and fault zones of this basin.

Reworked Permian palynomorphs in Carnian (Upper Triassic) sediments have higher maturation levels than the indigenous Carnian palynomorphs, indicated by spore colour and fluorescence. This implies exhumation and erosion of Permian aged successions located in the neighbouring Karoo basins during Middle Triassic times, and also suggests that peak burial palaeotemperatures, in those basins, were achieved during Permian to Lower Triassic times. Peak burial palaeotemperatures attained by the Upper Triassic (Carnian) sedimentary successions in the N'Condédzi sub-basin, were lower and did not overprint the effects of the earlier maturation episode of the neighbouring Karoo basins, indicated by the reworked Permian palynomorphs. Lastly, during Lower Jurassic times occurred a last maturation event related to dolerite intrusions. Though, the thermal effects of these intrusions were localised and limited to the contact aureoles.

8. Conclusion

The main conclusions of this work are:

- VR values measured from the exploration boreholes of the N'Condédzi sub-basin, range from 1.3 – 1.7%*Ro*, indicating a coal rank of medium rank B and A coals (ISO 11760, 2018). The range of VR values indicated, excludes the VR values of the heat-affected samples due to the dolerite intrusions. In terms of zones of hydrocarbons the majority of the succession of the boreholes lay at the end of the oil window and the beginning of the wet gas generative zone.
- The linear increase of VR with depth observed in the boreholes indicates an organic matter maturation process related to burial. The calculated regional palaeogeothermal gradient for the N'Condédzi sub-basin is 35-40°C/km. The doleritic intrusions observed in three boreholes, had localized thermal effects and only increased VR for the samples close to the intrusion walls. The abnormal geothermal gradients calculated for boreholes TGDH(C)005 and A1TR-018 located close to the south margin of the basin, are attributed to hot fluids flowing through permeable lithologies (sandstones) and faults zones that elevated the regional palaeogeothermal gradient in these parts of the basin margin. We proposed that the origin of the hot fluids were connate waters that moved due to lithostatic pressure during fault-induced subsidence, with a possible minor contribution of deep hot fluids originated by dewatering metamorphic reactions(?).
- Hot fluid flow was due to the accumulation of thick sedimentary piles (over 2 km in thickness) in periods of rapid subsidence during the Permian – Triassic times.
- Using the regional palaeogeothermal gradient calculated from VR, 4 to 5 km of cover was eroded since after Lopingian time in the depocentre of this sub-basin.
- The maturation data obtained, together with the age of the borehole successions, including the reworked Permian palynomorphs in Upper Triassic sedimentary rocks,

suggests that burial peak temperatures were reached during Upper Triassic – Lower Jurassic(?) times.

Disclosure of interest

The authors declare that they have no competing interest.

Acknowledgments

The authors would like to thank the Managers of Coal India Africana, Limitada, Companhia Carvoeira de Samoa, Limitada, Capitol Resources, Limitada, Gondwana Empreendimentos e Consultorias, Limitada, and Iain C. Pleas for borehole access and complementary information. Francesca Galasso acknowledges the University of Perugia, for the opportunity to participate in the program Erasmus+ Traineeship, funded by the European Commission. The authors gratefully acknowledge Centro de Investigação Marinha e Ambiental (CIMA) for the use of the services and laboratory facilities at the University of the Algarve. We would like to thank Professor Geoffrey Clayton from the Department of Geology, Trinity College, Dublin, and Doctor Elke Schneebeli-Hermann from University of Zurich, Paleontological Institute and Museum, Switzerland, for critical reading of the manuscript. The reviews and valuable comments of four anonymous reviewers, have greatly improved our manuscript. This research did not receive any specific grant from funding agencies in the public, commercial, or not-for-profit sectors.

References

Achimo, M., Vasconcelos, L., Marques, J., Ferrara, M., 2014. Sedimentologia dos depósitos tilíticos do vale do Rio Murrongódzi, Bacia Carbonífera de Moatize-Minjova, Tete,

Moçambique. In: 2º Congresso Nacional de Moçambique e 12º Congresso de Geoquímica dos Países de Língua Portuguesa, Vasconcelos, L. (ed.), Livro de Resumos, Maputo, 57-61.

Afonso, R.S., 1975. Contribuição para o conhecimento da area de Tambara-DÔa (Folha Sul-E-36, grau quadrado 1634). Bol. Serviços Geol. Minas, Lourenço Marques 38, 5e153.

Afonso, R.S., 1976. A geologia de Moçambique. (Notícia explicativa da carta geologica de Moçambique). Direcção dos Serviços de Geologia e Minas, Maputo, 1: 2.000.000. 175 pp.; 2 mapas.

Afonso, R. S., 1984. Ambiente geológico dos carvões gonduânicos de Moçambique - uma síntese. In: Lemos de Sousa, M.J. (Ed.), Symposium on Gondwana Coals, Lisbon, 1983. Proceedings and Papers. Comunicações dos Serviços Geológicos de Portugal, vol. 70 (2), 205-214.

ASTM D7708-14, 2014. Standard Test Method for Microscopical Determination of the Reflectance of Vitrinite Dispersed in Sedimentary Rocks. ASTM, International, West Conshohocken, PA, USA, p. 10.

Banks, N. L., Bardwell, K. A., Musiwa, S., 1995. Karoo Rift Basins of the Luangwa Valley, Zambia. Geological Society, London, 285-295. Special Publication, 80.

Barker, C. E., 1988. Geothermics of petroleum systems: implications of the stabilisation of kerogen thermal maturation after a geologically brief heating duration at peak temperature. In: Magoon, L.B. (Ed.), Petroleum Systems of the United States, vol. 1870. United States Geological Survey Bulletin, 26-29.

Bray, R., Green, P., Duddy, I., 1992. Thermal history reconstruction using apatite fission track analysis and vitrinite reflectance: a case study from the UK East Midlands and the Southern North Sea. In: Hardman, R. (Ed.), Exploration Britain: Geological Insight for the Next Decade, vol. 67. Geological Society of London Special Publication, 3-25.

Cairncross, B., 2001. An overview of the Permian (Karoo) coal deposits of Southern Africa. Journal of African Earth Sciences, 33, 529-562.

Carvalho, L.H.B., 1977. Formações vulcânicas de Carinde, Tete-Moçambique. Dissertação apresentada ao Instituto Superior Técnico para obtenção do grau de Doutor em Ciências da Engenharia (Geologia Aplicada), 213 p.

Catuneanu, O., Wopfner, H., Eriksson, P.G., Cairncross, B., Rubidge, B.S., Smith, R.M.H., Hancox, P.J., 2005. The Karoo basins of south-central Africa. Journal of African Earth Sciences, 43, 211-253.

Césari, S.N. and Colombi, C., 2016. Palynology of the Late Triassic Ischigualasto Formation, Argentina: Paleoecological and paleogeographic implications. Palaeogeography, Palaeoclimatology, Palaeoecology, 449, 365–384.

Formatted: English (United States)

Corcoran, D. and Clayton, J., 2001. Interpretation of Vitrinite Reflectance profile in sedimentary basin, onshore, offshore Ireland. Geol.Soc.London, Spec. Pub., 188, 61-90.

Correia, M., 1971. Diagenesis of sporopollenin and other comparable organic substances: application to hydrocarbon research. In: Brooks, J., Grant, P.R., Muir, M., van Gijzel, P., Shaw, G. (Eds.), Sporopollenin. Academic Press, New York, 569-620.

Daber, R., 1984. Plantas fósseis de Moçambique. Ciênc. Tecnol., Maputo, 9, 77-81.

Dawit, E.L., 2014. Permian and Triassic microfloral assemblages from the Blue Nile Basin, central Ethiopia. Journal of African Earth Sciences, 99, 408-426.

Duncan, R.A., Hooper, P.R., Rehacek, J., Marsh, J.S., Duncan, A.R., 1997. The timing and duration of the Karoo igneous event, southern Gondwana. Journal of Geophysical Research, 102, 18127-18138.

Fernandes, P., Musgrave, J.A., Clayton, G., Pereira, Z., Oliveira, J.T., Goodhe, R., Rodrigues, B., 2012. New evidence concerning the thermal history of Devonian and Carboniferous in South Portuguese Zone. Journal Geological Society, London, 169, 647-657.

Fernandes, P., Rodrigues, B., Borges, M., Matos, V., Clayton, G., 2013. Organic maturation of the Algarve Basin (Southern Portugal) bearing on thermal history and hydrocarbon exploration. Marine and Petroleum Geology, 46, 210-233.

Formatted: Italian (Italy)

Fernandes, P., Cogné, N., Chew, D.M., Rodrigues, B., Jorge, R.C.S, Marques, J., Jamal, D., Vasconcelos, L., 2015. The thermal history of Karoo Moatize Minjova Basin, Tete Province, Mozambique: an integrated vitrinite reflectance and apatite fission track thermochronology study. Journal of African Earth Sciences, 112, 55-72.

Götz, A. and Ruckwied, K., 2014. Palynological record of the Early Permian Postglacial climate amelioration (Karoo Basin, South Africa). Palebio. Paleoenv, 94, 229-235.

Götz, A., Hancox, P. J., Lloyd, A., 2017. Permian climate change recorded in palynomorph assemblages of Mozambique (Moatize Basin, eastern Tete Province). Acta Paleobotanica 57(1), 3-11.

Götz, A., Hancox, P. J., Lloyd, A., 2018. Southwestern Gondwana's Permian climate amelioration recorded in coal-bearing deposits of the Moatize sub-basin (Mozambique). Palaeoworld, https://doi.org/10.1016/j.palwor.2018.08.004

Grantham, G.H., Macey, P.H., Ingram, B.A., Roberts, M.P., Armstrong, R.A., Hokada, T., Shiraishi, K., Jackson, C., Bisnath, A., Manhiça, V., 2008. Terrane correlation between Antarctica, Mozambique and Sri Lanka; comparisons of geochronology, lithology, structure and metamorphism and possible implications for the geology of southern Africa and Antarctica. In: Satish-Kumar, M., Motoyoshi, Y., Osanoi, Y., Hiroi, Y., Shiraishi, K. (Eds.), Geodynamic Evolution of East Antarctica: a Key to the East-west Gondwana Connection, vol. 308. Geological Society, London, Special Publication, 91-119.

GTK Consortium, 2006. Map Explanation; Volume 2: Sheets 1631 - 1934. Geology of Degree Sheets, Mecumbura, Chioco, Tete, Tambara, Guro, Chemba, Manica, Catandica, Gorongosa, Rotanda, Chimoio and Beira, Mozambique. Ministério dos Recursos Minerais, Direcção Nacional de Geologia, Maputo.

Hancox, P. J., 2016. The Coalfields of South-Central Africa: a Current Perspective. Episodes, 39(2), 407-428.

Hankel, O., 1994. Early Permian to Middle Jurassic rifting and sedimentation in East Africa and Madagascar. Geol. Rundsch. 83, 703-710.

Hillier, S. and Marshall, J., 1988. A rapid technique to make thin sections of sedimentary organic matter concentrates. Journal of Sedimentary Petrology, 58, 754-755.

Hunt, J.M., 1996. Petroleum Geochemistry and Geology. W.H. Freeman and Co., 742 p.

International Committee for Coal and Organic Petrology, 1998. The new vitrinite classification (ICCP System 1994). Fuel, 77, 349-358.

Isbell, J.L., Cole, D.I., Catuneanu, O., 2008. Carboniferous-Permian glaciation in the main Karoo Basin, South Africa: stratigraphy, depositional controls, and glacial dynamics. In: Fielding, C.R., Frank, T.D., Isbell, J.L. (Eds.), Resolving the Late Palaeozoic Ice Age in Time and Space. Geological Society of America Special Paper, 441, 71-82.

ISO 7404-5, 2009. Methods for the Petrographic Analysis of Coal, Part 5: Methods of Determining Microscopically the Reflectance of Vitrinite. International Organization for Standardization, Geneva, Switzerland, p. 14.

ISO 11760, 2018. Classification of coals. International Organization for Standardization, Geneva, Switzerland, 2nd ed., p. 9.

Jamal, D.L., 2005. Crustal Studies across Selected Geotransects in NE Mozambique: Differentiating between Mozambican (Kibaran) and Pan African Events, with implications for Gondwana Studies. University of Cape Town, unpublished Ph.D. thesis, Cape Town, South Africa.

Johnson, M.R., van Vuuren, C.J., Hegenberger, W.F., Key, R., Shoko, U., 1996. Stratigraphy of the Karoo Supergroup in Southern Africa: an overview. Journal of African Earth Sciences, 23(1), 3-15.

Kreuser, T. and Woldu, G., 2010. Formation of euxinic lakes during the deglaciation phase in the Early Permian of East Africa. In: Late Paleozoic Glacial Events and Postglacial Transgressions in Gondwana, Oscar R. López-Gamundí (Ed.). Geological Society of America Special Paper, 468, 101-112.

Lächelt, S., 2004. Geology and Mineral Resources of Mozambique. Direcção Nacional de Geologia, Maputo, 515 p.

Lakshminarayana G., 2015. Geology of Barcode type coking coal seams, Mecondezi sub-basin, Moatize Coalfield, Mozambique. International Journal of Coal Geology, 146, 1-13.

Lopes, G., Pereira, Z., Fernandes, P., Marques, J., 2014. Datação palinológica dos sedimentos glaciogénicos da Formação Tilítica de Vúzi, sondagem ETA 65, Bacia Carbonífera de Moatize-Minjova, Moçambique: resultados preliminares. Comunicações Geológicas, 101, Especial I, 481-484

Mackowsky, M.T., 1982. Rank determination by measurement of reflectance of vitrinites. In: Stach, E., Mackowsky, M., Teichmuller, M., Taylor, G., Chandra, D., Teichmuller, R. (Eds.), Stach's Textbook of Coal Petrology, third ed. Gebrüder Borntraeger, Berlin and Stuttgart, 319-329.

Mariño, J, Marshak, S., Mastalerz M., 2015. Evidence for stratigraphically controlled paleogeotherms in the Illinois Basin based on vitrinite-reflectance analysis: Implications for interpreting coal-rank anomalies. Amer. Assoc. Petrol. Geol. Bulletin, 99(10), 1803-1825.

McPhilemy, B., 1988. The value of fluorescence microscopy in routine palynofacies analysis: Lower Carboniferous successions from Counties Armagh and Roscommon, Ireland. Review of Palaeobotany and Palynology, 56, 345-359.

Mendonça Filho, J.G., Araujo, C.V., Borrego, A.G., Cook, A., Flores, D., Hackley, P., Hower,

J.C., Kern, M.L., Kommeren, K., Kus, J., Mastalerz, M., Mendonça, J.O., Menezes, T.R., Newman, J., Ranasinghe, P., Souza, I.V.A.F., Suarez-Ruiz, I., Ujiié. Y., 2010. Effect of concentration of dispersed organic matter on optical maturity parameters: Interlaboratory results of the organic matter concentration working group of the ICCP. International Journal of Coal Geology, 84, 154-165.

Middleton, M.F., 1982.Tectonic history from Vitrinite Reflectance. Geophysical Journal of Royal Astronomical Society, 68, 121-132.

Montesi, G., 2016. Palynology and Organic Maturation studies of Permian Succession in the Moatize - Minjova Basin (N'Condédzi sub-basin, Karoo Supergroup, Mozambique) and the Zagros Basin (Iran). University of Perugia, unpublished MSc thesis, 123 p.

Mugabe, J.A., 1999. Karoo Deposits of Zambezi Graben - Moatize e Tete City Mozambique; Sedimentary Facies Distribution and Palynological Approach. Univ. Utrecht, unpublished Ph.D. thesis. 297 p.

Norconsult Consortium, 2007. Notícia Explicativa: Folhas 1039 Muidine, 1040 Palma, 1134 Ponta Messuli, 1135 Lupilichi, 1136 Milepa, 1137 Macalange, 1138, Negomano, 1139 Mueda, 1140 Mocímboa da Praia, 1234 Metangula, 1235 Macaloge-Chiconono, 1236 Mavago, 1237 Mecula, 1238 Xixano, 1239 Meluco, 1240 Quissanga-Pemba, 1334 Meponda, 1335 Lichinga, 1336 Majune, 1337 Marrupa, 1338 Namuno, 1339 Montepuez, 1340 Mecúfi, 1435 Mandimba, 1436 Cuamba, 1437 Malema, 1438 Ribáuè-Mecubúri, 1535 Insaca, 1536 Gúruè, 1635

Milange e 1636 Lugela-Mocuba, Moçambique. Direcção Nacional de Geologia, Ministério dos Recursos Minerais, Maputo.

Paterson, N.W.; Mangerud, G., Holen, L. H., Landa, J., Lundschien, B. A., Eide, F., 2018. Late Triassic (early Carnian–Norian) palynology of the Sentralbanken High, Norwegian Barents Sea. Palynology. doi: https://doi.org/10.1080/01916122.2017.1413018

Pearson, D. L., 1984. Pollen/Spore Color Standard, version No.2 Phillips Petroleum, Exploration Project Section. Bartelsville, Oklahoma.

Pereira, Z., Lopes, G., Fernandes, P., Marques, J., 2014. Estudo palinoestratigráfico da sondagem ETA 72 do Karoo Inferior da Bacia de Moatize, Moçambique - Resultados Preliminares. Actas do IX Congresso Nacional de Geologia/2º Congresso de Geologia dos Países de Língua Portuguesa, Porto, Portugal, 6 p..

Pereira, Z., Fernandes, P., Lopes, G., Marques, J., Vasconcelos, L. 2016. The Permian-Triassic transition in the Moatize-Minjova Basin, Karoo Supergroup, Mozambique: a Palynological Perspective. Review of Palaeobotany and Palynology, 226, 1-19.

Pinna, P., Jourde, G., Calvez, J.Y., Mroz, J.P., Marques, J.M., 1993. The Mozambique Belt in northern Mozambique: Neoproterozoic (1100-850 Ma) crustal growth and tectogenesis, and superimposed Pan-African (800-550 Ma) tectonism. Precambrian Research, 62, 1-59.

Price, L., 1983. Geological time as a parameter in organic methamorphism and vitrinite reflectance as an absolute paleogeothermomether. Journal of Petroleum Geology, 6, 5-38.

Real, F., 1966. Geologia da Bacia do Rio Zambeze (Moçambique). Características geológico-mineiras da Bacia do Rio Zambeze em território moçambicano. 183 p., 57 Plates; 2 Maps. Junta de Investigações do Ultramar. Lisboa.

Robert, P., 1988. Organic Metamorphism and Geothermal History. Elf-Aquitane and Reidel Publishing, Dordrecht, 311 p.

Silva, G.H., Barreto, L.S., Carvalho, L.H.B., 1967. *Dadoxylon nicoli* (Seward) do Karoo de Tete. Revista Est. Ger. Univ. Moçambique, 4. Série VI, Ciências Geológicas, 156pp., Lourenço Marques, Moçambique.

Staplin, F.L., 1982. How to assess maturation and palaeotemperatures: Introduction. In: Staplin, F.L., *et al*. (Eds.), How to Assess Maturation and Palaeotemperatures, pp. 1 and 5. Society of Economic Paleontologists and Mineralogists, Short Course No.7.

Suárez-Ruiz, I., Flores, D., Mendonça Filho, J.G., Hackley, P.C., 2012. Review and update of the applications of organic petrology: Part 1, geological applications. International Journal of Coal Geology, 99, 54-112.

Taylor, G.H., Teichmuller, M., Davis, A., Diessel, C.F.K., Littke, R., Robert, P., 1998. Organic Petrology. Gebruder Borntraeger, Berlin, p. 704.

Formatted: English (United Kingdom)

Thonnard, R., 1971/1972. Le graben de Moatize au Mozambique. Bulletin Séances, Académie Royale Sciences Outre-Mer, Bruxelles, 2.

Tissot, B. and Welte, D. H.,1978. Petroleum Formation and Occurrence: A new approach to oil and gas exploration. Springer-Velag Berlin.

Van Gijzel, P., 1979. Manual of the Techniques and Some Geological Applications of Fluorescence Microscopy. American Association of Stratigraphical Palynologists Foundation, Dallas.

Vasconcelos, L., 1995. Contribuição para o conhecimento dos carvões da Bacia Carbonífera de Moatize, Província de Tete, República de Moçambique. Tese de Doutoramento. Texto (Volume I), Tabelas, Figuras, Estampas (Volume II). Faculdade de Ciências, Universidade do Porto, Porto, Portugal.

Vasconcelos, L., 2000. Overview of the Moatize coal basin geology, Tete Province, Republic of Mozambique. Chron. Rech. Minière, Orléans, 538, 47-58.

Vasconcelos, L., 2013. Coal deposits in Mozambique an overview. Presentation at FFF Mozambique coal conference, October 2013 - Johannesburg, South Africa.

Viola, G., Henderson, I.H.C., Bingen, B., Thomas, R.J., Smethurst, M.A., Azevedo, S., 2008. Growth and collapse of a deeply eroded orogen: Insights from structural and geochronological constraints on the Pan-African evolution of NE Mozambique. Tectonics 27, TC5009.

Visser, J.N.J., 1989, The Permo-Carboniferous Dwyka Formation of Southern Africa; deposition by a predominantly subpolar marine ice sheet: Palaeogeography, Palaeoclimatology, Palaeoecology, v. 70, p. 377–391.

Figure Captions

Figure 1. Simplified geology of the Tete Province, Mozambique, with the location of Karoo basins of the Zambezi River valley and the N'Condédzi, Moatize and Muarádzì sub-basins. Adapted from Geological Map of Mozambique, Direcção Nacional de Geologia, Maputo (2006).

Figure 2. Simplified geology of N'Condédzi sub-basin showing the location of the studied boreholes. Map adapted from Geological Map of Mozambique, sheet no. 1533/1534, Cazula / Zóbuè, Geological Series 1/250000, Direcção Nacional de Geologia, Maputo, 2006.

Figure 3. Lithological log and vitrinite reflectance profile of borehole ZSA-32. The key to lithologies is the same as used in figures 3 to 9.

Figure 4. Lithological log, vitrinite reflectance profile and selected palynomorphs illustrating the variation of TAI of borehole A1TR-018.

Figure 5. Lithological log and vitrinite reflectance profile of borehole TGDH(C)005.

Figure 6. Lithological log, vitrinite reflectance profile and selected palynomorphs showing the range of TAI values and spore/pollen fluorescence of borehole A1TM-085.

Figure 7. Lithological log, vitrinite reflectance results and selected palynomorphs showing the range of TAI values and spore/pollen fluorescence of borehole CIMT-014.

Figure 8. Lithological log and vitrinite reflectance results and selected palynomorphs showing the range of TAI values and spore/pollen fluorescence of borehole A1TM-039.

Figure 9. Lithological log and vitrinite reflectance profile of borehole A1TM-058.

Figure 10. Selected palynomorphs showing the range of TAI values and spore/pollen fluorescence of boreholes A1TM-058 and TDGH(C)005.

Figure 11. Some examples of vitrinite grains found and measured in this study. Above each photograph of vitrinite grains is indicated the borehole, sample reference and the %Ro measured for that particular vitrinite grain, (vitrinite grains were chosen to illustrate grains with %*Ro* values close to the mean %*Ro* value of the sample).

Figure 12. Differences observed in transmitted and fluorescent light between the indigenous and recycled palynomorphs assemblages in borehole CIMT-014: a.) sp. reworked Permian spore (*Leiotriletes directus*) showing no fluorescence (a.1) and pl. Upper Triassic pollen

(*Platysaccus queenslandi*) showing yellow fluorescence colour (a.1), sample MQ115; b.) sp. reworked Permian spore (*Polycingulatisporites* sp.) showing no fluorescence (b.1) and pl. unidentified pollen grain, possible Upper Triassic age, showing yellow fluorescence colour (b.2), sample MQ115; c.) sp. Upper Triassic spore (*Rogalskaisporites cicatricosus*) showing strong yellor fluorescence colour (c.1) and sp.1, sp.2, sp.3 reworked Permian spores showing weak fluorescence or no fluorescence (c.1), sample MQ111; d.) sp. reworked Permian spore (*Densoisporites* sp.) showing no fluorescence (d.1) and pl. two unidentified pollen grains, possible Upper Triassic age, showing strong yellow fluorescence colour (d.1), sample MQ111.

Figure 13. Calculated palaeogeothermal gradients for the boreholes studied. For boreholes A1TM-039 and CIMT-014 due to the reduced number of samples with VR results palaeogeothermal gradients were not calculated.

Figure 14. Schematic cross-sections illustrating the tectonic and thermal evolution of the Permian - Triassic Karoo rocks of the N'Condédzi sub-basin. Figures not to scale. (**a**) Late Guadalupian: extensional basin initiation by the tectonic reactivation of Precambrian shear zones, forming half-graben sedimentary basins. (**b**) Late Lopingian to Lower Triassic: fault-induced subsidence and deposition of very thick sequences (>1000 m). Beginning of hot diagenetic fluid flow driven only by lithostatic pressure. **(c)** Upper Triassic: after a phase of non-deposition during the Middle Triassic, deposition of Upper Triassic red beds together with reworked Permian palynomorphs from the neighbouring Karoo basins, re-burial of the Permian – Lower Triassic sequences. (**d**) Schematic cross-section of the N'Condédzi region showing the position of some of the boreholes studied.

Table 1. Organic maturation results and palaeotemperatures (°C) calculated using method

described by Barker (1988) for the boreholes of the N'Condédzi sub-basin. All samples are black carbonaceous mudstones or black/grey mudstones. R_O (%) - vitrinite reflectance values, SD - standard deviation, Fluo. - spore fluorescence colours (Y – yellow, DY – dark yellow, DO - dark orange, R - red), spore colour TAI - Thermal Alteration Index, * - samples with vitrinite reflectance values due to heating effects of dolerite intrusions (details in Table 2), and TAI Reworked / Fluo. Reworked, refers to the reworked palynomorph population of boreholes CIMT-014 and A1TM-039.

Table 2. Vitrinite reflectance values of the dolerite heat affected samples, showing also its relations to the dolerite sills, namely the distance of the samples to the nearest intrusion wall and the thickness of the nearest intrusion (distance in metres).

Thermal history and basin evolution of the Moatize - Minjova Coal Basin (N'Condédzi sub-basin, Mozambique) constrained by organic maturation levels

Francesca Galasso[1,2]*, Paulo Fernandes[2], Giovanni Montesi[1], João Marques[3], Amalia Spina[1], Zélia Pereira[4]

1. Department of Physics and Geology, University of Perugia.Via Pascoli, 06123 Perugia, Italy
2. Centro de Investigação Marinha e Ambiental (CIMA), Universidade do Algarve, Campus de Gambelas, 8005-139 Faro, Portugal
3. Gondwana Empreendimentos e Consultorias, Limitada, Rua B, no. 233, Bairro da COOP, Caixa Postal 832, Maputo, Mozambique
4. Laboratório Nacional de Energia e Geologia (LNEG), Rua da Amieira, Apartado 1089, 4466-901 S. Mamede Infesta, Portugal

* Corresponding author: francescagalasso1992@gmail.com

Abstract

Kerogen concentrates obtained from Lopingian (Late Permian) to Upper Triassic mudrock lithologies of seven coal exploration boreholes, drilled in the Moatize – Minjova Coal Basin (N'Condédzi sub-basin, Mozambique), were studied by means of vitrinite reflectance (VR), spore fluorescence and spore colour, in order to constrain the thermal history and basin evolution by organic maturation levels. VR increases with depth, indicating organic maturation related to sediment burial for most of the boreholes. Modelled VR data indicate a

regional palaeogeothermal gradient between 35 and 40ºC/km. Lower Jurassic doleritic intrusions observed in three boreholes had only local thermal effects without affecting the regional palaeogeothermal gradient. Two boreholes located near the basin margin show high palaeogeothermal gradients suggesting thermal processes other than heating due to burial were involved. These processes may have involved hot diagenetic fluids circulating through fault zones and/or permeable lithologies, locally elevating geothermal gradients. Circulation of these fluids was induced by lithostatic pressure due to rapid rates of sedimentation. These high sedimentation rates lead to the accumulation of a thick succession (over 2000 m) of Lopingian (Late Permian) to Upper Triassic siliciclastic sediments. All the organic maturation indices measured and the age of the successions indicate that organic maturation occurred during or after Late Triassic times. However, the presence of reworked Permian palynomorphs into Upper Triassic sediments and the absence of Middle Triassic sediments indicate an exhumation and erosion of Permian strata in Middle Triassic times. The organic maturation levels of the reworked palynomorph population are considerably higher than the indigenous Upper Triassic population, indicating that they attained higher burial temperatures prior to being reworked.

Keywords: Karoo, Mozambique, Organic maturation, Permian – Triassic, Reworked palynomorphs, Moatize – Minjova Coal Basin, Vitrinite Reflectance

1. Introduction

The Karoo Supergroup (KSG) of Southeastern Africa comprises sedimentary and volcanic rock units that span a time interval of Late Carboniferous to Early Jurassic, and which attained a considerable thickness (more than 7000 m) in some basins (Johnson et al., 1996; Cairncross, 2001; Catuneanu et al., 2005). Regardless of tectonic processes related to individual basin formation and subsequent geological development the stratigraphy of the KSG is very consistent across all basins where it is preserved (Johnson et al., 1996; Catuneanu et al., 2005, Hancox, 2016). The sedimentary successions reflect major palaeogeographical and climatic changes during the development of the Karoo basins (Catuneanu et al., 2005; Götz and Ruckwied, 2014; Götz et al., 2017). In central-west Mozambique, sediments of the KSG are well represented in various basins situated along the Zambezi River valley in the Tete Province (GTK Consortium, 2006) (Fig. 1). In these basins the KSG, normally, rests unconformably over crystalline Precambrian basement rocks, and the base of the stratigraphic succession consists of conglomerates and mudrocks of the Dwyka Group (Pennsylvanian to Cisuralian) comparable to the Main Karoo Basin of South Africa. These conglomerates were, deposited by waning and waxing of glaciers of the Late Palaeozoic glaciations of Gondwana (Visser, 1989, Isbell et al., 2008). The northward drift of Gondwana to lower latitudes during the Permian, caused more temperate climate conditions to establish throughout this paleocontinent. Glaciation was terminated by late Palaeozoic times and in basins located north of the Main Karoo Basin (South Africa), sedimentation mostly took place in continental environments characterized by river systems and freshwater lakes (Cairncross, 2001; Kreuser and Woldu, 2010; Götz and Ruckwied, 2014). The sedimentary record of these times corresponds to the siliciclastic-dominated, coal-bearing lithologies of the Cisuralian to Guadalupian Ecca Group (Cairncross, 2001; Catuneanu et al., 2005, Hancox, 2016). At present, the existence of widespread coal seams interbedded in the Ecca Group stratigraphic

74 sequence, represents an important natural resource and asset for Mozambique's economy
75 (Vasconcelos, 2000, 2013). Overlying the Ecca Group are siliciclastic-dominated stratigraphic
76 sequences belonging to the Beaufort Group (Lopingian - Middle Triassic) and the Stormberg
77 Group (Late Triassic - Early Jurassic). The sediments of these two groups were deposited by
78 major river systems or aeolian processes in desert environments under hot and arid climatic
79 conditions (Johnson et al., 1996; Catuneanu et al., 2005). The contact between the Beaufort
80 Group and the overlying Stormberg Group corresponds to a hiatus that spans most of the
81 Middle Triassic (Catuneanu et al., 2005). The KSG is capped by the Lower Jurassic volcanic
82 rocks (*ca.* 183 Ma) of the Drakensberg Group, which are related to the Karoo - Ferrar Large
83 Igneous Province and pre-date the break-up of Gondwana (Duncan et al., 1997).
84
85 Thermal history analysis is an essential part of any study of sedimentary basins and their
86 hydrocarbon source rock potential. There are several optical methods that can be used to
87 estimate maximum temperatures attained by strata during subsidence and interpret their
88 thermal history (Price, 1983). Vitrinite reflectance (VR) is an optical method considered to be
89 a reliable indicator of the organic matter maturity levels of sedimentary rocks (Hunt, 1996;
90 Robert, 1988; Tissot and Welte, 1978). Since maturity levels are largely related to
91 temperature, VR is also a good indicator of peak (palaeo-) temperatures, which accounts for
92 its widespread use in basin analysis (Middleton, 1982; Corcoran and Clayton, 2001;
93 Fernandes et al., 2012, 2013, 2015; Mariño et al., 2015). Other optical methods, such as spore
94 colour (TAI) and spore fluorescence provide a rapid evaluation of organic maturation levels,
95 complementing the information attained by VR (Van Gijzel, 1979; McPhilemy, 1988; Suárez-
96 Ruiz et al., 2012). Fernandes et al. (2015) studied the thermal history of the Lopingian KSG
97 sediments of the Moatize – Minjova Coal Basin combining VR and Apatite Fission Track
98 Analysis (AFTA) of two boreholes located in the Moatize sub-basin (Fig. 1). These authors

99 concluded that maturation levels corresponded to a coal rank of medium rank B and A coals
100 (1.3 - 1.7%*Ro*). Maturation levels increase linearly downhole in the two studied boreholes,
101 indicating that burial with a constant geothermal gradient was the main process controlling
102 peak temperature. The thermal model for the history of the basin proposed by Fernandes et al.
103 (2015), indicates that peak burial temperatures were attained shortly (3 - 10 Ma) after
104 deposition in Lower Triassic times. The thermal model also indicates two episodes of cooling
105 and exhumation: a first period of rapid cooling between 240 and 230 Ma (Middle– Late
106 Triassic boundary) implying 2500 - 3000 m of denudation; and a second period, also of rapid
107 cooling, from 6 Ma (late Miocene) onwards implying 1000 - 1500 m of denudation.
108
109 In the present work, a detailed account of the organic maturation levels assessed by different
110 optical methods (VR, spore colour and spore fluorescence) of seven boreholes drilled for coal
111 exploration is described. The boreholes are located in the N'Condédzi sub-basin of the
112 Moatize – Minjova Coal Basin (Figs. 1 and 2). This study allowed the evaluation of the
113 maturity of organic matter and the thermal history of the KSG sedimentary succession in the
114 N'Condédzi region, and helps to constrain the tectonic model for the development of the
115 Karoo Basin in this region.
116
117 **2. Geological setting of the Moatize – Minjova Coal Basin in the N'Condédzi sub-basin**
118 Differences in the stratigraphy, tectonic setting and geographic position of KSG outcrops
119 along the Zambezi river valley in Mozambique, allow their division into three different coal-
120 bearing basins, which are, from west to east, the Chicôa – Mecúcoè, Sanângoè – Mefidézi and
121 the Moatize – Minjova Coal Basins, respectively (Lächelt, 2004; GTK Consortium, 2006)
122 (Fig. 1). These basins are part of a network of rift related basins that formed north of the
123 South African Main Karoo Basin, during the Permian to Lower Jurassic time interval. The

Zambezi River valley basins developed during brittle reactivation of high strain zones (e.g. the Sanângoé and Mzarabani shear zones) (Fig. 1) of the Zambezi Belt. This mobile belt formed between the Congo and Kalahari Cratons during the Pan-African Orogeny (620 – 530 Ma) (Carvalho, 1977; Afonso, 1984; Pinna et al., 1993; Jamal, 2005; GTK Consortium, 2006; Norconsult Consortium, 2007; Grantham et al., 2008; Viola et al., 2008). The tectonic fault-related reactivation started in the Cisuralian (early Permian) by the initiation of strike-slip faulting under a transtensional stress regime that formed extensional basins with a graben to half graben geometry (Carvalho, 1977; Hankel, 1994; Lächelt, 2004; Catuneanu et al., 2005; GTK Consortium, 2006).

The boreholes used in this study were drilled in the N'Condédzi sub-basin of the Moatize-Minjova Coal Basin, which is approximately 50 km long and 25 km wide, and is located *ca*. 70 km northeast of Tete City (Figs 1 and 2). Its margins are faulted against the Mesoproterozoic Tete Suite (Gabbro-Anorthosite) to the SW and the Mesoproterozoic gneiss and granite rocks of the Furancungo Suite to the N by the WNW –ESE trending Mwanza Fault.

The complete Karoo stratigraphic succession of the Moatize - Minjova Coal Basin is thicker than 800 m (Real, 1966; Thonnard, 1971/1972; Afonso, 1975; Vasconcelos, 1995; Mugabe, 1999; Lächelt, 2004; GTK Consortium, 2006), whereas in the N'Condédzi sub-basin Lakshminarayana (2015), a Lower Karoo succession with a thickness of more than 900 m is reported. The base of the succession consists of the tillites of the Vúzi Formation, which overly unconformably Precambrian basement rocks. However, the type section for this formation was defined in the area of the Mucanha and Vúzi Rivers (Carvalho, 1977) belonging to the Chicôa-Mecúcoè Basin, located upstream in the Zambezi River valley (Fig.

1). In the Mucanha-Vúzi area, the Vúzi Formation consists of 10 m-thick ill-bedded matrix supported red conglomerates that are conformably overlain by 10 m-thick mud supported grey-black conglomerates. Due to the lack of conclusive evidences of glacial action (transport and deposition), such as, striations on surfaces of the basement rocks and on surfaces of the clasts in the conglomerates, and dropstones and varve-like sedimentary rhythms, Carvalho (1977) interpreted these conglomerates, not as glacial deposits, but probably as coarse alluvial fans. These coarse clastic beds were probably deposited at the base of, and adjacent to, fault scraps, where the topographic relief was created by vertical fault movements coeval to the formation of the Karoo rift basins. Recently, a *ca.* 130 m thick succession of the Vúzi Formation, cropping out in the Murrongódzi River, was described in the Moatize - Minjova Basin by Achimo et al. (2014). The bulk of the succession consists of ill-sorted matrix-supported conglomerates showing typical features of glacial to sub-glacial transport and deposition, interpreted as being formed by the advance and retreat of ice caps over lakes and fluvio-glacial plains. From the description of the Vúzi Formation in the different Karoo basins of the Zambezi River valley, it is evident that it was deposited in a variety of sedimentary environments and tectonic conditions, which require further research in order to ascertain the relations between different processes and, possibly, the age and *tempus* of the accumulation of the sediments.

The coal-bearing Moatize Formation conformably overlies the Vúzi (Tillite) Formation and consists of interbedded carbonaceous mudstones, siltstones, sandstones and coal beds interpreted as fluvial and lacustrine sediments deposited under wet temperate climatic conditions. In the Moatize region, the formation attains a thickness of *ca*. 300 - 400 m (Real, 1966; Afonso, 1976; GTK Consortium, 2006) and has six main coal seams, which are known locally as “Carbonaceous Complexes.” These “Complexes” consist of interbedded plant-rich

carbonaceous mudstones and coal beds of variable thickness. Palaeoassemblages (plant macrofossils and palynomorphs) suggest Cisuralian-Guadalupian (Early to Middle Permian) age for the upper part of the Moatize Formation, correlated with the Middle-Late Permian age Ecca Group of the Main Karoo Basin in South Africa (Daber, 1984). However, recent palynological revision of the upper part of the Moatize Formation that was penetrated by two coal exploration boreholes (DW123 and DW132) indicates that this part of the Moatize Formation reaches the latest Permian, with the Permian-Triassic boundary identified at *ca.* 42 m depth in borehole DW132 (Pereira et al. 2016).

The Moatize (Sandstone) Formation is overlain by a thick sequence (*ca.* 4 km) of siliciclastic rocks divided into two stratigraphic units, the Matinde (Marl-Sandstone) Formation at the base, and the Cádzi (Sandstone) Formation at the top (GTK Consortium, 2006). Both formations were deposited in fluvial to possibly desert environments, recording the transition from seasonal temperate to hot arid climatic conditions. Due to the lack of biostratigraphic markers in both formations, the Matinde Formation is correlated to the Middle-Upper Ecca Group of the Main Karoo Basin of South Africa (Silva et al., 1967), whereas the Cádzi Formation is correlated with the Beaufort Group of the same basin. With the exception of few 1 - 3 m thick doleritic dykes and sills that intrude the sedimentary formations, the volcano-sedimentary lithologies of Lower Jurassic age that capped the KSG, and are correlated with the Stormberg Volcanics of the Main Karoo Basin, are not well represented in the Moatize-Minjova Coal Basin (Vasconcelos, 1995).

Lakshminarayana (2015) compared the stratigraphic succession of the KSG in the N'Condédzi sub-basin with the succession described for the Moatize sub-basin. The Vúzi Formation rests unconformably on gabbros and anorthosites of the Mesoproterozoic Tete

Suite. The Vúzi Formation consists of clast-supported conglomerates interbedded with sandstones, siltstones and carbonaceous shales forming thinning and fining upward cycles. The top part of the Vúzi Formation is characterized by a sequence known as the *Transitional Assemblage* consisting of sandstones, interbedded with carbonaceous shales and coal beds. This formation is *ca*. 60 – 140 m thick. The succeeding Moatize Formation attains a maximum of 900 m thick in the N'Condédzi sub-basin and consists of interbedded meter thick coal seam, sandstones, siltstones and carbonaceous shales. No new biostratigraphic information was provided by Lakshminarayana (2015) on the age of the Vúzi and Moatize formations in this sub-basin and, therefore, this author correlated these formations with the Pennsylvanian (Late Carboniferous) to Cisuralian (early Permian) Dwyka Group and the Permian Ecca Group, respectively.

3. Materials

The samples analysed in this study were obtained from seven coal exploration boreholes drilled in the N'Condédzi sub-basin (Fig. 2). Black carbonaceous shales, black shales, grey mudstones and grey siltstones, were the main lithologies sampled for organic maturation studies. Coal was not sampled because it was not present in the cores during the sampling. The coal seams were sampled earlier by the exploration companies that owned the mining rights of the area, and shipped to laboratories to assess its quality. The boreholes studied were chosen in order to represent all the stratigraphic units of the KSG present in the N'Condédzi sub-basin. Five of the boreholes studied intersected the basement at different depths, representing the coal bearing units that characterize the lower units of the stratigraphy (Moatize Formation), whereas two boreholes penetrated the *ca*. 500 m thick successions consisting mainly of red bed lithologies that represent the upper stratigraphic units (Matinde and Cádzi formations) of the KSG in sub-basin. One hundred and seventy two samples of the

lithologies indicated were processed for organic maturity analysis and palynology studies. One hundred and one samples yielded organic material suitable for these studies, however, seventy-one samples from boreholes A1TR-018, A1TM-039, TGDH(C)005 and CIMT-014 were barren.

3.1. Borehole ZSA-32

This borehole is located near the southern margin of the Karoo outcrop in the N'Condédzi sub-basin (Fig. 2). It has a total depth of 220 m, and penetrated at its base a 5 m thick sequence of the basement rocks of the Tete Suite, consisting of gabbros (Fig. 3). The latter lithologies are unconformably overlain by a 3 m thick bed of clast-supported conglomerates intercalated with very thin beds red siltstones and mudstones, positioned immediately above the unconformity. These red lithologies caused the red staining of the altered gabbros below the unconformity. These two features, red stain of the basement and red lithologies, are more compatible with deposition under oxidizing sub-aerial conditions, rather than glacial to peri-glacial environments of the Dwyka time. The succession in the borehole interval from 209 m to 180 m, consists of black carbonaceous shales capped by a 2 m thick coal bed. This is followed by an interval from 180 m to 62 m, characterized by coarse to medium grained sandstones interbedded with shales and siltstones and some coal beds. A 10 m thick coal bed caps the latter borehole interval. The upper part of the borehole from 50 m to the top of the borehole consists of sandstones interbedded with siltstones and shales. The succession in this borehole is also intruded by several doleritic sills (Fig. 3).

3.2. Borehole A1TR-018

Borehole A1TR-018 was drilled to a total depth of *ca*. 91 m, and penetrated Karoo sediments overlying crystalline basement rocks represented by gabbros of the Tete Suite at *ca*. 85 m

depth (Fig. 4). This borehole is located only 1 km (direction) from the outcrop, which includes the contact between the Tete Suite and Karoo Supergroup in the N'Condédzi sub-basin (Fig. 2). A 1 m clast-supported conglomerate bed unconformably overlies the Precambrian basement. The conglomerate grades upward into a 4 m thick bed of carbonaceous shales, followed upwards by *ca.* 6 m thick sandstone-siltstone dominated interval and a 4 m thick clast-supported conglomerate interval interbedded with very thin beds of shale. The upper part of the core consists of a 70 m sequence dominated by sandstones and siltstones beds interbedded with thin to very thin beds of shales, followed upward by a 10 m thick shale dominated interval.

3.3. Borehole TGDH(C)005

This borehole was drilled in a small outcrop area of the Karoo Supergroup surrounded by the Mesoproterozoic Tete Suite (Fig. 2). It has a total depth of *ca*. 230 m and penetrated, an 11 m thick sequence of basement rocks consisting of anorthosites (Fig. 5) at the base. These are unconformably overlain by about 38 m of coarse- to medium-grained sandstone and siltstone beds interbedded with thin to very thin beds of shales belonging to the KSG. This situation indicates the absence of the conglomerate beds that usually characterize the base of the KSG, in the Moatize and in other Karoo basins, suggesting that the base of Karoo Supergroup is diachronous in this sub-basin. The latter sandstone-siltstone interval is followed by approximately 70 m of dominantly siltstones and shales with thin beds of coal concentrated in the 162 – 168 m and 110 – 123 m depth intervals. In the interval between 98 m and 68 m, coarse- to medium-grained sandstone beds are interbedded with very thin beds of siltstones and shales. The interval from 68 m depth up to the top of the core consists of shales, carbonaceous shales and several thin beds of coal, typical of barcode coals.

3.5. Borehole A1TM-085

This borehole has a total depth of ca. 727 m and penetrated a 2 m thick sequence of basement rocks consisting of anorthosites belonging to the Tete Suite at its base (Fig. 6). The basement rocks are unconformably overlain by about 55 m of clast to matrix support conglomerates interbedded with siltstones, sandstones, and shales. Approximately 160 m of dominantly shales, carbonaceous shales, siltstones and thin beds of coals follow the latter conglomerate dominant interval. A coarser-grained interval consisting of siltstones, medium- to coarse-grained sandstones and thin beds of shales are positioned between approximately 415 m and 282 m depth. From 282 m to 18 m depth the succession consists of shales, carbonaceous shales and several thin beds of coal. The top, 18 m of this core consists of coarse- to medium-grained sandstones. The succession in this core is intruded by dolerite sills concentrated in the depth interval between 340 m and 90 m. The sill thickness is 1 – 2 m on average but at approximately 160 m, a conspicuous 12 m thick doleritic sill occurs that caused sufficient heating to affect the VR results (section 5).

3.4. Borehole CIMT-014

This borehole has a total depth of 500 m and mostly consists of siliciclastic red bed lithologies (Fig. 7). The top of the Mesoproterozoic basement was not penetrated. From the base to 470 m, the succession changes in both lithology and sedimentary features. This basal 30 m thick succession consists of medium- to coarse-grained grey sandstones interbedded with laminated grey siltstones and carbonaceous shales, the red sediment colours, which is characteristic for most of the core is absent in this basal interval. Two prominent coarse-grained sandstone dominant intervals are present, the first between 310 m and ca. 470 m, and the second between 210 m and 260 m depth. These intervals consist of coarse-grained (sometimes

conglomeratic) to medium-grained red sandstones interbedded with red to brown mudstones and siltstones. The interval from 310 m and 260 m depth of the is characterized by fine-grained lithologies dominated by red mudstones interbedded with thin beds of grey mudstones and brown siltstones, with few beds of coarse-to medium-grained red sandstones. Another fine-grained dominated interval with the same lithological features is found between 210 m depth and the top of the borehole.

3.6. Borehole A1TM-039

This borehole was drilled to total depth of *ca*. 600 m, and consists mainly of red siliciclastic lithologies (Fig. 8). This succession exhibits many lithological similarities with borehole CIMT-014. However, it differs by a higher dominance of coarse-grained siliciclastic rocks. Accordingly, from the base to 470 m depth, the succession is dominated by red to brown siltstone beds interbedded with red mudstones and few thin beds of grey mudstones and red sandstones, whereas the interval between 470 m and 350 m is characterized by thick, red to purple sandstone beds. Between 350 m and the top of the core, the succession consists of thick beds of coarse- to medium-grained red sandstones intercalated with thick beds of brown siltstones and red mudstones.

3.7. Borehole A1TM-058

With a total depth of 1000 m, borehole A1TM-058 (Fig. 9) is the deepest of all the boreholes studied, consisting mainly of fine-grained siliciclastic lithologies (shales and siltstones). At its base a 4 m sequence of gabbros – anorthosites belonging to the Tete Suite was penetrated. The latter lithologies are unconformably overlain by red siltstones, fine-grained sandstones, and red mudstones that grade upwards immediately into black carbonaceous shales interbedded with two intervals of clast- to matrix-supported conglomerates up to *ca*. 930 m

depth. The top of the basement rocks is red stained and the features of the lithologies above the unconformity, also suggest sub-aerial sedimentary conditions and the probable formation of soils, rather than sedimentation under glacial to peri-glacial conditions prevalent during the deposition of the Dwyka type lithologies. The interval between 930 m and 750 m in the succession is characterized by a cyclic repetition of siltstone and sandstone interbedded with shales. This is followed by a very thick interval from 750 m to 190 m, consisting mainly of black carbonaceous shales, shales, siltstones and coal beds. The latter interval also included more coarse-grained lithologies, consisting of sandstones and siltstones especially between 610 m and 490 m depth. From 190 m depth to the top of the core, the succession consists of coarse- to medium-grained grey sandstones alternating with laminated siltstones, carbonaceous shale and thin beds of coal. The occurrence of several doleritic sills is characteristic for the succession of this borehole.

4. Organic matter extraction techniques and methods of organic maturation assessment

One hundred and seventy two mudrock core samples were used for thermal maturity analysis using the laboratory facilities of CIMA, Universidade do Algarve. Twenty grams of mudrock were crushed and placed in a 50 mL Falcon tube. To the crushed rocks was added a few drops of HCl to test for carbonates. Since all the samples proved to be devoid of carbonates, the crushed mudrock samples were treated with HF (40%) until all the silicates were dissolved. Then the organic residue obtained was rinsed and decanted several times using distilled water until the organic residue was fully neutralized. Afterwards, the samples were sieved using a 15µm mesh sieve. For spore fluorescence, spore colour and palynological analysis, the organic residues were mounted on palynological slides using acrylic resin Elvacite®.

4.1. Vitrinite Reflectance

The obtained organic residues were mounted and polished after the method by Hillier and Marshall (1988). Mean random vitrinite reflectance in oil immersion (%*Ro*) was the vitrinite reflectance (VR) parameter chosen for thermal maturity assessment, because the methodology adopted accounts non-oriented vitrinite particles. For vitrinite identification and measurement several criteria were taken into account following the guidelines recommended by the ASTM D7708-14 (2014), ISO 7404-5 (2009) and the International Committee for Coal and Organic Petrology (1998). VR measurements on all samples was performed at the University of the Algarve, Portugal, using an Olympus BX 51 microscope equipped with a black and white Olympus XC-50 digital camera. The greyscale (8-bit) digital images of vitrinite particles were analysed using the graphical tool VITRINITE, which runs within the Mirone Suite and calibrates the scale of 256 grey levels with standards of known reflectivity (Fernandes *et al.*, 2015). The reflectance values of the standards used were: 0.00 %, 0.428 %, 0.595 %, 0.897 %, 1.314 %, 1.715 %, 3.15% and 5.37 %. VR was measured in non-polarized incident light with a wavelength of 546 nm and immersion oil with a refractive index of 1.518 at a room temperature of 20ºC. Figure 11 shows some photographs of vitrinite particles which reflectance values was measured for this study. One hundred random reflectance values were measured across the polished thin sections and their arithmetic mean and standard deviation were calculated (Table 1). The arithmetic mean was considered to be the true $\%R_O$ for the sample.

As described in Section 3, the stratigraphic sections of three of the boreholes studied (ZSA-32, A1TM-058 and A1TM-085) were intruded by doleritic sills. Some of the samples of these three boreholes, close to the intrusion walls, have high vitrinite reflectance values (Table 2).

372 The high vitrinite reflectance values measured for these samples, are attributed to the
373 localized heat effect of the igneous intrusion in the aureoles and not to burial heat (see Section
374 7. Discussion). Hence, the vitrinite reflectance measured in the later samples (Table 2) were
375 not included neither in the calculation of burial palaeotemperatures and palaeogeothermal
376 gradients, nor in the estimation of eroded covers (see Section 6. Interpretation of organic
377 maturation results). However, the vitrinite reflectance values of the heat affected were
378 important for the thermal history discussion of the studied region.

379

380 ***4.2. Spore fluorescence and spore colour***

381 Qualitative spore fluorescence and spore colour are two optical parameters of thermal
382 maturity of organic maturation, useful for evaluating maturation levels of low-rank rocks until
383 the end of the oil window (1.35 - 1.5%*Ro*) (Van Gijzel, 1979; McPhilemy, 1988; Suárez-Ruiz
384 et al., 2012). When correlated with the quantitative VR method, spore fluorescence and colour
385 parameters can provide additional support for the thermal maturity of the rocks. Maturation
386 causes a gradual shift in organic matter fluorescence colours (red shift) from the shorter to the
387 longer wavelengths, that is, blue and green to yellow, orange and finally red. Of all the
388 macerals of the liptinite group, sporinite is the one that shows the most consistent changes in
389 fluorescence colour spectra and intensity with increasing maturation. Under fluorescence
390 excitation, it changes colour from green through yellow to orange and finally red, with
391 increasing maturity to the top of the oil-window, after which it no longer fluoresces. A
392 phenomenon frequently noticed in fluorescent palynomorphs is the fading effect (van Gijzel,
393 1979). The fading effect is due to a photochemical modification of the fluorescing organic
394 matter during prolonged blue light exposure, (30 minutes to 2 hours or more). During this
395 lengthy exposure the intensity of fluorescence may increase or decrease; if it increases, the

fading is said to be positive, conversely, if it diminishes is negative. In other words, the emitted fluorescence spectrum may move either towards higher wavelengths (red band) or towards shorter wavelengths (green band), the fading is said to be positive in the first case and negative in the second.

The analysis of qualitative spore fluorescence colours was undertaken in the University of the Algarve using an Olympus BX 51 microscope equipped with a metal halide lamp fluorescence unit; XCite Series 120Q and with a violet and Blue +12 filter block that generates a wavelength band of 390 - 490 nm. This system was allowed to stabilize for 5 min before any observation of the fluorescence of palynomorphs was attempted. Suitable spore species with smooth and medium thick exine, such as *Densoisporites* spp., were subjected to 5 minutes of excitation, after which their fluorescence colours were recorded. The same spores were exposed for a further thirty minutes to record any fading effects. The terminology used for describing fluorescence colours was blue (B), green (G), yellow (Y), dark yellow (DY), orange (O), dark orange (DO) and red (R).

Spore exine colour has long been suggested by palynologists as a method to assess the thermal maturity of sedimentary rocks, because they observed that, with increasing burial depth, spore colour changes from light to dark and that the change is progressive and irreversible (Correia, 1971; Staplin, 1982). In this study, spore colour was recorded using the Phillips Petroleum Colour Standard version no. 2 (Pearson, 1984), which is an adaptation of Staplin's Thermal Alteration Index (TAI) chart, because it includes more shades for the same colour index. The spore colour index for the samples was given by the colour of the dominant and lightest spores observed and compared with the Phillips Petroleum Colour Standard chart. The results of spore colour determination are presented together with VR measurements and

spore fluorescence colours for each sample (Table 1). Figures 3 to 10 show the main features of spore colour and spore fluorescence in the boreholes studied. Spore colours were recorded for acamerate, azonate trilete or monolete spores with a smooth exine of medium thickness, such as *Densoisporites* spp. and *Laevigatosporites* spp., which occurs throughout the section of both boreholes studied by (Pereira et al., 2016).

As mentioned above, both spore fluorescence and spore colour are qualitative methods for assessing organic maturation. The visual evaluation of the fluorescence colours and the colours the palynomorph walls is subjective, depending on the experience of the operator and lacking, therefore, the objectivity of VR. The lack of universally accepted standards of organic maturation, as VR, is another drawback of these two methods. Moreover, it has been reported (Mendonça Filho et al., 2010), that the acid treatment used to obtain kerogen concentrates (HCl and HF maceration) affects the fluorescence spectra of liptinites, shifting it to higher wavelengths (red-shift), when compared with the fluorescence spectra of whole rock samples. Despite these problems, spore fluorescence and spore colour, used together with VR are still important parameters of organic maturation, especially for low and medium rank rocks.

5. Organic Maturation and Palynological Results

Data of the thermal maturity analyses, both quantitative (VR) and qualitative (spore fluorescence and TAI), are shown in Table 1 and in VR profiles of the studied boreholes, which illustrate the change of the organic maturation indicators with burial depth (Figs. 3 to 9).

5.1. Borehole ZSA-32

Thirteen samples were processed from ZSA-32 and they were all suitable for organic maturation studies, whereas only three samples of the thirteen were suitable for palynological studies. The VR values measured show a linear increase with depth in the borehole, ranging from 1.21%*Ro* at the top to 1.31%*Ro* at the bottom (Fig. 3). Spore fluorescence colours change intensity from orange at the top, to dark orange at the bottom of the borehole, indicating palaeotemperatures close to the fluorescence extinction. TAI values also change from 3 to 3/3+ with increasing depth. Six samples were affected by heating by dolerite intrusions and have TAI colours of 4-/4 or 5. In general, TAI and fluorescence of the samples not affected by the intrusions indicate a thermal maturity at the onset of the oil-window, and VR values indicate a coal rank of medium rank B (ISO 11760, 2018).

Palynological analysis of ZSA-32 samples revealed an assemblage characterized by bisaccate taeniate pollen grain such as *Luckiesporites virkkiae*, *Lunatisporites pellucidus*, *Guttulapollenites hannonicus* and monolete spores such as *Laevigatosporites colliensis.* These assemblages indicate a Lopingian (late Permian) age for the entire succession of this core (Montesi, 2016).

5.2. Borehole A1TR-018

Twenty-two samples from A1TR-018 were studied for palynology and organic maturation, but after laboratory processing, only six samples were suitable for maturation studies and thirteen samples yielded palynomorphs. VR values measured from the *ca*. 80 m thick succession of this borehole increase downhole, from 1.51%*Ro* at the top to 1.72%*Ro* at the bottom at depth of *ca*. 70 m (Fig. 4). Spore colours showed consistent TAI values of 3+/4- throughout the succession, which is fully consistent with the VR values measured. The thermal maturity obtained from this core indicates that the sedimentary succession straddles in the wet and dry gas zone of hydrocarbon generation. In terms of coal rank, VR values indicate

a medium rank A (ISO 11760, 2018). All the samples studied for palynology yielded an assemblage characterized by rare trilete spores and colpate pollen grains, abundant monossaccate and rare to common bissaccate (taeniate and non-taeniate) pollen. This assemblage shows similarity to the one described by Pereira *et al*. (2014) from the borehole ETA 72 located in the Muarádzi sub-basin (Fig. 1) and, therefore, is interpreted to be of Kungurian / Roadian age with *Alisporites* sp., *Cycadopites* sp., *Florinites* spp., *Potoniesporites* sp., *Striatopodocarpites cancellatus, S. fusus Protohaploxypinus* sp. and *Vittatina* sp.

5.3. Borehole TGDH(C)005

Twenty five samples were processed for both thermal maturity and palynological analysis but just twenty and twelve samples from borehole TGDH(C)005 were studied for palynology and organic maturation, respectively. The lowest maturation levels in this part of the Moatize – Minjova Basin were detected in this borehole. VR values range from 0.97%*Ro* at ca. 20 m depth to 1.15%*Ro* at 206 m depth. VR increases linearly with depth with a good correlation coefficient of $R^2 = 0.92$ (Fig. 5). In terms of hydrocarbon generation the entire succession in this borehole lies within the oil-window. Consistent TAI values of 2 were recorded for this borehole, with the exception of one sample from the bottom of the borehole with a TAI value of 2+. All samples show positive fluorescence with yellow to dark yellow colours (Fig. 10). Fluorescent samples also show a positive fading effect. The maturation levels measured straddle the boundary between medium rank C and B coals (ISO 11760, 2018) in terms of coal rank. The microfloristic assemblage recorded in this borehole show affinities with the assemblage described by Pereira et al. (2016) from borehole DW 123 located in the Muarádzi sub-basin (Fig. 1), that indicates a Lopingian age based on the presence of the key species, as *Lueckiesporites virkkiae*, *Guttullapollenites hannonicus, Polypodiisporites* sp., *Thymospora*

494 sp., and *Weylandites lucifer*.

495

496 ***5.4. Borehole A1TM-085***

497 Ten samples were processed for both maturity and palynological studies, being all suitable for
498 these studies. VR values measured increase downhole from 1.43%*Ro* at 138 m depth to
499 1.56%*Ro* at 731 m depth (Fig. 6). The VR profile shows a linear increase in reflectance with
500 depth of burial, defining a gradient with a correlation coefficient of $R^2 = 0.83$. Maturation
501 levels indicated by VR fall in the wet gas zone for all the samples of this borehole. TAI values
502 of 3+/4- were obtained from most of the samples that contained suitable spores. However, in
503 three samples between depths *ca*. 455 m and 222 m, spores with a TAI of 3/3+ were recorded,
504 showing also feint fluorescence with brown to dark orange colours, indicating a position close
505 to the spore fluorescence extinction level. Below 454 m depth, no palynomorphs fluoresce. In
506 this borehole, the cut-off of fluorescence correlates with VR of ca. 1.49%*Ro*. According to
507 Taylor et al. 1998 all fluorescence disappeared during the second coalification jump, which is
508 between 1.2 % *Ro* and 1.6% *Ro*, therefore not all spores fluorescence coincide with 1.35%*Ro*
509 taken as the end of oil-window. Fluorescent samples also showed a negative fading effect.
510 The maturation levels measured correspond to a coal rank of medium rank A (ISO 11760,
511 2018). As in borehole A1TM-058, this borehole also shows effects of conductive heating
512 related to the intrusion of doleritic sills in a sample at *ca*. 187 m depth.
513 Palynological studies performed on samples from this borehole highlighted an assemblage
514 similar to the one found in borehole TGDH(C)005 indicating a Lopingian age with
515 *Calamospora*sp., *Horriditriletes* sp, *Krauselisporites rallus, Osmundacidites senectus* and
516 *Guttullapollenites hannonicus* and *Weylandites lucifer* for the whole succession penetrated by
517 this borehole.

518

519 ***5.5. Borehole CIMT-014***

520 As mentioned in the borehole descriptions, most of the lithologies penetrated by borehole
521 CIMT-014 consist of red beds (mudstones, siltstones and sandstones), which are not suitable
522 for organic maturation and palynological studies due to the oxic conditions that prevailed
523 during deposition.

524

525 Fifty samples were processed for both maturity and palynological studies for CIMT-014
526 borehole. However, the majority of samples were barren with only 10 samples for palynology
527 and 4 samples for maturation proving to be suitable for these studies. In borehole CIMT-014,
528 a VR value of 1.07%*Ro* was measured from sample MQ111 at *ca*. 132 m depth. In general,
529 VR increases downhole and a VR value of 1.47%*Ro* was measured for sample MQ147 near
530 the bottom of the borehole (Fig. 7). However, the most important information regarding the
531 maturation and thermal history of this borehole came from spore colour (TAI) and
532 fluorescence. The observation of these two optical organic maturation indicators revealed two
533 different palynomorph populations, in terms of both age and organic maturation level. All
534 samples investigated contain an indigenous palynomorph population but samples MQ127,
535 MQ115 and MQ111 also includes a reworked palynomorph population (Fig. 12). It is
536 noteworthy that reworked vitrinite populations were not identified in these last three samples.
537 TAI values of 2 and 3+/4- were recorded for the indigenous palynomorph population from *ca*.
538 132 m depth and at the bottom of the CIMT-014 borehole, respectively. Fluorescence
539 intensity and colour also change downhole for the indigenous palynomorph population, from
540 bright yellow colour in sample MQ111 to dark orange colour in sample MQ147. The
541 reworked palynomorph population is absent in sample MQ147, but in the other three samples
542 it is common, making up to 30 – 40% of all palynomorphs. The TAI values of the reworked
543 palynomorphs are always 3+/4- and spore fluorescence is either orange colour or the spores

do not fluoresce (Table 1). Non-fluorescent spores are more abundant in samples MQ111 and MQ115 (Fig. 12). The organic maturation levels indicated by VR indicate that this borehole falls within the late oil-window, with sample MQ147 (at the bottom of the borehole) indicating a position at the beginning of the wet-gas generation zone. VR values also indicate a coal rank of medium rank B (ISO 11760, 2018) for most of the sedimentary succession in this borehole.

The palynological assemblage found in sample MQ111 suggest an Upper Triassic (Carnian) age, based on the presence of the spores *Anapiculatisporites spiniger/Carnisporites anteriscus, Densoisporites* spp., *Dictyophyllidites* sp. *Limatulasporites limatus, Lophotriletes novicus, Lundbladispora* spp., *Nevesisporites fossulatus, Retitriletes* sp., *Stiattella seebergensis* and *Uvaesporites* sp. and the pollen grains of *Camerozonosporites secatus*, *Cycadopites* sp., and *Samaropollenites speciosus,* that typifies to these ages (César and Colombi, 2016; Dawit, 2014; Paterson et al., 2018). The assemblages found in samples MQ115, MQ127 strongly suggests a Lower Triassic age, containing the spores *Aratisporites* sp., *Densoisporites nejburgi, D. playfordii Lundbladispora* spp. and *Playfordidiaspora cancellosa* and the pollen grains *Alisporites nuthallensis*, *Lunatisporites pellucidus, Falcisporites stabilis ,* and *Platysaccus queenslandii*. The assemblages of these two samples are characterized by *Alisporites nuthallensis*, *Lunatisporites pellucidus, Densoisporites playfordii, Falcisporites stabilis* and *Lundbladispora obsoleta*, *Platysaccus queenslandii*, *Uvaesporites* sp. and *Carnisporites* sp. that typifies to these ages (Dawit, 2014). Between samples MQ111 and MQ115, separated vertical in the borehole by only *ca*. 15 m no palynomorphs were recorded in three samples located in this interval, suggesting an important hiatus, since no Middle Triassic palynomorphs were identified. Samples MQ111, MQ115 and MQ127 also have a considerable amount of reworked palynomorphs of Lopingian (Permian age) as for instance *Polypodiisporites* sp., *Thymospora* sp. The Permian-Triassic boundary is tentatively placed at

569 *ca*. 489 m depth according to the scheme described by Pereira et al. (2016) from borehole
570 DW132, where the Permian-Triassic boundary was identified at *ca.* 42 m depth.
571
572 ***5.6. Borehole A1TM-039***
573 For A1TM-039 borehole, twenty samples were processed, but only two samples were suitable
574 for organic maturation studies and three yielded palynomorphs suitable for palynological
575 analysis. VR values measured are 1.15%*Ro* (MQ231) and 1.17%*Ro* (MQ233) and the
576 indigenous palynomorphs population shows yellow fluorescence colours and TAI values of
577 2+ (Fig. 8). The reworked palynomorph population either shows no fluorescence or dull dark
578 orange colours and TAI values of 3+/4- (Table 1). The maturation levels suggested by the VR
579 results and the indigenous palynomorph population indicate a position within the oil-window
580 and a coal rank of medium rank B (ISO 11760, 2018), whereas the maturation levels of the
581 reworked population indicate a position at the end of the oil-window and at the beginning of
582 the wet-gas generation zone.
583 The three productive samples studied are located near the bottom of the borehole and contain
584 an assemblage assigned to Carnian age (Upper Triassic) age. The palynoassemblage included
585 the pollen grains *Alisporites nuthallensis, Enzonalasporites virgens, Platysaccus queenslandi*.
586 and *Samaropollenites speciosus* and the spores *Aratrisporites* sp.*, Anapiculatisporites*
587 *spiniger/Carnisporites anteriscus*, *Densoisporites* spp., *Lundibladispora* spp.*, Playfordispora*
588 *cancellosa, Stiattella seebergensis* and *Uvaesporites* sp. A second assemblage comprising
589 reworked palynomorphs was also identified in the same samples. The reworded assemblage is
590 assign to a Permian age due to the presence of*, Alisporites parvus, Cyclogranisporites*
591 *gondwaniensis, Polypodiisporites* sp.*, Thymospora* sp.*,* described as key species for this age in
592 other Karoo basins.
593

5.7. Borehole A1TM-058

The twenty-nine samples processed were all suitable for maturity studies, whereas, only twelve samples were suitable for palynological studies. In borehole A1TM-058, VR values increase downhole from 1.19%*Ro* at 23.5 m depth to 1.51%*Ro* at 970 m depth, with a clear linear VR *vs.* depth relationship (Fig. 9). The boundary between the base of the oil-window and the wet gas zone, indicated by the VR profile, occurs at *ca*. 500 m depth, with VR values ranging from 1.31 to 1.36%*Ro*. Samples above 490 m depth show positive fluorescence with orange to dark orange colours (Fig. 10), whereas for samples below that depth, no palynomorphs (spores and pollen) were observed to fluoresce. The depth of fluorescence extinction in this borehole correlates with VR values between 1.31 and 1.33%*Ro*. Spore colour increases from a TAI of 3/3+ at the top of the borehole to values of 3+/4- at the bottom of the borehole. TAI values of 3+/4- were recorded for spores at the horizon of fluorescence extinction. All thermal maturity indices recorded correspond to medium rank B and A coals in terms of coal rank (ISO 11760, 2018). In this borehole, VR measured from samples between the depth intervals of 68 to 180 m and 610 to 625 m, yielded anomalously high values, that do not lie on the VR vs. depth profile (Fig. 9). These samples are positioned close to the margins of several doleritic intrusions that were intersected by the borehole. Therefore, the VR values from these samples were not included in the calculation of the VR profile, since they were interpreted as the result of post burial igneous activity, most likely related to the Jurassic Karoo - Ferrar Large Igneous Province (*op. cit.* Duncan et al., 1997). Palynological studies performed in this borehole, shows a palynoassemblages similar to the assemblage studied in the borehole A1TM-085. Present are the diagnostic species *Guttullapollenites hannonicus*, *Klausipollenites schaubergeri, Lueckiesporites virkkiae*, *Osmundacites senectus*, *Polypodiisporites* sp., *Protohaploxypinus microcorpus*, *Thymospora* sp.and *Weylandites lucifer*, that indicates a Lopingian age (Late Permian). The assemblages investigated are also

very similar and correlate with those described for the borehole DW 123, Muarádzi sub-basin (see Fig. 1) (Pereira et al., 2016).

6. Interpretation of Organic Maturation Results

6.1. Palaeogeothermal gradient estimates

Except for boreholes CIMT-014 and A1TM-039, the thermal maturity obtained from the non-heat affected samples (Table 1), indicates a clear relationship between maturity and depth of the sedimentary beds despite the different techniques used (Figs. 3 to 10). This type of relation suggests that burial was the main factor controlling organic maturation. However, organic maturation profiles indicate that the boreholes located in close proximity to the southern basin boundary have less steep gradient indicating higher geothermal gradients at those locations. In order to investigate this aspect further, palaeotemperatures were calculated using Barker's (1988) empirical equation T(°C)= 104ln(%*Ro*)+148, where T(°C) is the maximum palaeotemperature attained by the sedimentary rock that yielded vitrinite particles with a measured VR of %*Ro*.

The palaeotemperatures calculated by this equation are shown in the Table 1. These were then used to estimate palaeogeothermal gradients (Fig. 13) and the amount the rock cover eroded in the N'Condédzi sub-basin of the Moatize - Minjova Coal Basin.

The palaeogeothermal gradients calculated vary significantly from a maximum of *ca*. 300°C/km in borehole A1TM-018 to a minimum of ca. 35°C/km in borehole A1TM-085. Palaeogeothermal gradients were not calculated for boreholes CIMT-014 and A1TM-039 due to insufficient numbers of samples studied.

643 Notably, the higher palaeogeothermal gradients were from the boreholes located near the
644 basin margin and in the small isolated occurrence of the Karoo Supergroup where borehole
645 TGDH(C)005 was drilled. Anomalously high VR values were measured in boreholes A1TM-
646 085, A1TM-058 and ZSA-32 through several depth intervals that were interpreted as the
647 results of conductive heating associated with Jurassic age doleritic intrusions. These
648 anomalous VR values were not included in the construction of palaeogeothermal gradients.
649
650 However, there is no evidence that boreholes that have the highest calculated
651 palaeogeothermal gradients were affected by igneous intrusion and, therefore, another thermal
652 event was responsible for such high geothermal gradients. The calculated palaeogeothermal
653 gradients of 35-40°C/km is considered to be the regional geothermal gradients for the
654 N'Condédzi sub-basin of the Moatize - Minjova Coal Basin, and is similar to the 40°C/km
655 geothermal gradient calculated by Fernandes et al. (2015) for the Muarádzi sub-basin of the
656 same basin.
657
658 The calculated palaeogeothermal gradients are characteristic of extensional continental rift
659 basins (Fernandes et al. 2015). However, the higher geothermal gradients calculated for the
660 boreholes near the basin boundary, suggest that high heat flux rather than the regional
661 geothermal gradient was responsible for locally elevated the geothermal gradients. A likely
662 cause for this high palaeogeothermal gradient is the circulation of hot fluids associated with
663 fault zones and permeable beds (sandstones).
664
665 ***6.2. Eroded cover estimates***
666 The calculated palaeogeothermal gradients were used to estimate the amount of eroded
667 sedimentary cover in sedimentary basins where rocks have already attained maximum

668 temperatures. The eroded sedimentary cover refers to the thickness of sedimentary section
669 necessary to account for the measured VR results. In the boreholes studied, the shallowest
670 samples, from 11 to 138 m depth, reached peak palaeotemperature of 185-190°C. The method
671 used to calculate the eroded cover is after Bray et al. (1992). Applying this methodology to
672 the estimates of exhumation in the study area suggests a maximum of *ca*. 5300 m and a
673 minimum of 550 m. This range can be explained by different palaeogeothermal gradients used
674 in calculations for these boreholes. Since the highest palaeogeothermal gradients are
675 considered abnormal and related to high temperature fluid flow through fault zones and
676 permeable lithologies, the amount of post-late Permian exhumation is between 4.3-5.3 km;
677 values slightly higher than the 2.5 – 3 km calculated by Fernandes et al. (2015).
678
679 Thick sedimentary sections are found in other external rift-related Karoo basins in Eastern
680 Africa, which are geometrically related to the Moatize Minjova Basin (Cairncross, 2001;
681 Catuneanu et al. 2005). For example, Banks et al. (1995) reported at 8 km thick Permian-
682 Triassic sedimentary section preserved in the Karoo rift basin of the Luargwa Valley in
683 Zambia.
684
685 **7. Discussion**
686 The VR values measured from the N'Condédzi sub-basin, range from 1.3-1.7%*Ro*, indicating
687 a coal rank of medium rank B and A coals (ISO 11760, 2018), and are similar to those
688 reported by Fernandes et al. (2015) of dispersed organic matter, and Vasconcelos (1995) of
689 coals, for the Moatize sub-basin (Fig. 1). In terms of zones of hydrocarbon generation,
690 boreholes ZSA-32, A1TM-39 and TGDH(C)005 are within or at the end of the oil-window,
691 boreholes A1TR-018 and A1TM-085 are within the wet gas generative zone, and boreholes

692 A1TM-058 and CIMT-014 span the base of oil window at depths of *ca*. 600 m depth and 400
693 m, respectively.
694
695 The linear increase of VR with depth observed in the boreholes indicates an organic matter
696 maturation process related to burial. The calculated regional palaeogeothermal gradient for the
697 N'Condédzi sub-basin is 35-40°C/km. The doleritic intrusions observed in three boreholes
698 (A1TM-058, A1TM-085 and ZSA-32), had only local thermal effects and only increased VR
699 for the samples in the contact aureoles. If the igneous episode, responsible for the doleritic
700 intrusions, had a major effect on the regional organic matter maturity, a homogenisation of all
701 maturity indicators will be expected for the sedimentary successions of these boreholes, this
702 was not observed and supports our argument for the local thermal affects of the intrusions.
703 However, boreholes TGDH(C)005 and A1TR-018 do not show evidence of igneous
704 intrusions and have higher palaeogeothermal gradients suggesting that a thermal process other
705 than burial heating, was responsible for these abnormal gradients. The close proximity of
706 these boreholes to the southern fault-bounded basin margin suggests that hot fluids circulating
707 through permeable lithologies (sandstones) and faults zones, as a likely processes capable of
708 elevate the regional palaeogeothermal gradients in these parts of the basin margin (Fig. 14).
709 The origin of the hot fluids may have been connate waters that moved through the
710 sedimentary pile due to lithostatic pressure during fault-induced subsidence, or may have a
711 deeper origin resulting from metamorphic dewatering reactions(?). The flow of hot fluids,
712 expelled from the basal beds of the basin by lithostatic pressure, through permeable
713 lithologies and fracture zones, allowed the advective and convective transmission of heat,
714 which heated up the sedimentary successions located near the southern basin margin (Fig. 14).
715 The rock successions in these zones were in equilibrium with the temperature of the hot fluids
716 that overprinted the initial thermal maturity caused by burial heat only.

The initiation of fluid flow due to lithostatic pressure in this basin is probably due to the high sedimentation rates consequence of fault-induced subsidence, leading to the accumulation of the thick succession of sediments. In borehole A1TM-058, *ca*. 1 km of Lopingian age sediments are preserved and Lakshminarayana (2015) reported a Lower Karoo succession with more than 900 m thickness. Boreholes A1TM-039 and CIMT-014 encompass a *ca*. 500 – 600 m sedimentary succession of mostly Lower to Middle/Upper Triassic age, demonstrating the continuation of high sedimentation rates throughout Triassic times in this basin. An additional cause for the initiation of fluid flow is the structural geometry of the basin. The N'Condédzi sub-basin is half-graben, where the main fault, the Mwanza Fault, was formed by tectonic reactivation of the Sanângoe Shear Zone (Fig. 1). The Mwanza Fault was probably active since the early Permian and lead to the accumulation of a thick pile of sediments adjacent to the fault zone. Due to the half-graben geometry, the thicknesses of the sedimentary successions were considerably less near the southern margin of the basin. For example, borehole TGDH(C)005 located in the isolated occurrence of Karroo Supergroup sediments within the Tete Suite contains *ca.* 230 m of Lopingian aged strata, whereas borehole A1TM-058 includes a *ca*. 1 km succession of the same age.

Using the regional palaeogeothermal gradient calculated from VR, 4 to 5 km of cover was eroded after Lopingian times in the depocentre of this basin, whereas near the S-SW basin margin, the estimated eroded cover is significantly less from *ca*. 544 m to *ca.* 2.4 km. However, these estimates may be inaccurate, as they do not take account of the palaeogeothermal gradient probably having been elevated by hot fluids flowing through fault zone at the basin margin.

742 The maturation data and the age of the successions of boreholes A1TM-058, A1TM-085,
743 TGDH(C)005, ZSA-32 and A1TR-018, indicate that the timing of organic matter maturation,
744 when peak temperatures were attained, is prior to Lower Triassic times. This can be better
745 constrained by taking into account the cooling episode that occurred between 240 and 230 Ma
746 in the Moatize - Minjova Basin (Fernandes et al., 2015). The latter study also indicated that
747 peak burial temperatures and consequently organic maturation levels, were attained shortly
748 after deposition (3 - 10 Ma), implying high subsidence rates during Lopingian to Lower
749 Triassic time in this region. In borehole CIMT-015 palynological results indicate that Lower
750 Triassic and the Upper Triassic (Carnian) rocks, samples MQ115 and MQ111, respectively
751 (section 5.5 and Fig. 7), are only vertically separated in the borehole by a 15 m thick section
752 of coarse clastic sedimentary rocks. Although, the samples processed in the borehole interval,
753 between these two samples, for organic maturation and palynology were barren, it is unlike
754 that Middle Triassic rocks are condensed in this 15 m thick section. This suggests that the
755 N'Condédzi sub-basin was affected by the same Middle Triassic erosion event described by
756 Fernandes *et al*. (2015) for the Moatize - Minjova Basin in the region of the Muarádzi sub-
757 basin (Fig. 1). Also, the presence of common reworked palynomorphs of Permian age in
758 Upper Triassic (Carnian) sediments in boreholes A1TM-039 and CIMT-014 indicates
759 exhumation and erosion of Permian aged Karoo sedimentary rocks during Middle Triassic
760 times in the neighbouring Karoo basins, *e.g*. in the Moatize and Muarádzi sub-basins (Lopes
761 et al., 2014; Pereira et al., 2016; Götz, et al., 2018) (Fig. 1). Furthermore, the spore
762 fluorescence colours and TAI values recorded from the reworked Permian age palynomorphs
763 in boreholes CIMT-014 and A1TM-039, are considerably higher than those of the indigenous
764 Triassic palynomorphs. Therefore, the Upper Triassic sedimentary rocks never attained higher
765 temperatures than those indicated by the reworked palynomorph population. Unconformities
766 between the late Permian and the Lower Triassic sedimentary successions are described in

767 several Karoo rift basins located to the north of the Main Karoo Basin of South Africa
768 (Catuneanu et al., 2005 and references herein). In the Ruhuhu, Selous and Tanga basins of
769 southern Tanzania this unconformity is well documented and corresponds, for example, to the
770 unconformity between the Lopingian Usili Formation and the Lower Triassic Manda
771 Formation. In Zambia it is the unconformity between the Lopingian Upper Madumabisa
772 Formation and the overlying Lower Triassic Escarpment Grit, and in Madagascar, in the
773 Morondova Basin, it is the unconformity between the Lower Sakamena Formation and the
774 overlying Middle to Upper Sakamena Formation. However, the effects of this Middle Triassic
775 erosion event on the organic maturation and thermal history of the N'Condédzi sub-basin are
776 still uncertain. This is due to the similarity of VR values measured for the Lower and Upper
777 Triassic samples in boreholes CIMT-014 and A1TM-039, together with the impossibility of
778 constructing VR profiles for these two boreholes (see sections 5.5, 5.6 and 6.1), capable of
779 identifying distinct geothermal gradients, below and above the Middle Triassic erosion event.
780 Accordingly, the organic maturation results attained in this study indicate that the effects of
781 the Upper Triassic reburial on the organic maturation, as a distinct thermal event of this sub-
782 basin were not detected, suggesting that a single episode of burial under a sedimentary cover
783 that ended in Upper Triassic – Lower Jurassic(?) times, was responsible for the organic
784 maturation levels measured. The similar VR results, for example, between the Carnian age
785 samples (MQ231 and MQ233) in borehole A1TM-039 and the same age sample (MQ111) in
786 borehole CIMT-014, separated vertically *ca.* 470 m (both boreholes were drilled on a ground
787 at *ca*. 300 m above sea level), could be due to different burial cover thicknesses. In this case
788 borehole A1TM-038 was located in an area of the sedimentary basin that was buried under a
789 thicker sedimentary cover (a depocentre area) than borehole CIMT-014.
790

Organic maturation levels measured for the N'Condédzi sub-basin suggest a complex thermal history (Fig. 14). The VR profiles of the boreholes studied indicate a maturation process related to burial heat. Though, the high palaeogeothermal gradients observed near the South margin of this basin, suggest the flow of hot fluids through permeable lithologies and fractures with discharge points located near the South boundary of this basin. The flow of hot fluids was due, most probably, to compaction-driven fluid flow. The movement of major extensional faults in the N'Condédzi sub-basin led to high fault-induced subsidence rates. The sediment accommodation space created by these processes was matched also by high sedimentation rates during Permian to Lower Triassic times, which increased considerably compaction pressures and may have originated hot overpressure fluids that initiated the fluid flow through the permeable lithologies and fault zones of this basin.

Reworked Permian palynomorphs in Carnian (Upper Triassic) sediments have higher maturation levels than the indigenous Carnian palynomorphs, indicated by spore colour and fluorescence. This implies exhumation and erosion of Permian aged successions located in the neighbouring Karoo basins during Middle Triassic times, and also suggests that peak burial palaeotemperatures, in those basins, were achieved during Permian to Lower Triassic times. Peak burial palaeotemperatures attained by the Upper Triassic (Carnian) sedimentary successions in the N'Condédzi sub-basin, were lower and did not overprint the effects of the earlier maturation episode of the neighbouring Karoo basins, indicated by the reworked Permian palynomorphs. Lastly, during Lower Jurassic times occurred a last maturation event related to dolerite intrusions. Though, the thermal effects of these intrusions were localised and limited to the contact aureoles.

8. Conclusion

The main conclusions of this work are:

- VR values measured from the exploration boreholes of the N'Condédzi sub-basin, range from 1.3 – 1.7%*Ro*, indicating a coal rank of medium rank B and A coals (ISO 11760, 2018). The range of VR values indicated, excludes the VR values of the heat-affected samples due to the dolerite intrusions. In terms of zones of hydrocarbons the majority of the succession of the boreholes lay at the end of the oil window and the beginning of the wet gas generative zone.
- The linear increase of VR with depth observed in the boreholes indicates an organic matter maturation process related to burial. The calculated regional palaeogeothermal gradient for the N'Condédzi sub-basin is 35-40°C/km. The doleritic intrusions observed in three boreholes, had localized thermal effects and only increased VR for the samples close to the intrusion walls. The abnormal geothermal gradients calculated for boreholes TGDH(C)005 and A1TR-018 located close to the south margin of the basin, are attributed to hot fluids flowing through permeable lithologies (sandstones) and faults zones that elevated the regional palaeogeothermal gradient in these parts of the basin margin. We proposed that the origin of the hot fluids were connate waters that moved due to lithostatic pressure during fault-induced subsidence, with a possible minor contribution of deep hot fluids originated by dewatering metamorphic reactions(?).
- Hot fluid flow was due to the accumulation of thick sedimentary piles (over 2 km in thickness) in periods of rapid subsidence during the Permian – Triassic times.
- Using the regional palaeogeothermal gradient calculated from VR, 4 to 5 km of cover was eroded since after Lopingian time in the depocentre of this sub-basin.
- The maturation data obtained, together with the age of the borehole successions, including the reworked Permian palynomorphs in Upper Triassic sedimentary rocks,

suggests that burial peak temperatures were reached during Upper Triassic – Lower Jurassic(?) times.

Disclosure of interest

The authors declare that they have no competing interest.

Acknowledgments

The authors would like to thank the Managers of Coal India Africana, Limitada, Companhia Carvoeira de Samoa, Limitada, Capitol Resources, Limitada, Gondwana Empreendimentos e Consultorias, Limitada, and Iain C. Pleas for borehole access and complementary information. Francesca Galasso acknowledges the University of Perugia, for the opportunity to participate in the program Erasmus+ Traineeship, funded by the European Commission. The authors gratefully acknowledge Centro de Investigação Marinha e Ambiental (CIMA) for the use of the services and laboratory facilities at the University of the Algarve. We would like to thank Professor Geoffrey Clayton from the Department of Geology, Trinity College, Dublin, and Doctor Elke Schneebeli-Hermann from University of Zurich, Paleontological Institute and Museum, Switzerland, for critical reading of the manuscript. The reviews and valuable comments of four anonymous reviewers, have greatly improved our manuscript. This research did not receive any specific grant from funding agencies in the public, commercial, or not-for-profit sectors.

References

Achimo, M., Vasconcelos, L., Marques, J., Ferrara, M., 2014. Sedimentologia dos depósitos tilíticos do vale do Rio Murrongódzi, Bacia Carbonífera de Moatize-Minjova, Tete,

Moçambique. In: 2º Congresso Nacional de Moçambique e 12º Congresso de Geoquímica dos Países de Língua Portuguesa, Vasconcelos, L. (ed.), Livro de Resumos, Maputo, 57-61.

Afonso, R.S., 1975. Contribuição para o conhecimento da area de Tambara-DÔa (Folha Sul-E-36, grau quadrado 1634). Bol. Serviços Geol. Minas, Lourenço Marques 38, 5e153.

Afonso, R.S., 1976. A geologia de Moçambique. (Notícia explicativa da carta geologica de Moçambique). Direcção dos Serviços de Geologia e Minas, Maputo, 1: 2.000.000. 175 pp.; 2 mapas.

Afonso, R. S., 1984. Ambiente geológico dos carvões gonduânicos de Moçambique - uma síntese. In: Lemos de Sousa, M.J. (Ed.), Symposium on Gondwana Coals, Lisbon, 1983. Proceedings and Papers. Comunicações dos Serviços Geológicos de Portugal, vol. 70 (2), 205-214.

ASTM D7708-14, 2014. Standard Test Method for Microscopical Determination of the Reflectance of Vitrinite Dispersed in Sedimentary Rocks. ASTM, International, West Conshohocken, PA, USA, p. 10.

Banks, N. L., Bardwell, K. A., Musiwa, S., 1995. Karoo Rift Basins of the Luangwa Valley, Zambia. Geological Society, London, 285-295. Special Publication, 80.

888 Barker, C. E., 1988. Geothermics of petroleum systems: implications of the stabilisation of
889 kerogen thermal maturation after a geologically brief heating duration at peak temperature.
890 In: Magoon, L.B. (Ed.), Petroleum Systems of the United States, vol. 1870. United States
891 Geological Survey Bulletin, 26-29.
892
893 Bray, R., Green, P., Duddy, I., 1992. Thermal history reconstruction using apatite fission track
894 analysis and vitrinite reflectance: a case study from the UK East Midlands and the Southern
895 North Sea. In: Hardman, R. (Ed.), Exploration Britain: Geological Insight for the Next Decade,
896 vol. 67. Geological Society of London Special Publication, 3-25.
897
898 Cairncross, B., 2001. An overview of the Permian (Karoo) coal deposits of Southern Africa.
899 Journal of African Earth Sciences, 33, 529-562.
900
901 Carvalho, L.H.B., 1977. Formações vulcânicas de Carinde, Tete-Moçambique. Dissertação
902 apresentada ao Instituto Superior Técnico para obtenção do grau de Doutor em Ciências da
903 Engenharia (Geologia Aplicada), 213 p.
904
905 Catuneanu, O., Wopfner, H., Eriksson, P.G., Cairncross, B., Rubidge, B.S., Smith, R.M.H.,
906 Hancox, P.J., 2005. The Karoo basins of south-central Africa. Journal of African Earth
907 Sciences, 43, 211-253.
908
909 Césari, S.N. and Colombi, C., 2016. Palynology of the Late Triassic Ischigualasto Formation,
910 Argentina: Paleoecological and paleogeographic implications. Palaeogeography,
911 Palaeoclimatology, Palaeoecology, 449, 365–384.

912

913 Corcoran, D. and Clayton, J., 2001. Interpretation of Vitrinite Reflectance profile in
914 sedimentary basin, onshore, offshore Ireland. Geol.Soc.London, Spec. Pub., 188, 61-90.
915
916 Correia, M., 1971. Diagenesis of sporopollenin and other comparable organic substances:
917 application to hydrocarbon research. In: Brooks, J., Grant, P.R., Muir, M., van Gijzel, P.,
918 Shaw, G. (Eds.), Sporopollenin. Academic Press, New York, 569-620.
919
920 Daber, R., 1984. Plantas fósseis de Moçambique. Ciênc. Tecnol., Maputo, 9, 77-81.
921
922 Dawit, E.L., 2014. Permian and Triassic microfloral assemblages from the Blue Nile Basin,
923 central Ethiopia. Journal of African Earth Sciences, 99, 408-426.
924
925 Duncan, R.A., Hooper, P.R., Rehacek, J., Marsh, J.S., Duncan, A.R., 1997. The timing and
926 duration of the Karoo igneous event, southern Gondwana. Journal of Geophysical Research,
927 102, 18127-18138.
928
929 Fernandes, P., Musgrave, J.A., Clayton, G., Pereira, Z., Oliveira, J.T., Goodhe, R., Rodrigues,
930 B., 2012. New evidence concerning the thermal history of Devonian and Carboniferous in
931 South Portuguese Zone. Journal Geological Society, London, 169, 647-657.
932
933 Fernandes, P., Rodrigues, B., Borges, M., Matos, V., Clayton, G., 2013. Organic maturation
934 of the Algarve Basin (Southern Portugal) bearing on thermal history and hydrocarbon
935 exploration. Marine and Petroleum Geology, 46, 210-233.

936

937 Fernandes, P., Cogné, N., Chew, D.M., Rodrigues, B., Jorge, R.C.S, Marques, J., Jamal, D.,
938 Vasconcelos, L., 2015. The thermal history of Karoo Moatize Minjova Basin, Tete Province,
939 Mozambique: an integrated vitrinite reflectance and apatite fission track thermochronology
940 study. Journal of African Earth Sciences, 112, 55-72.

941

942 Götz, A. and Ruckwied, K., 2014. Palynological record of the Early Permian Postglacial
943 climate amelioration (Karoo Basin, South Africa). Palebio. Paleoenv, 94, 229-235.

944

945 Götz, A., Hancox, P. J., Lloyd, A., 2017. Permian climate change recorded in palynomorph
946 assemblages of Mozambique (Moatize Basin, eastern Tete Province). Acta Paleobotanica
947 57(1), 3-11.

948

949 Götz, A., Hancox, P. J., Lloyd, A., 2018. Southwestern Gondwana's Permian climate
950 amelioration recorded in coal-bearing deposits of the Moatize sub-basin (Mozambique).
951 Palaeoworld, https://doi.org/10.1016/j.palwor.2018.08.004

952

953 Grantham, G.H., Macey, P.H., Ingram, B.A., Roberts, M.P., Armstrong, R.A., Hokada, T.,
954 Shiraishi, K., Jackson, C., Bisnath, A., Manhiça, V., 2008. Terrane correlation between
955 Antarctica, Mozambique and Sri Lanka; comparisons of geochronology, lithology, structure
956 and metamorphism and possible implications for the geology of southern Africa and
957 Antarctica. In: Satish-Kumar, M., Motoyoshi, Y., Osanoi, Y., Hiroi, Y., Shiraishi, K. (Eds.),
958 Geodynamic Evolution of East Antarctica: a Key to the East-west Gondwana Connection, vol.
959 308. Geological Society, London, Special Publication, 91-119.

GTK Consortium, 2006. Map Explanation; Volume 2: Sheets 1631 - 1934. Geology of Degree Sheets, Mecumbura, Chioco, Tete, Tambara, Guro, Chemba, Manica, Catandica, Gorongosa, Rotanda, Chimoio and Beira, Mozambique. Ministério dos Recursos Minerais, Direcção Nacional de Geologia, Maputo.

Hancox, P. J., 2016. The Coalfields of South-Central Africa: a Current Perspective. Episodes, 39(2), 407-428.

Hankel, O., 1994. Early Permian to Middle Jurassic rifting and sedimentation in East Africa and Madagascar. Geol. Rundsch. 83, 703-710.

Hillier, S. and Marshall, J., 1988. A rapid technique to make thin sections of sedimentary organic matter concentrates. Journal of Sedimentary Petrology, 58, 754-755.

Hunt, J.M., 1996. Petroleum Geochemistry and Geology. W.H. Freeman and Co., 742 p.

International Committee for Coal and Organic Petrology, 1998. The new vitrinite classification (ICCP System 1994). Fuel, 77, 349-358.

Isbell, J.L., Cole, D.I., Catuneanu, O., 2008. Carboniferous-Permian glaciation in the main Karoo Basin, South Africa: stratigraphy, depositional controls, and glacial dynamics. In: Fielding, C.R., Frank, T.D., Isbell, J.L. (Eds.), Resolving the Late Palaeozoic Ice Age in Time and Space. Geological Society of America Special Paper, 441, 71-82.

ISO 7404-5, 2009. Methods for the Petrographic Analysis of Coal, Part 5: Methods of Determining Microscopically the Reflectance of Vitrinite. International Organization for Standardization, Geneva, Switzerland, p. 14.

ISO 11760, 2018. Classification of coals. International Organization for Standardization, Geneva, Switzerland, 2nd ed., p. 9.

Jamal, D.L., 2005. Crustal Studies across Selected Geotransects in NE Mozambique: Differentiating between Mozambican (Kibaran) and Pan African Events, with implications for Gondwana Studies. University of Cape Town, unpublished Ph.D. thesis, Cape Town, South Africa.

Johnson, M.R., van Vuuren, C.J., Hegenberger, W.F., Key, R., Shoko, U., 1996. Stratigraphy of the Karoo Supergroup in Southern Africa: an overview. Journal of African Earth Sciences, 23(1), 3-15.

Kreuser, T. and Woldu, G., 2010. Formation of euxinic lakes during the deglaciation phase in the Early Permian of East Africa. In: Late Paleozoic Glacial Events and Postglacial Transgressions in Gondwana, Oscar R. López-Gamundí (Ed.). Geological Society of America Special Paper, 468, 101-112.

Lächelt, S., 2004. Geology and Mineral Resources of Mozambique. Direcção Nacional de Geologia, Maputo, 515 p.

1008

1009 Lakshminarayana G., 2015. Geology of Barcode type coking coal seams, Mecondezi sub-
1010 basin, Moatize Coalfield, Mozambique. International Journal of Coal Geology, 146, 1-13.

1011

1012 Lopes, G., Pereira, Z., Fernandes, P., Marques, J., 2014. Datação palinológica dos sedimentos
1013 glaciogénicos da Formação Tilítica de Vúzi, sondagem ETA 65, Bacia Carbonífera de
1014 Moatize-Minjova, Moçambique: resultados preliminares. Comunicações Geológicas, 101,
1015 Especial I, 481-484

1016

1017 Mariño, J, Marshak, S., Mastalerz M., 2015. Evidence for stratigraphically controlled
1018 paleogeotherms in the Illinois Basin based on vitrinite-reflectance analysis: Implications for
1019 interpreting coal-rank anomalies**.** Amer. Assoc. Petrol. Geol. Bulletin, 99(10), 1803-1825.

1020

1021 McPhilemy, B., 1988. The value of fluorescence microscopy in routine palynofacies
1022 analysis: Lower Carboniferous successions from Counties Armagh and
1023 Roscommon, Ireland. Review of Palaeobotany and Palynology, 56, 345-359.

1024

1025 Mendonça Filho, J.G., Araujo, C.V., Borrego, A.G., Cook, A., Flores, D., Hackley, P., Hower,
1026 J.C., Kern, M.L., Kommeren, K., Kus, J., Mastalerz, M., Mendonça, J.O., Menezes, T.R.,
1027 Newman, J., Ranasinghe, P., Souza, I.V.A.F., Suarez-Ruiz, I., Ujiié. Y., 2010. Effect of
1028 concentration of dispersed organic matter on optical maturity parameters: Interlaboratory
1029 results of the organic matter concentration working group of the ICCP. International Journal
1030 of Coal Geology, 84, 154-165.

1031

1032

1033 Middleton, M.F., 1982.Tectonic history from Vitrinite Reflectance. Geophysical Journal of
1034 Royal Astronomical Society, 68, 121-132.

1035

1036 Montesi, G., 2016. Palynology and Organic Maturation studies of Permian Succession in the
1037 Moatize - Minjova Basin (N'Condédzi sub-basin, Karoo Supergroup, Mozambique) and the
1038 Zagros Basin (Iran). University of Perugia, unpublished MSc thesis, 123 p.

1039

1040 Mugabe, J.A., 1999. Karoo Deposits of Zambezi Graben - Moatize e Tete City Mozambique;
1041 Sedimentary Facies Distribution and Palynological Approach. Univ. Utrecht, unpublished
1042 Ph.D. thesis. 297 p.

1043

1044 Norconsult Consortium, 2007. Notícia Explicativa: Folhas 1039 Muidine, 1040 Palma, 1134
1045 Ponta Messuli, 1135 Lupilichi, 1136 Milepa, 1137 Macalange, 1138, Negomano, 1139 Mueda,
1046 1140 Mocímboa da Praia, 1234 Metangula, 1235 Macaloge-Chiconono, 1236 Mavago, 1237
1047 Mecula, 1238 Xixano, 1239 Meluco, 1240 Quissanga-Pemba, 1334 Meponda, 1335 Lichinga,
1048 1336 Majune, 1337 Marrupa, 1338 Namuno, 1339 Montepuez, 1340 Mecúfi, 1435 Mandimba,
1049 1436 Cuamba, 1437 Malema, 1438 Ribáuè-Mecubúri, 1535 Insaca, 1536 Gúruè, 1635
1050 Milange e 1636 Lugela-Mocuba, Moçambique. Direcção Nacional de Geologia, Ministério
1051 dos Recursos Minerais, Maputo.

1052

1053 Paterson, N.W.; Mangerud, G., Holen, L. H., Landa, J., Lundschien, B. A., Eide, F.,
1054 2018. Late Triassic (early Carnian–Norian) palynology of the Sentralbanken High, Norwegian
1055 Barents Sea. Palynology. doi: https://doi.org/10.1080/01916122.2017.1413018

Pearson, D. L., 1984. Pollen/Spore Color Standard, version No.2 Phillips Petroleum, Exploration Project Section. Bartelsville, Oklahoma.

Pereira, Z., Lopes, G., Fernandes, P., Marques, J., 2014. Estudo palinoestratigráfico da sondagem ETA 72 do Karoo Inferior da Bacia de Moatize, Moçambique - Resultados Preliminares. Actas do IX Congresso Nacional de Geologia/2º Congresso de Geologia dos Países de Língua Portuguesa, Porto, Portugal, 6 p..

Pereira, Z., Fernandes, P., Lopes, G., Marques, J., Vasconcelos, L. 2016. The Permian-Triassic transition in the Moatize-Minjova Basin, Karoo Supergroup, Mozambique: a Palynological Perspective. Review of Palaeobotany and Palynology, 226, 1-19.

Pinna, P., Jourde, G., Calvez, J.Y., Mroz, J.P., Marques, J.M., 1993. The Mozambique Belt in northern Mozambique: Neoproterozoic (1100-850 Ma) crustal growth and tectogenesis, and superimposed Pan-African (800-550 Ma) tectonism. Precambrian Research, 62, 1-59.

Price, L., 1983. Geological time as a parameter in organic methamorphism and vitrinite reflectance as an absolute paleogeothermomether. Journal of Petroleum Geology, 6, 5-38.

Real, F., 1966. Geologia da Bacia do Rio Zambeze (Moçambique). Características geológico-mineiras da Bacia do Rio Zambeze em território moçambicano. 183 p., 57 Plates; 2 Maps. Junta de Investigações do Ultramar. Lisboa.

1080 Robert, P., 1988. Organic Metamorphism and Geothermal History. Elf-Aquitane and Reidel
1081 Publishing, Dordrecht, 311 p.
1082
1083 Silva, G.H., Barreto, L.S., Carvalho, L.H.B., 1967. *Dadoxylon nicoli* (Seward) do Karoo
1084 de Tete. Revista Est. Ger. Univ. Moçambique, 4. Série VI, Ciências Geológicas,
1085 156pp., Lourenço Marques, Moçambique.
1086
1087 Staplin, F.L., 1982. How to assess maturation and palaeotemperatures: Introduction. In:
1088 Staplin, F.L., *et al*. (Eds.), How to Assess Maturation and Palaeotemperatures, pp. 1 and 5.
1089 Society of Economic Paleontologists and Mineralogists, Short Course No.7.
1090
1091 Suárez-Ruiz, I., Flores, D., Mendonça Filho, J.G., Hackley, P.C., 2012. Review and
1092 update of the applications of organic petrology: Part 1, geological applications.
1093 International Journal of Coal Geology, 99, 54-112.
1094
1095 Taylor, G.H., Teichmuller, M., Davis, A., Diessel, C.F.K., Littke, R., Robert, P., 1998.
1096 Organic Petrology. Gebruder Borntraeger, Berlin, p. 704.
1097
1098 Thonnard, R., 1971/1972. Le graben de Moatize au Mozambique. Bulletin Séances,
1099 Académie Royale Sciences Outre-Mer, Bruxelles, 2.
1100
1101 Tissot, B. and Welte, D. H.,1978. Petroleum Formation and Occurrence: A new approach to
1102 oil and gas exploration. Springer-Velag Berlin.
1103
1104 Van Gijzel, P., 1979. Manual of the Techniques and Some Geological Applications of

1105 Fluorescence Microscopy. American Association of Stratigraphical Palynologists Foundation,
1106 Dallas.
1107
1108 Vasconcelos, L., 1995. Contribuição para o conhecimento dos carvões da Bacia Carbonífera
1109 de Moatize, Província de Tete, República de Moçambique. Tese de Doutoramento. Texto
1110 (Volume I), Tabelas, Figuras, Estampas (Volume II). Faculdade de Ciências, Universidade do
1111 Porto, Porto, Portugal.
1112
1113 Vasconcelos, L., 2000. Overview of the Moatize coal basin geology, Tete Province, Republic
1114 of Mozambique. Chron. Rech. Minière, Orléans, 538, 47-58.
1115
1116 Vasconcelos, L., 2013. Coal deposits in Mozambique an overview. Presentation at FFF
1117 Mozambique coal conference, October 2013 - Johannesburg, South Africa.
1118
1119 Viola, G., Henderson, I.H.C., Bingen, B., Thomas, R.J., Smethurst, M.A., Azevedo, S.,
1120 2008. Growth and collapse of a deeply eroded orogen: Insights from structural and
1121 geochronological constraints on the Pan-African evolution of NE
1122 Mozambique. Tectonics 27, TC5009.
1123
1124 Visser, J.N.J., 1989, The Permo-Carboniferous Dwyka Formation of Southern Africa;
1125 deposition by a predominantly subpolar marine ice sheet: Palaeogeography,
1126 Palaeoclimatology, Palaeoecology, v. 70, p. 377–391.
1127
1128
1129

Figure Captions

Figure 1. Simplified geology of the Tete Province, Mozambique, with the location of Karoo basins of the Zambezi River valley and the N'Condédzi, Moatize and Muarádzì sub-basins. Adapted from Geological Map of Mozambique, Direcção Nacional de Geologia, Maputo (2006).

Figure 2. Simplified geology of N'Condédzi sub-basin showing the location of the studied boreholes. Map adapted from Geological Map of Mozambique, sheet no. 1533/1534, Cazula / Zóbuè, Geological Series 1/250000, Direcção Nacional de Geologia, Maputo, 2006.

Figure 3. Lithological log and vitrinite reflectance profile of borehole ZSA-32. The key to lithologies is the same as used in figures 3 to 9.

Figure 4. Lithological log, vitrinite reflectance profile and selected palynomorphs illustrating the variation of TAI of borehole A1TR-018.

Figure 5. Lithological log and vitrinite reflectance profile of borehole TGDH(C)005.

Figure 6. Lithological log, vitrinite reflectance profile and selected palynomorphs showing the range of TAI values and spore/pollen fluorescence of borehole A1TM-085.

Figure 7. Lithological log, vitrinite reflectance results and selected palynomorphs showing the range of TAI values and spore/pollen fluorescence of borehole CIMT-014.

Figure 8. Lithological log and vitrinite reflectance results and selected palynomorphs showing the range of TAI values and spore/pollen fluorescence of borehole A1TM-039.

Figure 9. Lithological log and vitrinite reflectance profile of borehole A1TM-058.

Figure 10. Selected palynomorphs showing the range of TAI values and spore/pollen fluorescence of boreholes A1TM-058 and TDGH(C)005.

Figure 11. Some examples of vitrinite particles found and measured in this study. Above each photograph of vitrinite particles is indicated the borehole, sample reference and the %Ro measured for that particular vitrinite particles, (vitrinite particles were chosen to illustrate grains with %*Ro* values close to the mean %*Ro* value of the sample).

Figure 12. Differences observed in transmitted and fluorescent light between the indigenous and recycled palynomorphs assemblages in borehole CIMT-014: a.) sp. reworked Permian spore (*Leiotriletes directus*) showing no fluorescence (a.1) and pl. Upper Triassic pollen (*Platysaccus queenslandi*) showing yellow fluorescence colour (a.1), sample MQ115; b.) sp. reworked Permian spore (*Polycingulatisporites* sp.) showing no fluorescence (b.1) and pl. unidentified pollen grain, possible Upper Triassic age, showing yellow fluorescence colour (b.2), sample MQ115; c.) sp. Upper Triassic spore (*Rogalskaisporites cicatricosus*) showing strong yellor fluorescence colour (c.1) and sp.1, sp.2, sp.3 reworked Permian spores showing weak fluorescence or no fluorescence (c.1), sample MQ111; d.) sp. reworked Permian spore

(*Densoisporites* sp.) showing no fluorescence (d.1) and pl. two unidentified pollen grains, possible Upper Triassic age, showing strong yellow fluorescence colour (d.1), sample MQ111.

Figure 13. Calculated palaeogeothermal gradients for the boreholes studied. For boreholes A1TM-039 and CIMT-014 due to the reduced number of samples with VR results palaeogeothermal gradients were not calculated.

Figure 14. Schematic cross-sections illustrating the tectonic and thermal evolution of the Permian - Triassic Karoo rocks of the N'Condédzi sub-basin. Figures not to scale. (**a**) Late Guadalupian: extensional basin initiation by the tectonic reactivation of Precambrian shear zones, forming half-graben sedimentary basins. (**b**) Late Lopingian to Lower Triassic: fault-induced subsidence and deposition of very thick sequences (>1000 m). Beginning of hot diagenetic fluid flow driven only by lithostatic pressure. **(c)** Upper Triassic: after a phase of non-deposition during the Middle Triassic, deposition of Upper Triassic red beds together with reworked Permian palynomorphs from the neighbouring Karoo basins, re-burial of the Permian – Lower Triassic sequences. (**d**) Schematic cross-section of the N'Condédzi region showing the position of some of the boreholes studied.

Table 1. Organic maturation results and palaeotemperatures (^{o}C) calculated using method described by Barker (1988) for the boreholes of the N'Condédzi sub-basin. All samples are black carbonaceous mudstones or black/grey mudstones. R_O (%) - vitrinite reflectance values, SD - standard deviation, Fluo. - spore fluorescence colours (Y – yellow, DY – dark yellow, DO - dark orange, R - red), spore colour TAI - Thermal Alteration Index, * - samples with vitrinite reflectance values due to heating effects of dolerite intrusions (details in Table 2), and TAI Reworked / Fluo. Reworked, refers to the reworked palynomorph population of

boreholes CIMT-014 and A1TM-039.

Table 2. Vitrinite reflectance values of the dolerite heat affected samples, showing also its relations to the dolerite sills, namely the distance of the samples to the nearest intrusion wall and the thickness of the nearest intrusion (distance in metres).

Thermal history and basin evolution of the Moatize - Minjova Coal Basin (N'Condédzi sub-basin, Mozambique) constrained by organic maturation levels

Francesca Galasso[1,2]*, Paulo Fernandes[2], Giovanni Montesi[1], João Marques[3], Amalia Spina[1], Zélia Pereira[4]

1. Department of Physics and Geology, University of Perugia.Via Pascoli, 06123 Perugia, Italy
2. Centro de Investigação Marinha e Ambiental (CIMA), Universidade do Algarve, Campus de Gambelas, 8005-139 Faro, Portugal
3. Gondwana Empreendimentos e Consultorias, Limitada, Rua B, no. 233, Bairro da COOP, Caixa Postal 832, Maputo, Mozambique
4. Laboratório Nacional de Energia e Geologia (LNEG), Rua da Amieira, Apartado 1089, 4466-901 S. Mamede Infesta, Portugal

* Corresponding author: francescagalasso1992@gmail.com

Abstract

Kerogen concentrates obtained from Lopingian (Late Permian) to Upper Triassic mudrock lithologies of seven coal exploration boreholes, drilled in the Moatize – Minjova Coal Basin (N'Condédzi sub-basin, Mozambique), were studied by means of vitrinite reflectance (VR), spore fluorescence and spore colour, in order to constrain the thermal history and basin evolution by organic maturation levels. VR increases with depth, indicating organic maturation related to sediment burial for most of the boreholes. Modelled VR data indicate a

regional palaeogeothermal gradient between 35 and 40ºC/km. Lower Jurassic doleritic intrusions observed in three boreholes had only local thermal effects without affecting the regional palaeogeothermal gradient. Two boreholes located near the basin margin show high palaeogeothermal gradients suggesting thermal processes other than heating due to burial were involved. These processes may have involved hot diagenetic fluids circulating through fault zones and/or permeable lithologies, locally elevating geothermal gradients. Circulation of these fluids was induced by lithostatic pressure due to rapid rates of sedimentation. These high sedimentation rates lead to the accumulation of a thick succession (over 2000 m) of Lopingian (Late Permian) to Upper Triassic siliciclastic sediments. All the organic maturation indices measured and the age of the successions indicate that organic maturation occurred during or after Late Triassic times. However, the presence of reworked Permian palynomorphs into Upper Triassic sediments and the absence of Middle Triassic sediments indicate an exhumation and erosion of Permian strata in Middle Triassic times. The organic maturation levels of the reworked palynomorph population are considerably higher than the indigenous Upper Triassic population, indicating that they attained higher burial temperatures prior to being reworked.

Keywords: Karoo, Mozambique, Organic maturation, Permian – Triassic, Reworked palynomorphs, Moatize – Minjova Coal Basin, Vitrinite Reflectance

1. Introduction

The Karoo Supergroup (KSG) of Southeastern Africa comprises sedimentary and volcanic rock units that span a time interval of Late Carboniferous to Early Jurassic, and which attained a considerable thickness (more than 7000 m) in some basins (Johnson et al., 1996; Cairncross, 2001; Catuneanu et al., 2005). Regardless of tectonic processes related to individual basin formation and subsequent geological development the stratigraphy of the KSG is very consistent across all basins where it is preserved (Johnson et al., 1996; Catuneanu et al., 2005, Hancox, 2016). The sedimentary successions reflect major palaeogeographical and climatic changes during the development of the Karoo basins (Catuneanu et al., 2005; Götz and Ruckwied, 2014; Götz et al., 2017). In central-west Mozambique, sediments of the KSG are well represented in various basins situated along the Zambezi River valley in the Tete Province (GTK Consortium, 2006) (Fig. 1). In these basins the KSG, normally, rests unconformably over crystalline Precambrian basement rocks, and the base of the stratigraphic succession consists of conglomerates and mudrocks of the Dwyka Group (Pennsylvanian to Cisuralian) comparable to the Main Karoo Basin of South Africa. These conglomerates were, deposited by waning and waxing of glaciers of the Late Palaeozoic glaciations of Gondwana (Visser, 1989, Isbell et al., 2008). The northward drift of Gondwana to lower latitudes during the Permian, caused more temperate climate conditions to establish throughout this paleocontinent. Glaciation was terminated by late Palaeozoic times and in basins located north of the Main Karoo Basin (South Africa), sedimentation mostly took place in continental environments characterized by river systems and freshwater lakes (Cairncross, 2001; Kreuser and Woldu, 2010; Götz and Ruckwied, 2014). The sedimentary record of these times corresponds to the siliciclastic-dominated, coal-bearing lithologies of the Cisuralian to Guadalupian Ecca Group (Cairncross, 2001; Catuneanu et al., 2005, Hancox, 2016). At present, the existence of widespread coal seams interbedded in the Ecca Group stratigraphic

74 sequence, represents an important natural resource and asset for Mozambique's economy
75 (Vasconcelos, 2000, 2013). Overlying the Ecca Group are siliciclastic-dominated stratigraphic
76 sequences belonging to the Beaufort Group (Lopingian - Middle Triassic) and the Stormberg
77 Group (Late Triassic - Early Jurassic). The sediments of these two groups were deposited by
78 major river systems or aeolian processes in desert environments under hot and arid climatic
79 conditions (Johnson et al., 1996; Catuneanu et al., 2005). The contact between the Beaufort
80 Group and the overlying Stormberg Group corresponds to a hiatus that spans most of the
81 Middle Triassic (Catuneanu et al., 2005). The KSG is capped by the Lower Jurassic volcanic
82 rocks (*ca.* 183 Ma) of the Drakensberg Group, which are related to the Karoo - Ferrar Large
83 Igneous Province and pre-date the break-up of Gondwana (Duncan et al., 1997).
84
85 Thermal history analysis is an essential part of any study of sedimentary basins and their
86 hydrocarbon source rock potential. There are several optical methods that can be used to
87 estimate maximum temperatures attained by strata during subsidence and interpret their
88 thermal history (Price, 1983). Vitrinite reflectance (VR) is an optical method considered to be
89 a reliable indicator of the organic matter maturity levels of sedimentary rocks (Hunt, 1996;
90 Robert, 1988; Tissot and Welte, 1978). Since maturity levels are largely related to
91 temperature, VR is also a good indicator of peak (palaeo-) temperatures, which accounts for
92 its widespread use in basin analysis (Middleton, 1982; Corcoran and Clayton, 2001;
93 Fernandes et al., 2012, 2013, 2015; Mariño et al., 2015). Other optical methods, such as spore
94 colour (TAI) and spore fluorescence provide a rapid evaluation of organic maturation levels,
95 complementing the information attained by VR (Van Gijzel, 1979; McPhilemy, 1988; Suárez-
96 Ruiz et al., 2012). Fernandes et al. (2015) studied the thermal history of the Lopingian KSG
97 sediments of the Moatize – Minjova Coal Basin combining VR and Apatite Fission Track
98 Analysis (AFTA) of two boreholes located in the Moatize sub-basin (Fig. 1). These authors

99 concluded that maturation levels corresponded to a coal rank of medium rank B and A coals
100 (1.3 - 1.7%*Ro*). Maturation levels increase linearly downhole in the two studied boreholes,
101 indicating that burial with a constant geothermal gradient was the main process controlling
102 peak temperature. The thermal model for the history of the basin proposed by Fernandes et al.
103 (2015), indicates that peak burial temperatures were attained shortly (3 - 10 Ma) after
104 deposition in Lower Triassic times. The thermal model also indicates two episodes of cooling
105 and exhumation: a first period of rapid cooling between 240 and 230 Ma (Middle– Late
106 Triassic boundary) implying 2500 - 3000 m of denudation; and a second period, also of rapid
107 cooling, from 6 Ma (late Miocene) onwards implying 1000 - 1500 m of denudation.
108
109 In the present work, a detailed account of the organic maturation levels assessed by different
110 optical methods (VR, spore colour and spore fluorescence) of seven boreholes drilled for coal
111 exploration is described. The boreholes are located in the N'Condédzi sub-basin of the
112 Moatize – Minjova Coal Basin (Figs. 1 and 2). This study allowed the evaluation of the
113 maturity of organic matter and the thermal history of the KSG sedimentary succession in the
114 N'Condédzi region, and helps to constrain the tectonic model for the development of the
115 Karoo Basin in this region.
116
117 **2. Geological setting of the Moatize – Minjova Coal Basin in the N'Condédzi sub-basin**
118 Differences in the stratigraphy, tectonic setting and geographic position of KSG outcrops
119 along the Zambezi river valley in Mozambique, allow their division into three different coal-
120 bearing basins, which are, from west to east, the Chicôa – Mecúcoè, Sanângoè – Mefidézi and
121 the Moatize – Minjova Coal Basins, respectively (Lächelt, 2004; GTK Consortium, 2006)
122 (Fig. 1). These basins are part of a network of rift related basins that formed north of the
123 South African Main Karoo Basin, during the Permian to Lower Jurassic time interval. The

Zambezi River valley basins developed during brittle reactivation of high strain zones (e.g. the Sanângoé and Mzarabani shear zones) (Fig. 1) of the Zambezi Belt. This mobile belt formed between the Congo and Kalahari Cratons during the Pan-African Orogeny (620 – 530 Ma) (Carvalho, 1977; Afonso, 1984; Pinna et al., 1993; Jamal, 2005; GTK Consortium, 2006; Norconsult Consortium, 2007; Grantham et al., 2008; Viola et al., 2008). The tectonic fault-related reactivation started in the Cisuralian (early Permian) by the initiation of strike-slip faulting under a transtensional stress regime that formed extensional basins with a graben to half graben geometry (Carvalho, 1977; Hankel, 1994; Lächelt, 2004; Catuneanu et al., 2005; GTK Consortium, 2006).

The boreholes used in this study were drilled in the N'Condédzi sub-basin of the Moatize-Minjova Coal Basin, which is approximately 50 km long and 25 km wide, and is located *ca*. 70 km northeast of Tete City (Figs 1 and 2). Its margins are faulted against the Mesoproterozoic Tete Suite (Gabbro-Anorthosite) to the SW and the Mesoproterozoic gneiss and granite rocks of the Furancungo Suite to the N by the WNW –ESE trending Mwanza Fault.

The complete Karoo stratigraphic succession of the Moatize - Minjova Coal Basin is thicker than 800 m (Real, 1966; Thonnard, 1971/1972; Afonso, 1975; Vasconcelos, 1995; Mugabe, 1999; Lächelt, 2004; GTK Consortium, 2006), whereas in the N'Condédzi sub-basin Lakshminarayana (2015), a Lower Karoo succession with a thickness of more than 900 m is reported. The base of the succession consists of the tillites of the Vúzi Formation, which overly unconformably Precambrian basement rocks. However, the type section for this formation was defined in the area of the Mucanha and Vúzi Rivers (Carvalho, 1977) belonging to the Chicôa-Mecúcoè Basin, located upstream in the Zambezi River valley (Fig.

1). In the Mucanha-Vúzi area, the Vúzi Formation consists of 10 m-thick ill-bedded matrix supported red conglomerates that are conformably overlain by 10 m-thick mud supported grey-black conglomerates. Due to the lack of conclusive evidences of glacial action (transport and deposition), such as, striations on surfaces of the basement rocks and on surfaces of the clasts in the conglomerates, and dropstones and varve-like sedimentary rhythms, Carvalho (1977) interpreted these conglomerates, not as glacial deposits, but probably as coarse alluvial fans. These coarse clastic beds were probably deposited at the base of, and adjacent to, fault scraps, where the topographic relief was created by vertical fault movements coeval to the formation of the Karoo rift basins. Recently, a *ca.* 130 m thick succession of the Vúzi Formation, cropping out in the Murrongódzi River, was described in the Moatize - Minjova Basin by Achimo et al. (2014). The bulk of the succession consists of ill-sorted matrix-supported conglomerates showing typical features of glacial to sub-glacial transport and deposition, interpreted as being formed by the advance and retreat of ice caps over lakes and fluvio-glacial plains. From the description of the Vúzi Formation in the different Karoo basins of the Zambezi River valley, it is evident that it was deposited in a variety of sedimentary environments and tectonic conditions, which require further research in order to ascertain the relations between different processes and, possibly, the age and *tempus* of the accumulation of the sediments.

The coal-bearing Moatize Formation conformably overlies the Vúzi (Tillite) Formation and consists of interbedded carbonaceous mudstones, siltstones, sandstones and coal beds interpreted as fluvial and lacustrine sediments deposited under wet temperate climatic conditions. In the Moatize region, the formation attains a thickness of *ca*. 300 - 400 m (Real, 1966; Afonso, 1976; GTK Consortium, 2006) and has six main coal seams, which are known locally as “Carbonaceous Complexes.” These “Complexes” consist of interbedded plant-rich

carbonaceous mudstones and coal beds of variable thickness. Palaeoassemblages (plant macrofossils and palynomorphs) suggest Cisuralian-Guadalupian (Early to Middle Permian) age for the upper part of the Moatize Formation, correlated with the Middle-Late Permian age Ecca Group of the Main Karoo Basin in South Africa (Daber, 1984). However, recent palynological revision of the upper part of the Moatize Formation that was penetrated by two coal exploration boreholes (DW123 and DW132) indicates that this part of the Moatize Formation reaches the latest Permian, with the Permian-Triassic boundary identified at *ca.* 42 m depth in borehole DW132 (Pereira et al. 2016).

The Moatize (Sandstone) Formation is overlain by a thick sequence (*ca.* 4 km) of siliciclastic rocks divided into two stratigraphic units, the Matinde (Marl-Sandstone) Formation at the base, and the Cádzi (Sandstone) Formation at the top (GTK Consortium, 2006). Both formations were deposited in fluvial to possibly desert environments, recording the transition from seasonal temperate to hot arid climatic conditions. Due to the lack of biostratigraphic markers in both formations, the Matinde Formation is correlated to the Middle-Upper Ecca Group of the Main Karoo Basin of South Africa (Silva et al., 1967), whereas the Cádzi Formation is correlated with the Beaufort Group of the same basin. With the exception of few 1 - 3 m thick doleritic dykes and sills that intrude the sedimentary formations, the volcano-sedimentary lithologies of Lower Jurassic age that capped the KSG, and are correlated with the Stormberg Volcanics of the Main Karoo Basin, are not well represented in the Moatize-Minjova Coal Basin (Vasconcelos, 1995).

Lakshminarayana (2015) compared the stratigraphic succession of the KSG in the N'Condédzi sub-basin with the succession described for the Moatize sub-basin. The Vúzi Formation rests unconformably on gabbros and anorthosites of the Mesoproterozoic Tete

Suite. The Vúzi Formation consists of clast-supported conglomerates interbedded with sandstones, siltstones and carbonaceous shales forming thinning and fining upward cycles. The top part of the Vúzi Formation is characterized by a sequence known as the *Transitional Assemblage* consisting of sandstones, interbedded with carbonaceous shales and coal beds. This formation is *ca*. 60 – 140 m thick. The succeeding Moatize Formation attains a maximum of 900 m thick in the N'Condédzi sub-basin and consists of interbedded meter thick coal seam, sandstones, siltstones and carbonaceous shales. No new biostratigraphic information was provided by Lakshminarayana (2015) on the age of the Vúzi and Moatize formations in this sub-basin and, therefore, this author correlated these formations with the Pennsylvanian (Late Carboniferous) to Cisuralian (early Permian) Dwyka Group and the Permian Ecca Group, respectively.

3. Materials

The samples analysed in this study were obtained from seven coal exploration boreholes drilled in the N'Condédzi sub-basin (Fig. 2). Black carbonaceous shales, black shales, grey mudstones and grey siltstones, were the main lithologies sampled for organic maturation studies. Coal was not sampled because it was not present in the cores during the sampling. The coal seams were sampled earlier by the exploration companies that owned the mining rights of the area, and shipped to laboratories to assess its quality. The boreholes studied were chosen in order to represent all the stratigraphic units of the KSG present in the N'Condédzi sub-basin. Five of the boreholes studied intersected the basement at different depths, representing the coal bearing units that characterize the lower units of the stratigraphy (Moatize Formation), whereas two boreholes penetrated the *ca*. 500 m thick successions consisting mainly of red bed lithologies that represent the upper stratigraphic units (Matinde and Cádzi formations) of the KSG in sub-basin. One hundred and seventy two samples of the

lithologies indicated were processed for organic maturity analysis and palynology studies. One hundred and one samples yielded organic material suitable for these studies, however, seventy-one samples from boreholes A1TR-018, A1TM-039, TGDH(C)005 and CIMT-014 were barren.

3.1. Borehole ZSA-32

This borehole is located near the southern margin of the Karoo outcrop in the N'Condédzi sub-basin (Fig. 2). It has a total depth of 220 m, and penetrated at its base a 5 m thick sequence of the basement rocks of the Tete Suite, consisting of gabbros (Fig. 3). The latter lithologies are unconformably overlain by a 3 m thick bed of clast-supported conglomerates intercalated with very thin beds red siltstones and mudstones, positioned immediately above the unconformity. These red lithologies caused the red staining of the altered gabbros below the unconformity. These two features, red stain of the basement and red lithologies, are more compatible with deposition under oxidizing sub-aerial conditions, rather than glacial to peri-glacial environments of the Dwyka time. The succession in the borehole interval from 209 m to 180 m, consists of black carbonaceous shales capped by a 2 m thick coal bed. This is followed by an interval from 180 m to 62 m, characterized by coarse to medium grained sandstones interbedded with shales and siltstones and some coal beds. A 10 m thick coal bed caps the latter borehole interval. The upper part of the borehole from 50 m to the top of the borehole consists of sandstones interbedded with siltstones and shales. The succession in this borehole is also intruded by several doleritic sills (Fig. 3).

3.2. Borehole A1TR-018

Borehole A1TR-018 was drilled to a total depth of *ca*. 91 m, and penetrated Karoo sediments overlying crystalline basement rocks represented by gabbros of the Tete Suite at *ca*. 85 m

depth (Fig. 4). This borehole is located only 1 km (direction) from the outcrop, which includes the contact between the Tete Suite and Karoo Supergroup in the N'Condédzi sub-basin (Fig. 2). A 1 m clast-supported conglomerate bed unconformably overlies the Precambrian basement. The conglomerate grades upward into a 4 m thick bed of carbonaceous shales, followed upwards by *ca.* 6 m thick sandstone-siltstone dominated interval and a 4 m thick clast-supported conglomerate interval interbedded with very thin beds of shale. The upper part of the core consists of a 70 m sequence dominated by sandstones and siltstones beds interbedded with thin to very thin beds of shales, followed upward by a 10 m thick shale dominated interval.

3.3. Borehole TGDH(C)005

This borehole was drilled in a small outcrop area of the Karoo Supergroup surrounded by the Mesoproterozoic Tete Suite (Fig. 2). It has a total depth of *ca*. 230 m and penetrated, an 11 m thick sequence of basement rocks consisting of anorthosites (Fig. 5) at the base. These are unconformably overlain by about 38 m of coarse- to medium-grained sandstone and siltstone beds interbedded with thin to very thin beds of shales belonging to the KSG. This situation indicates the absence of the conglomerate beds that usually characterize the base of the KSG, in the Moatize and in other Karoo basins, suggesting that the base of Karoo Supergroup is diachronous in this sub-basin. The latter sandstone-siltstone interval is followed by approximately 70 m of dominantly siltstones and shales with thin beds of coal concentrated in the 162 – 168 m and 110 – 123 m depth intervals. In the interval between 98 m and 68 m, coarse- to medium-grained sandstone beds are interbedded with very thin beds of siltstones and shales. The interval from 68 m depth up to the top of the core consists of shales, carbonaceous shales and several thin beds of coal, typical of barcode coals.

3.5. Borehole A1TM-085

This borehole has a total depth of ca. 727 m and penetrated a 2 m thick sequence of basement rocks consisting of anorthosites belonging to the Tete Suite at its base (Fig. 6). The basement rocks are unconformably overlain by about 55 m of clast to matrix support conglomerates interbedded with siltstones, sandstones, and shales. Approximately 160 m of dominantly shales, carbonaceous shales, siltstones and thin beds of coals follow the latter conglomerate dominant interval. A coarser-grained interval consisting of siltstones, medium- to coarse-grained sandstones and thin beds of shales are positioned between approximately 415 m and 282 m depth. From 282 m to 18 m depth the succession consists of shales, carbonaceous shales and several thin beds of coal. The top, 18 m of this core consists of coarse- to medium-grained sandstones. The succession in this core is intruded by dolerite sills concentrated in the depth interval between 340 m and 90 m. The sill thickness is 1 – 2 m on average but at approximately 160 m, a conspicuous 12 m thick doleritic sill occurs that caused sufficient heating to affect the VR results (section 5).

3.4. Borehole CIMT-014

This borehole has a total depth of 500 m and mostly consists of siliciclastic red bed lithologies (Fig. 7). The top of the Mesoproterozoic basement was not penetrated. From the base to 470 m, the succession changes in both lithology and sedimentary features. This basal 30 m thick succession consists of medium- to coarse-grained grey sandstones interbedded with laminated grey siltstones and carbonaceous shales, the red sediment colours, which is characteristic for most of the core is absent in this basal interval. Two prominent coarse-grained sandstone dominant intervals are present, the first between 310 m and ca. 470 m, and the second between 210 m and 260 m depth. These intervals consist of coarse-grained (sometimes

conglomeratic) to medium-grained red sandstones interbedded with red to brown mudstones and siltstones. The interval from 310 m and 260 m depth of the is characterized by fine-grained lithologies dominated by red mudstones interbedded with thin beds of grey mudstones and brown siltstones, with few beds of coarse-to medium-grained red sandstones. Another fine-grained dominated interval with the same lithological features is found between 210 m depth and the top of the borehole.

3.6. Borehole A1TM-039

This borehole was drilled to total depth of *ca*. 600 m, and consists mainly of red siliciclastic lithologies (Fig. 8). This succession exhibits many lithological similarities with borehole CIMT-014. However, it differs by a higher dominance of coarse-grained siliciclastic rocks. Accordingly, from the base to 470 m depth, the succession is dominated by red to brown siltstone beds interbedded with red mudstones and few thin beds of grey mudstones and red sandstones, whereas the interval between 470 m and 350 m is characterized by thick, red to purple sandstone beds. Between 350 m and the top of the core, the succession consists of thick beds of coarse- to medium-grained red sandstones intercalated with thick beds of brown siltstones and red mudstones.

3.7. Borehole A1TM-058

With a total depth of 1000 m, borehole A1TM-058 (Fig. 9) is the deepest of all the boreholes studied, consisting mainly of fine-grained siliciclastic lithologies (shales and siltstones). At its base a 4 m sequence of gabbros – anorthosites belonging to the Tete Suite was penetrated. The latter lithologies are unconformably overlain by red siltstones, fine-grained sandstones, and red mudstones that grade upwards immediately into black carbonaceous shales interbedded with two intervals of clast- to matrix-supported conglomerates up to *ca*. 930 m

depth. The top of the basement rocks is red stained and the features of the lithologies above the unconformity, also suggest sub-aerial sedimentary conditions and the probable formation of soils, rather than sedimentation under glacial to peri-glacial conditions prevalent during the deposition of the Dwyka type lithologies. The interval between 930 m and 750 m in the succession is characterized by a cyclic repetition of siltstone and sandstone interbedded with shales. This is followed by a very thick interval from 750 m to 190 m, consisting mainly of black carbonaceous shales, shales, siltstones and coal beds. The latter interval also included more coarse-grained lithologies, consisting of sandstones and siltstones especially between 610 m and 490 m depth. From 190 m depth to the top of the core, the succession consists of coarse- to medium-grained grey sandstones alternating with laminated siltstones, carbonaceous shale and thin beds of coal. The occurrence of several doleritic sills is characteristic for the succession of this borehole.

4. Organic matter extraction techniques and methods of organic maturation assessment

One hundred and seventy two mudrock core samples were used for thermal maturity analysis using the laboratory facilities of CIMA, Universidade do Algarve. Twenty grams of mudrock were crushed and placed in a 50 mL Falcon tube. To the crushed rocks was added a few drops of HCl to test for carbonates. Since all the samples proved to be devoid of carbonates, the crushed mudrock samples were treated with HF (40%) until all the silicates were dissolved. Then the organic residue obtained was rinsed and decanted several times using distilled water until the organic residue was fully neutralized. Afterwards, the samples were sieved using a 15µm mesh sieve. For spore fluorescence, spore colour and palynological analysis, the organic residues were mounted on palynological slides using acrylic resin Elvacite®.

4.1. Vitrinite Reflectance

The obtained organic residues were mounted and polished after the method by Hillier and Marshall (1988). Mean random vitrinite reflectance in oil immersion (%*Ro*) was the vitrinite reflectance (VR) parameter chosen for thermal maturity assessment, because the methodology adopted accounts non-oriented vitrinite particles. For vitrinite identification and measurement several criteria were taken into account following the guidelines recommended by the ASTM D7708-14 (2014), ISO 7404-5 (2009) and the International Committee for Coal and Organic Petrology (1998). VR measurements on all samples was performed at the University of the Algarve, Portugal, using an Olympus BX 51 microscope equipped with a black and white Olympus XC-50 digital camera. The greyscale (8-bit) digital images of vitrinite particles were analysed using the graphical tool VITRINITE, which runs within the Mirone Suite and calibrates the scale of 256 grey levels with standards of known reflectivity (Fernandes *et al.*, 2015). The reflectance values of the standards used were: 0.00 %, 0.428 %, 0.595 %, 0.897 %, 1.314 %, 1.715 %, 3.15% and 5.37 %. VR was measured in non-polarized incident light with a wavelength of 546 nm and immersion oil with a refractive index of 1.518 at a room temperature of 20ºC. Figure 11 shows some photographs of vitrinite particles which reflectance values was measured for this study. One hundred random reflectance values were measured across the polished thin sections and their arithmetic mean and standard deviation were calculated (Table 1). The arithmetic mean was considered to be the true $\%R_O$ for the sample.

As described in Section 3, the stratigraphic sections of three of the boreholes studied (ZSA-32, A1TM-058 and A1TM-085) were intruded by doleritic sills. Some of the samples of these three boreholes, close to the intrusion walls, have high vitrinite reflectance values (Table 2).

372 The high vitrinite reflectance values measured for these samples, are attributed to the
373 localized heat effect of the igneous intrusion in the aureoles and not to burial heat (see Section
374 7. Discussion). Hence, the vitrinite reflectance measured in the later samples (Table 2) were
375 not included neither in the calculation of burial palaeotemperatures and palaeogeothermal
376 gradients, nor in the estimation of eroded covers (see Section 6. Interpretation of organic
377 maturation results). However, the vitrinite reflectance values of the heat affected were
378 important for the thermal history discussion of the studied region.

379

380 ***4.2. Spore fluorescence and spore colour***

381 Qualitative spore fluorescence and spore colour are two optical parameters of thermal
382 maturity of organic maturation, useful for evaluating maturation levels of low-rank rocks until
383 the end of the oil window (1.35 - 1.5%*Ro*) (Van Gijzel, 1979; McPhilemy, 1988; Suárez-Ruiz
384 et al., 2012). When correlated with the quantitative VR method, spore fluorescence and colour
385 parameters can provide additional support for the thermal maturity of the rocks. Maturation
386 causes a gradual shift in organic matter fluorescence colours (red shift) from the shorter to the
387 longer wavelengths, that is, blue and green to yellow, orange and finally red. Of all the
388 macerals of the liptinite group, sporinite is the one that shows the most consistent changes in
389 fluorescence colour spectra and intensity with increasing maturation. Under fluorescence
390 excitation, it changes colour from green through yellow to orange and finally red, with
391 increasing maturity to the top of the oil-window, after which it no longer fluoresces. A
392 phenomenon frequently noticed in fluorescent palynomorphs is the fading effect (van Gijzel,
393 1979). The fading effect is due to a photochemical modification of the fluorescing organic
394 matter during prolonged blue light exposure, (30 minutes to 2 hours or more). During this
395 lengthy exposure the intensity of fluorescence may increase or decrease; if it increases, the

fading is said to be positive, conversely, if it diminishes is negative. In other words, the emitted fluorescence spectrum may move either towards higher wavelengths (red band) or towards shorter wavelengths (green band), the fading is said to be positive in the first case and negative in the second.

The analysis of qualitative spore fluorescence colours was undertaken in the University of the Algarve using an Olympus BX 51 microscope equipped with a metal halide lamp fluorescence unit; XCite Series 120Q and with a violet and Blue +12 filter block that generates a wavelength band of 390 - 490 nm. This system was allowed to stabilize for 5 min before any observation of the fluorescence of palynomorphs was attempted. Suitable spore species with smooth and medium thick exine, such as *Densoisporites* spp., were subjected to 5 minutes of excitation, after which their fluorescence colours were recorded. The same spores were exposed for a further thirty minutes to record any fading effects. The terminology used for describing fluorescence colours was blue (B), green (G), yellow (Y), dark yellow (DY), orange (O), dark orange (DO) and red (R).

Spore exine colour has long been suggested by palynologists as a method to assess the thermal maturity of sedimentary rocks, because they observed that, with increasing burial depth, spore colour changes from light to dark and that the change is progressive and irreversible (Correia, 1971; Staplin, 1982). In this study, spore colour was recorded using the Phillips Petroleum Colour Standard version no. 2 (Pearson, 1984), which is an adaptation of Staplin's Thermal Alteration Index (TAI) chart, because it includes more shades for the same colour index. The spore colour index for the samples was given by the colour of the dominant and lightest spores observed and compared with the Phillips Petroleum Colour Standard chart. The results of spore colour determination are presented together with VR measurements and

spore fluorescence colours for each sample (Table 1). Figures 3 to 10 show the main features of spore colour and spore fluorescence in the boreholes studied. Spore colours were recorded for acamerate, azonate trilete or monolete spores with a smooth exine of medium thickness, such as *Densoisporites* spp. and *Laevigatosporites* spp., which occurs throughout the section of both boreholes studied by (Pereira et al., 2016).

As mentioned above, both spore fluorescence and spore colour are qualitative methods for assessing organic maturation. The visual evaluation of the fluorescence colours and the colours the palynomorph walls is subjective, depending on the experience of the operator and lacking, therefore, the objectivity of VR. The lack of universally accepted standards of organic maturation, as VR, is another drawback of these two methods. Moreover, it has been reported (Mendonça Filho et al., 2010), that the acid treatment used to obtain kerogen concentrates (HCl and HF maceration) affects the fluorescence spectra of liptinites, shifting it to higher wavelengths (red-shift), when compared with the fluorescence spectra of whole rock samples. Despite these problems, spore fluorescence and spore colour, used together with VR are still important parameters of organic maturation, especially for low and medium rank rocks.

5. Organic Maturation and Palynological Results

Data of the thermal maturity analyses, both quantitative (VR) and qualitative (spore fluorescence and TAI), are shown in Table 1 and in VR profiles of the studied boreholes, which illustrate the change of the organic maturation indicators with burial depth (Figs. 3 to 9).

5.1. Borehole ZSA-32

Thirteen samples were processed from ZSA-32 and they were all suitable for organic maturation studies, whereas only three samples of the thirteen were suitable for palynological studies. The VR values measured show a linear increase with depth in the borehole, ranging from 1.21%*Ro* at the top to 1.31%*Ro* at the bottom (Fig. 3). Spore fluorescence colours change intensity from orange at the top, to dark orange at the bottom of the borehole, indicating palaeotemperatures close to the fluorescence extinction. TAI values also change from 3 to 3/3+ with increasing depth. Six samples were affected by heating by dolerite intrusions and have TAI colours of 4-/4 or 5. In general, TAI and fluorescence of the samples not affected by the intrusions indicate a thermal maturity at the onset of the oil-window, and VR values indicate a coal rank of medium rank B (ISO 11760, 2018).

Palynological analysis of ZSA-32 samples revealed an assemblage characterized by bisaccate taeniate pollen grain such as *Luckiesporites virkkiae*, *Lunatisporites pellucidus*, *Guttulapollenites hannonicus* and monolete spores such as *Laevigatosporites colliensis.* These assemblages indicate a Lopingian (late Permian) age for the entire succession of this core (Montesi, 2016).

5.2. Borehole A1TR-018

Twenty-two samples from A1TR-018 were studied for palynology and organic maturation, but after laboratory processing, only six samples were suitable for maturation studies and thirteen samples yielded palynomorphs. VR values measured from the *ca*. 80 m thick succession of this borehole increase downhole, from 1.51%*Ro* at the top to 1.72%*Ro* at the bottom at depth of *ca*. 70 m (Fig. 4). Spore colours showed consistent TAI values of 3+/4- throughout the succession, which is fully consistent with the VR values measured. The thermal maturity obtained from this core indicates that the sedimentary succession straddles in the wet and dry gas zone of hydrocarbon generation. In terms of coal rank, VR values indicate

a medium rank A (ISO 11760, 2018). All the samples studied for palynology yielded an assemblage characterized by rare trilete spores and colpate pollen grains, abundant monossaccate and rare to common bissaccate (taeniate and non-taeniate) pollen. This assemblage shows similarity to the one described by Pereira *et al*. (2014) from the borehole ETA 72 located in the Muarádzi sub-basin (Fig. 1) and, therefore, is interpreted to be of Kungurian / Roadian age with *Alisporites* sp., *Cycadopites* sp., *Florinites* spp., *Potoniesporites* sp., *Striatopodocarpites cancellatus, S. fusus Protohaploxypinus* sp. and *Vittatina* sp.

5.3. Borehole TGDH(C)005

Twenty five samples were processed for both thermal maturity and palynological analysis but just twenty and twelve samples from borehole TGDH(C)005 were studied for palynology and organic maturation, respectively. The lowest maturation levels in this part of the Moatize – Minjova Basin were detected in this borehole. VR values range from 0.97%*Ro* at ca. 20 m depth to 1.15%*Ro* at 206 m depth. VR increases linearly with depth with a good correlation coefficient of $R^2 = 0.92$ (Fig. 5). In terms of hydrocarbon generation the entire succession in this borehole lies within the oil-window. Consistent TAI values of 2 were recorded for this borehole, with the exception of one sample from the bottom of the borehole with a TAI value of 2+. All samples show positive fluorescence with yellow to dark yellow colours (Fig. 10). Fluorescent samples also show a positive fading effect. The maturation levels measured straddle the boundary between medium rank C and B coals (ISO 11760, 2018) in terms of coal rank. The microfloristic assemblage recorded in this borehole show affinities with the assemblage described by Pereira et al. (2016) from borehole DW 123 located in the Muarádzi sub-basin (Fig. 1), that indicates a Lopingian age based on the presence of the key species, as *Lueckiesporites virkkiae*, *Guttullapollenites hannonicus, Polypodiisporites* sp., *Thymospora*

494 sp., and *Weylandites lucifer*.

495

496 ***5.4. Borehole A1TM-085***

497 Ten samples were processed for both maturity and palynological studies, being all suitable for
498 these studies. VR values measured increase downhole from 1.43%*Ro* at 138 m depth to
499 1.56%*Ro* at 731 m depth (Fig. 6). The VR profile shows a linear increase in reflectance with
500 depth of burial, defining a gradient with a correlation coefficient of $R^2 = 0.83$. Maturation
501 levels indicated by VR fall in the wet gas zone for all the samples of this borehole. TAI values
502 of 3+/4- were obtained from most of the samples that contained suitable spores. However, in
503 three samples between depths *ca*. 455 m and 222 m, spores with a TAI of 3/3+ were recorded,
504 showing also feint fluorescence with brown to dark orange colours, indicating a position close
505 to the spore fluorescence extinction level. Below 454 m depth, no palynomorphs fluoresce. In
506 this borehole, the cut-off of fluorescence correlates with VR of ca. 1.49%*Ro*. According to
507 Taylor et al. 1998 all fluorescence disappeared during the second coalification jump, which is
508 between 1.2 % *Ro* and 1.6% *Ro*, therefore not all spores fluorescence coincide with 1.35%*Ro*
509 taken as the end of oil-window. Fluorescent samples also showed a negative fading effect.
510 The maturation levels measured correspond to a coal rank of medium rank A (ISO 11760,
511 2018). As in borehole A1TM-058, this borehole also shows effects of conductive heating
512 related to the intrusion of doleritic sills in a sample at *ca*. 187 m depth.
513 Palynological studies performed on samples from this borehole highlighted an assemblage
514 similar to the one found in borehole TGDH(C)005 indicating a Lopingian age with
515 *Calamospora*sp., *Horriditriletes* sp, *Krauselisporites rallus, Osmundacidites senectus* and
516 *Guttullapollenites hannonicus* and *Weylandites lucifer* for the whole succession penetrated by
517 this borehole.

518

519 ***5.5. Borehole CIMT-014***

520 As mentioned in the borehole descriptions, most of the lithologies penetrated by borehole
521 CIMT-014 consist of red beds (mudstones, siltstones and sandstones), which are not suitable
522 for organic maturation and palynological studies due to the oxic conditions that prevailed
523 during deposition.

524

525 Fifty samples were processed for both maturity and palynological studies for CIMT-014
526 borehole. However, the majority of samples were barren with only 10 samples for palynology
527 and 4 samples for maturation proving to be suitable for these studies. In borehole CIMT-014,
528 a VR value of 1.07%*Ro* was measured from sample MQ111 at *ca*. 132 m depth. In general,
529 VR increases downhole and a VR value of 1.47%*Ro* was measured for sample MQ147 near
530 the bottom of the borehole (Fig. 7). However, the most important information regarding the
531 maturation and thermal history of this borehole came from spore colour (TAI) and
532 fluorescence. The observation of these two optical organic maturation indicators revealed two
533 different palynomorph populations, in terms of both age and organic maturation level. All
534 samples investigated contain an indigenous palynomorph population but samples MQ127,
535 MQ115 and MQ111 also includes a reworked palynomorph population (Fig. 12). It is
536 noteworthy that reworked vitrinite populations were not identified in these last three samples.
537 TAI values of 2 and 3+/4- were recorded for the indigenous palynomorph population from *ca*.
538 132 m depth and at the bottom of the CIMT-014 borehole, respectively. Fluorescence
539 intensity and colour also change downhole for the indigenous palynomorph population, from
540 bright yellow colour in sample MQ111 to dark orange colour in sample MQ147. The
541 reworked palynomorph population is absent in sample MQ147, but in the other three samples
542 it is common, making up to 30 – 40% of all palynomorphs. The TAI values of the reworked
543 palynomorphs are always 3+/4- and spore fluorescence is either orange colour or the spores

do not fluoresce (Table 1). Non-fluorescent spores are more abundant in samples MQ111 and MQ115 (Fig. 12). The organic maturation levels indicated by VR indicate that this borehole falls within the late oil-window, with sample MQ147 (at the bottom of the borehole) indicating a position at the beginning of the wet-gas generation zone. VR values also indicate a coal rank of medium rank B (ISO 11760, 2018) for most of the sedimentary succession in this borehole.

The palynological assemblage found in sample MQ111 suggest an Upper Triassic (Carnian) age, based on the presence of the spores *Anapiculatisporites spiniger/Carnisporites anteriscus, Densoisporites* spp., *Dictyophyllidites* sp. *Limatulasporites limatus, Lophotriletes novicus, Lundbladispora* spp., *Nevesisporites fossulatus, Retitriletes* sp., *Stiattella seebergensis* and *Uvaesporites* sp. and the pollen grains of *Camerozonosporites secatus*, *Cycadopites* sp., and *Samaropollenites speciosus,* that typifies to these ages (César and Colombi, 2016; Dawit, 2014; Paterson et al., 2018). The assemblages found in samples MQ115, MQ127 strongly suggests a Lower Triassic age, containing the spores *Aratisporites* sp., *Densoisporites nejburgi, D. playfordii Lundbladispora* spp. and *Playfordidiaspora cancellosa* and the pollen grains *Alisporites nuthallensis*, *Lunatisporites pellucidus, Falcisporites stabilis ,* and *Platysaccus queenslandii*. The assemblages of these two samples are characterized by *Alisporites nuthallensis*, *Lunatisporites pellucidus, Densoisporites playfordii, Falcisporites stabilis* and *Lundbladispora obsoleta*, *Platysaccus queenslandii*, *Uvaesporites* sp. and *Carnisporites* sp. that typifies to these ages (Dawit, 2014). Between samples MQ111 and MQ115, separated vertical in the borehole by only *ca*. 15 m no palynomorphs were recorded in three samples located in this interval, suggesting an important hiatus, since no Middle Triassic palynomorphs were identified. Samples MQ111, MQ115 and MQ127 also have a considerable amount of reworked palynomorphs of Lopingian (Permian age) as for instance *Polypodiisporites* sp., *Thymospora* sp. The Permian-Triassic boundary is tentatively placed at

569 *ca*. 489 m depth according to the scheme described by Pereira et al. (2016) from borehole
570 DW132, where the Permian-Triassic boundary was identified at *ca.* 42 m depth.
571
572 ***5.6. Borehole A1TM-039***
573 For A1TM-039 borehole, twenty samples were processed, but only two samples were suitable
574 for organic maturation studies and three yielded palynomorphs suitable for palynological
575 analysis. VR values measured are 1.15%*Ro* (MQ231) and 1.17%*Ro* (MQ233) and the
576 indigenous palynomorphs population shows yellow fluorescence colours and TAI values of
577 2+ (Fig. 8). The reworked palynomorph population either shows no fluorescence or dull dark
578 orange colours and TAI values of 3+/4- (Table 1). The maturation levels suggested by the VR
579 results and the indigenous palynomorph population indicate a position within the oil-window
580 and a coal rank of medium rank B (ISO 11760, 2018), whereas the maturation levels of the
581 reworked population indicate a position at the end of the oil-window and at the beginning of
582 the wet-gas generation zone.
583 The three productive samples studied are located near the bottom of the borehole and contain
584 an assemblage assigned to Carnian age (Upper Triassic) age. The palynoassemblage included
585 the pollen grains *Alisporites nuthallensis, Enzonalasporites virgens, Platysaccus queenslandi*.
586 and *Samaropollenites speciosus* and the spores *Aratrisporites* sp.*, Anapiculatisporites*
587 *spiniger/Carnisporites anteriscus*, *Densoisporites* spp., *Lundibladispora* spp.*, Playfordispora*
588 *cancellosa, Stiattella seebergensis* and *Uvaesporites* sp. A second assemblage comprising
589 reworked palynomorphs was also identified in the same samples. The reworded assemblage is
590 assign to a Permian age due to the presence of*, Alisporites parvus, Cyclogranisporites*
591 *gondwaniensis, Polypodiisporites* sp.*, Thymospora* sp.*,* described as key species for this age in
592 other Karoo basins.
593

5.7. Borehole A1TM-058

The twenty-nine samples processed were all suitable for maturity studies, whereas, only twelve samples were suitable for palynological studies. In borehole A1TM-058, VR values increase downhole from 1.19%*Ro* at 23.5 m depth to 1.51%*Ro* at 970 m depth, with a clear linear VR *vs.* depth relationship (Fig. 9). The boundary between the base of the oil-window and the wet gas zone, indicated by the VR profile, occurs at *ca*. 500 m depth, with VR values ranging from 1.31 to 1.36%*Ro*. Samples above 490 m depth show positive fluorescence with orange to dark orange colours (Fig. 10), whereas for samples below that depth, no palynomorphs (spores and pollen) were observed to fluoresce. The depth of fluorescence extinction in this borehole correlates with VR values between 1.31 and 1.33%*Ro*. Spore colour increases from a TAI of 3/3+ at the top of the borehole to values of 3+/4- at the bottom of the borehole. TAI values of 3+/4- were recorded for spores at the horizon of fluorescence extinction. All thermal maturity indices recorded correspond to medium rank B and A coals in terms of coal rank (ISO 11760, 2018). In this borehole, VR measured from samples between the depth intervals of 68 to 180 m and 610 to 625 m, yielded anomalously high values, that do not lie on the VR vs. depth profile (Fig. 9). These samples are positioned close to the margins of several doleritic intrusions that were intersected by the borehole. Therefore, the VR values from these samples were not included in the calculation of the VR profile, since they were interpreted as the result of post burial igneous activity, most likely related to the Jurassic Karoo - Ferrar Large Igneous Province (*op. cit.* Duncan et al., 1997). Palynological studies performed in this borehole, shows a palynoassemblages similar to the assemblage studied in the borehole A1TM-085. Present are the diagnostic species *Guttullapollenites hannonicus*, *Klausipollenites schaubergeri, Lueckiesporites virkkiae*, *Osmundacites senectus*, *Polypodiisporites* sp., *Protohaploxypinus microcorpus*, *Thymospora* sp.and *Weylandites lucifer*, that indicates a Lopingian age (Late Permian). The assemblages investigated are also

very similar and correlate with those described for the borehole DW 123, Muarádzi sub-basin (see Fig. 1) (Pereira et al., 2016).

6. Interpretation of Organic Maturation Results

6.1. Palaeogeothermal gradient estimates

Except for boreholes CIMT-014 and A1TM-039, the thermal maturity obtained from the non-heat affected samples (Table 1), indicates a clear relationship between maturity and depth of the sedimentary beds despite the different techniques used (Figs. 3 to 10). This type of relation suggests that burial was the main factor controlling organic maturation. However, organic maturation profiles indicate that the boreholes located in close proximity to the southern basin boundary have less steep gradient indicating higher geothermal gradients at those locations. In order to investigate this aspect further, palaeotemperatures were calculated using Barker's (1988) empirical equation T(°C)= 104ln(%*Ro*)+148, where T(°C) is the maximum palaeotemperature attained by the sedimentary rock that yielded vitrinite particles with a measured VR of %*Ro*.

The palaeotemperatures calculated by this equation are shown in the Table 1. These were then used to estimate palaeogeothermal gradients (Fig. 13) and the amount the rock cover eroded in the N'Condédzi sub-basin of the Moatize - Minjova Coal Basin.

The palaeogeothermal gradients calculated vary significantly from a maximum of *ca*. 300°C/km in borehole A1TM-018 to a minimum of ca. 35°C/km in borehole A1TM-085. Palaeogeothermal gradients were not calculated for boreholes CIMT-014 and A1TM-039 due to insufficient numbers of samples studied.

643 Notably, the higher palaeogeothermal gradients were from the boreholes located near the
644 basin margin and in the small isolated occurrence of the Karoo Supergroup where borehole
645 TGDH(C)005 was drilled. Anomalously high VR values were measured in boreholes A1TM-
646 085, A1TM-058 and ZSA-32 through several depth intervals that were interpreted as the
647 results of conductive heating associated with Jurassic age doleritic intrusions. These
648 anomalous VR values were not included in the construction of palaeogeothermal gradients.
649
650 However, there is no evidence that boreholes that have the highest calculated
651 palaeogeothermal gradients were affected by igneous intrusion and, therefore, another thermal
652 event was responsible for such high geothermal gradients. The calculated palaeogeothermal
653 gradients of 35-40°C/km is considered to be the regional geothermal gradients for the
654 N'Condédzi sub-basin of the Moatize - Minjova Coal Basin, and is similar to the 40°C/km
655 geothermal gradient calculated by Fernandes et al. (2015) for the Muarádzi sub-basin of the
656 same basin.
657
658 The calculated palaeogeothermal gradients are characteristic of extensional continental rift
659 basins (Fernandes et al. 2015). However, the higher geothermal gradients calculated for the
660 boreholes near the basin boundary, suggest that high heat flux rather than the regional
661 geothermal gradient was responsible for locally elevated the geothermal gradients. A likely
662 cause for this high palaeogeothermal gradient is the circulation of hot fluids associated with
663 fault zones and permeable beds (sandstones).
664
665 ***6.2. Eroded cover estimates***
666 The calculated palaeogeothermal gradients were used to estimate the amount of eroded
667 sedimentary cover in sedimentary basins where rocks have already attained maximum

668 temperatures. The eroded sedimentary cover refers to the thickness of sedimentary section
669 necessary to account for the measured VR results. In the boreholes studied, the shallowest
670 samples, from 11 to 138 m depth, reached peak palaeotemperature of 185-190°C. The method
671 used to calculate the eroded cover is after Bray et al. (1992). Applying this methodology to
672 the estimates of exhumation in the study area suggests a maximum of *ca*. 5300 m and a
673 minimum of 550 m. This range can be explained by different palaeogeothermal gradients used
674 in calculations for these boreholes. Since the highest palaeogeothermal gradients are
675 considered abnormal and related to high temperature fluid flow through fault zones and
676 permeable lithologies, the amount of post-late Permian exhumation is between 4.3-5.3 km;
677 values slightly higher than the 2.5 – 3 km calculated by Fernandes et al. (2015).
678
679 Thick sedimentary sections are found in other external rift-related Karoo basins in Eastern
680 Africa, which are geometrically related to the Moatize Minjova Basin (Cairncross, 2001;
681 Catuneanu et al. 2005). For example, Banks et al. (1995) reported at 8 km thick Permian-
682 Triassic sedimentary section preserved in the Karoo rift basin of the Luargwa Valley in
683 Zambia.
684
685 **7. Discussion**
686 The VR values measured from the N'Condédzi sub-basin, range from 1.3-1.7%*Ro*, indicating
687 a coal rank of medium rank B and A coals (ISO 11760, 2018), and are similar to those
688 reported by Fernandes et al. (2015) of dispersed organic matter, and Vasconcelos (1995) of
689 coals, for the Moatize sub-basin (Fig. 1). In terms of zones of hydrocarbon generation,
690 boreholes ZSA-32, A1TM-39 and TGDH(C)005 are within or at the end of the oil-window,
691 boreholes A1TR-018 and A1TM-085 are within the wet gas generative zone, and boreholes

692 A1TM-058 and CIMT-014 span the base of oil window at depths of *ca*. 600 m depth and 400
693 m, respectively.
694
695 The linear increase of VR with depth observed in the boreholes indicates an organic matter
696 maturation process related to burial. The calculated regional palaeogeothermal gradient for the
697 N'Condédzi sub-basin is 35-40°C/km. The doleritic intrusions observed in three boreholes
698 (A1TM-058, A1TM-085 and ZSA-32), had only local thermal effects and only increased VR
699 for the samples in the contact aureoles. If the igneous episode, responsible for the doleritic
700 intrusions, had a major effect on the regional organic matter maturity, a homogenisation of all
701 maturity indicators will be expected for the sedimentary successions of these boreholes, this
702 was not observed and supports our argument for the local thermal affects of the intrusions.
703 However, boreholes TGDH(C)005 and A1TR-018 do not show evidence of igneous
704 intrusions and have higher palaeogeothermal gradients suggesting that a thermal process other
705 than burial heating, was responsible for these abnormal gradients. The close proximity of
706 these boreholes to the southern fault-bounded basin margin suggests that hot fluids circulating
707 through permeable lithologies (sandstones) and faults zones, as a likely processes capable of
708 elevate the regional palaeogeothermal gradients in these parts of the basin margin (Fig. 14).
709 The origin of the hot fluids may have been connate waters that moved through the
710 sedimentary pile due to lithostatic pressure during fault-induced subsidence, or may have a
711 deeper origin resulting from metamorphic dewatering reactions(?). The flow of hot fluids,
712 expelled from the basal beds of the basin by lithostatic pressure, through permeable
713 lithologies and fracture zones, allowed the advective and convective transmission of heat,
714 which heated up the sedimentary successions located near the southern basin margin (Fig. 14).
715 The rock successions in these zones were in equilibrium with the temperature of the hot fluids
716 that overprinted the initial thermal maturity caused by burial heat only.

The initiation of fluid flow due to lithostatic pressure in this basin is probably due to the high sedimentation rates consequence of fault-induced subsidence, leading to the accumulation of the thick succession of sediments. In borehole A1TM-058, *ca*. 1 km of Lopingian age sediments are preserved and Lakshminarayana (2015) reported a Lower Karoo succession with more than 900 m thickness. Boreholes A1TM-039 and CIMT-014 encompass a *ca*. 500 – 600 m sedimentary succession of mostly Lower to Middle/Upper Triassic age, demonstrating the continuation of high sedimentation rates throughout Triassic times in this basin. An additional cause for the initiation of fluid flow is the structural geometry of the basin. The N'Condédzi sub-basin is half-graben, where the main fault, the Mwanza Fault, was formed by tectonic reactivation of the Sanângoe Shear Zone (Fig. 1). The Mwanza Fault was probably active since the early Permian and lead to the accumulation of a thick pile of sediments adjacent to the fault zone. Due to the half-graben geometry, the thicknesses of the sedimentary successions were considerably less near the southern margin of the basin. For example, borehole TGDH(C)005 located in the isolated occurrence of Karroo Supergroup sediments within the Tete Suite contains *ca.* 230 m of Lopingian aged strata, whereas borehole A1TM-058 includes a *ca*. 1 km succession of the same age.

Using the regional palaeogeothermal gradient calculated from VR, 4 to 5 km of cover was eroded after Lopingian times in the depocentre of this basin, whereas near the S-SW basin margin, the estimated eroded cover is significantly less from *ca*. 544 m to *ca.* 2.4 km. However, these estimates may be inaccurate, as they do not take account of the palaeogeothermal gradient probably having been elevated by hot fluids flowing through fault zone at the basin margin.

742 The maturation data and the age of the successions of boreholes A1TM-058, A1TM-085,
743 TGDH(C)005, ZSA-32 and A1TR-018, indicate that the timing of organic matter maturation,
744 when peak temperatures were attained, is prior to Lower Triassic times. This can be better
745 constrained by taking into account the cooling episode that occurred between 240 and 230 Ma
746 in the Moatize - Minjova Basin (Fernandes et al., 2015). The latter study also indicated that
747 peak burial temperatures and consequently organic maturation levels, were attained shortly
748 after deposition (3 - 10 Ma), implying high subsidence rates during Lopingian to Lower
749 Triassic time in this region. In borehole CIMT-015 palynological results indicate that Lower
750 Triassic and the Upper Triassic (Carnian) rocks, samples MQ115 and MQ111, respectively
751 (section 5.5 and Fig. 7), are only vertically separated in the borehole by a 15 m thick section
752 of coarse clastic sedimentary rocks. Although, the samples processed in the borehole interval,
753 between these two samples, for organic maturation and palynology were barren, it is unlike
754 that Middle Triassic rocks are condensed in this 15 m thick section. This suggests that the
755 N'Condédzi sub-basin was affected by the same Middle Triassic erosion event described by
756 Fernandes *et al*. (2015) for the Moatize - Minjova Basin in the region of the Muarádzi sub-
757 basin (Fig. 1). Also, the presence of common reworked palynomorphs of Permian age in
758 Upper Triassic (Carnian) sediments in boreholes A1TM-039 and CIMT-014 indicates
759 exhumation and erosion of Permian aged Karoo sedimentary rocks during Middle Triassic
760 times in the neighbouring Karoo basins, *e.g*. in the Moatize and Muarádzi sub-basins (Lopes
761 et al., 2014; Pereira et al., 2016; Götz, et al., 2018) (Fig. 1). Furthermore, the spore
762 fluorescence colours and TAI values recorded from the reworked Permian age palynomorphs
763 in boreholes CIMT-014 and A1TM-039, are considerably higher than those of the indigenous
764 Triassic palynomorphs. Therefore, the Upper Triassic sedimentary rocks never attained higher
765 temperatures than those indicated by the reworked palynomorph population. Unconformities
766 between the late Permian and the Lower Triassic sedimentary successions are described in

767 several Karoo rift basins located to the north of the Main Karoo Basin of South Africa
768 (Catuneanu et al., 2005 and references herein). In the Ruhuhu, Selous and Tanga basins of
769 southern Tanzania this unconformity is well documented and corresponds, for example, to the
770 unconformity between the Lopingian Usili Formation and the Lower Triassic Manda
771 Formation. In Zambia it is the unconformity between the Lopingian Upper Madumabisa
772 Formation and the overlying Lower Triassic Escarpment Grit, and in Madagascar, in the
773 Morondova Basin, it is the unconformity between the Lower Sakamena Formation and the
774 overlying Middle to Upper Sakamena Formation. However, the effects of this Middle Triassic
775 erosion event on the organic maturation and thermal history of the N'Condédzi sub-basin are
776 still uncertain. This is due to the similarity of VR values measured for the Lower and Upper
777 Triassic samples in boreholes CIMT-014 and A1TM-039, together with the impossibility of
778 constructing VR profiles for these two boreholes (see sections 5.5, 5.6 and 6.1), capable of
779 identifying distinct geothermal gradients, below and above the Middle Triassic erosion event.
780 Accordingly, the organic maturation results attained in this study indicate that the effects of
781 the Upper Triassic reburial on the organic maturation, as a distinct thermal event of this sub-
782 basin were not detected, suggesting that a single episode of burial under a sedimentary cover
783 that ended in Upper Triassic – Lower Jurassic(?) times, was responsible for the organic
784 maturation levels measured. The similar VR results, for example, between the Carnian age
785 samples (MQ231 and MQ233) in borehole A1TM-039 and the same age sample (MQ111) in
786 borehole CIMT-014, separated vertically *ca.* 470 m (both boreholes were drilled on a ground
787 at *ca*. 300 m above sea level), could be due to different burial cover thicknesses. In this case
788 borehole A1TM-038 was located in an area of the sedimentary basin that was buried under a
789 thicker sedimentary cover (a depocentre area) than borehole CIMT-014.
790

Organic maturation levels measured for the N'Condédzi sub-basin suggest a complex thermal history (Fig. 14). The VR profiles of the boreholes studied indicate a maturation process related to burial heat. Though, the high palaeogeothermal gradients observed near the South margin of this basin, suggest the flow of hot fluids through permeable lithologies and fractures with discharge points located near the South boundary of this basin. The flow of hot fluids was due, most probably, to compaction-driven fluid flow. The movement of major extensional faults in the N'Condédzi sub-basin led to high fault-induced subsidence rates. The sediment accommodation space created by these processes was matched also by high sedimentation rates during Permian to Lower Triassic times, which increased considerably compaction pressures and may have originated hot overpressure fluids that initiated the fluid flow through the permeable lithologies and fault zones of this basin.

Reworked Permian palynomorphs in Carnian (Upper Triassic) sediments have higher maturation levels than the indigenous Carnian palynomorphs, indicated by spore colour and fluorescence. This implies exhumation and erosion of Permian aged successions located in the neighbouring Karoo basins during Middle Triassic times, and also suggests that peak burial palaeotemperatures, in those basins, were achieved during Permian to Lower Triassic times. Peak burial palaeotemperatures attained by the Upper Triassic (Carnian) sedimentary successions in the N'Condédzi sub-basin, were lower and did not overprint the effects of the earlier maturation episode of the neighbouring Karoo basins, indicated by the reworked Permian palynomorphs. Lastly, during Lower Jurassic times occurred a last maturation event related to dolerite intrusions. Though, the thermal effects of these intrusions were localised and limited to the contact aureoles.

8. Conclusion

The main conclusions of this work are:

- VR values measured from the exploration boreholes of the N'Condédzi sub-basin, range from 1.3 – 1.7%*Ro*, indicating a coal rank of medium rank B and A coals (ISO 11760, 2018). The range of VR values indicated, excludes the VR values of the heat-affected samples due to the dolerite intrusions. In terms of zones of hydrocarbons the majority of the succession of the boreholes lay at the end of the oil window and the beginning of the wet gas generative zone.
- The linear increase of VR with depth observed in the boreholes indicates an organic matter maturation process related to burial. The calculated regional palaeogeothermal gradient for the N'Condédzi sub-basin is 35-40°C/km. The doleritic intrusions observed in three boreholes, had localized thermal effects and only increased VR for the samples close to the intrusion walls. The abnormal geothermal gradients calculated for boreholes TGDH(C)005 and A1TR-018 located close to the south margin of the basin, are attributed to hot fluids flowing through permeable lithologies (sandstones) and faults zones that elevated the regional palaeogeothermal gradient in these parts of the basin margin. We proposed that the origin of the hot fluids were connate waters that moved due to lithostatic pressure during fault-induced subsidence, with a possible minor contribution of deep hot fluids originated by dewatering metamorphic reactions(?).
- Hot fluid flow was due to the accumulation of thick sedimentary piles (over 2 km in thickness) in periods of rapid subsidence during the Permian – Triassic times.
- Using the regional palaeogeothermal gradient calculated from VR, 4 to 5 km of cover was eroded since after Lopingian time in the depocentre of this sub-basin.
- The maturation data obtained, together with the age of the borehole successions, including the reworked Permian palynomorphs in Upper Triassic sedimentary rocks,

suggests that burial peak temperatures were reached during Upper Triassic – Lower Jurassic(?) times.

Disclosure of interest

The authors declare that they have no competing interest.

Acknowledgments

The authors would like to thank the Managers of Coal India Africana, Limitada, Companhia Carvoeira de Samoa, Limitada, Capitol Resources, Limitada, Gondwana Empreendimentos e Consultorias, Limitada, and Iain C. Pleas for borehole access and complementary information. Francesca Galasso acknowledges the University of Perugia, for the opportunity to participate in the program Erasmus+ Traineeship, funded by the European Commission. The authors gratefully acknowledge Centro de Investigação Marinha e Ambiental (CIMA) for the use of the services and laboratory facilities at the University of the Algarve. We would like to thank Professor Geoffrey Clayton from the Department of Geology, Trinity College, Dublin, and Doctor Elke Schneebeli-Hermann from University of Zurich, Paleontological Institute and Museum, Switzerland, for critical reading of the manuscript. The reviews and valuable comments of four anonymous reviewers, have greatly improved our manuscript. This research did not receive any specific grant from funding agencies in the public, commercial, or not-for-profit sectors.

References

Achimo, M., Vasconcelos, L., Marques, J., Ferrara, M., 2014. Sedimentologia dos depósitos tilíticos do vale do Rio Murrongódzi, Bacia Carbonífera de Moatize-Minjova, Tete,

Moçambique. In: 2º Congresso Nacional de Moçambique e 12º Congresso de Geoquímica dos Países de Língua Portuguesa, Vasconcelos, L. (ed.), Livro de Resumos, Maputo, 57-61.

Afonso, R.S., 1975. Contribuição para o conhecimento da area de Tambara-DÔa (Folha Sul-E-36, grau quadrado 1634). Bol. Serviços Geol. Minas, Lourenço Marques 38, 5e153.

Afonso, R.S., 1976. A geologia de Moçambique. (Notícia explicativa da carta geologica de Moçambique). Direcção dos Serviços de Geologia e Minas, Maputo, 1: 2.000.000. 175 pp.; 2 mapas.

Afonso, R. S., 1984. Ambiente geológico dos carvões gonduânicos de Moçambique - uma síntese. In: Lemos de Sousa, M.J. (Ed.), Symposium on Gondwana Coals, Lisbon, 1983. Proceedings and Papers. Comunicações dos Serviços Geológicos de Portugal, vol. 70 (2), 205-214.

ASTM D7708-14, 2014. Standard Test Method for Microscopical Determination of the Reflectance of Vitrinite Dispersed in Sedimentary Rocks. ASTM, International, West Conshohocken, PA, USA, p. 10.

Banks, N. L., Bardwell, K. A., Musiwa, S., 1995. Karoo Rift Basins of the Luangwa Valley, Zambia. Geological Society, London, 285-295. Special Publication, 80.

888 Barker, C. E., 1988. Geothermics of petroleum systems: implications of the stabilisation of
889 kerogen thermal maturation after a geologically brief heating duration at peak temperature.
890 In: Magoon, L.B. (Ed.), Petroleum Systems of the United States, vol. 1870. United States
891 Geological Survey Bulletin, 26-29.
892
893 Bray, R., Green, P., Duddy, I., 1992. Thermal history reconstruction using apatite fission track
894 analysis and vitrinite reflectance: a case study from the UK East Midlands and the Southern
895 North Sea. In: Hardman, R. (Ed.), Exploration Britain: Geological Insight for the Next Decade,
896 vol. 67. Geological Society of London Special Publication, 3-25.
897
898 Cairncross, B., 2001. An overview of the Permian (Karoo) coal deposits of Southern Africa.
899 Journal of African Earth Sciences, 33, 529-562.
900
901 Carvalho, L.H.B., 1977. Formações vulcânicas de Carinde, Tete-Moçambique. Dissertação
902 apresentada ao Instituto Superior Técnico para obtenção do grau de Doutor em Ciências da
903 Engenharia (Geologia Aplicada), 213 p.
904
905 Catuneanu, O., Wopfner, H., Eriksson, P.G., Cairncross, B., Rubidge, B.S., Smith, R.M.H.,
906 Hancox, P.J., 2005. The Karoo basins of south-central Africa. Journal of African Earth
907 Sciences, 43, 211-253.
908
909 Césari, S.N. and Colombi, C., 2016. Palynology of the Late Triassic Ischigualasto Formation,
910 Argentina: Paleoecological and paleogeographic implications. Palaeogeography,
911 Palaeoclimatology, Palaeoecology, 449, 365–384.

912

913 Corcoran, D. and Clayton, J., 2001. Interpretation of Vitrinite Reflectance profile in
914 sedimentary basin, onshore, offshore Ireland. Geol.Soc.London, Spec. Pub., 188, 61-90.
915
916 Correia, M., 1971. Diagenesis of sporopollenin and other comparable organic substances:
917 application to hydrocarbon research. In: Brooks, J., Grant, P.R., Muir, M., van Gijzel, P.,
918 Shaw, G. (Eds.), Sporopollenin. Academic Press, New York, 569-620.
919
920 Daber, R., 1984. Plantas fósseis de Moçambique. Ciênc. Tecnol., Maputo, 9, 77-81.
921
922 Dawit, E.L., 2014. Permian and Triassic microfloral assemblages from the Blue Nile Basin,
923 central Ethiopia. Journal of African Earth Sciences, 99, 408-426.
924
925 Duncan, R.A., Hooper, P.R., Rehacek, J., Marsh, J.S., Duncan, A.R., 1997. The timing and
926 duration of the Karoo igneous event, southern Gondwana. Journal of Geophysical Research,
927 102, 18127-18138.
928
929 Fernandes, P., Musgrave, J.A., Clayton, G., Pereira, Z., Oliveira, J.T., Goodhe, R., Rodrigues,
930 B., 2012. New evidence concerning the thermal history of Devonian and Carboniferous in
931 South Portuguese Zone. Journal Geological Society, London, 169, 647-657.
932
933 Fernandes, P., Rodrigues, B., Borges, M., Matos, V., Clayton, G., 2013. Organic maturation
934 of the Algarve Basin (Southern Portugal) bearing on thermal history and hydrocarbon
935 exploration. Marine and Petroleum Geology, 46, 210-233.

936

937 Fernandes, P., Cogné, N., Chew, D.M., Rodrigues, B., Jorge, R.C.S, Marques, J., Jamal, D.,
938 Vasconcelos, L., 2015. The thermal history of Karoo Moatize Minjova Basin, Tete Province,
939 Mozambique: an integrated vitrinite reflectance and apatite fission track thermochronology
940 study. Journal of African Earth Sciences, 112, 55-72.

941

942 Götz, A. and Ruckwied, K., 2014. Palynological record of the Early Permian Postglacial
943 climate amelioration (Karoo Basin, South Africa). Palebio. Paleoenv, 94, 229-235.

944

945 Götz, A., Hancox, P. J., Lloyd, A., 2017. Permian climate change recorded in palynomorph
946 assemblages of Mozambique (Moatize Basin, eastern Tete Province). Acta Paleobotanica
947 57(1), 3-11.

948

949 Götz, A., Hancox, P. J., Lloyd, A., 2018. Southwestern Gondwana's Permian climate
950 amelioration recorded in coal-bearing deposits of the Moatize sub-basin (Mozambique).
951 Palaeoworld, https://doi.org/10.1016/j.palwor.2018.08.004

952

953 Grantham, G.H., Macey, P.H., Ingram, B.A., Roberts, M.P., Armstrong, R.A., Hokada, T.,
954 Shiraishi, K., Jackson, C., Bisnath, A., Manhiça, V., 2008. Terrane correlation between
955 Antarctica, Mozambique and Sri Lanka; comparisons of geochronology, lithology, structure
956 and metamorphism and possible implications for the geology of southern Africa and
957 Antarctica. In: Satish-Kumar, M., Motoyoshi, Y., Osanoi, Y., Hiroi, Y., Shiraishi, K. (Eds.),
958 Geodynamic Evolution of East Antarctica: a Key to the East-west Gondwana Connection, vol.
959 308. Geological Society, London, Special Publication, 91-119.

GTK Consortium, 2006. Map Explanation; Volume 2: Sheets 1631 - 1934. Geology of Degree Sheets, Mecumbura, Chioco, Tete, Tambara, Guro, Chemba, Manica, Catandica, Gorongosa, Rotanda, Chimoio and Beira, Mozambique. Ministério dos Recursos Minerais, Direcção Nacional de Geologia, Maputo.

Hancox, P. J., 2016. The Coalfields of South-Central Africa: a Current Perspective. Episodes, 39(2), 407-428.

Hankel, O., 1994. Early Permian to Middle Jurassic rifting and sedimentation in East Africa and Madagascar. Geol. Rundsch. 83, 703-710.

Hillier, S. and Marshall, J., 1988. A rapid technique to make thin sections of sedimentary organic matter concentrates. Journal of Sedimentary Petrology, 58, 754-755.

Hunt, J.M., 1996. Petroleum Geochemistry and Geology. W.H. Freeman and Co., 742 p.

International Committee for Coal and Organic Petrology, 1998. The new vitrinite classification (ICCP System 1994). Fuel, 77, 349-358.

Isbell, J.L., Cole, D.I., Catuneanu, O., 2008. Carboniferous-Permian glaciation in the main Karoo Basin, South Africa: stratigraphy, depositional controls, and glacial dynamics. In: Fielding, C.R., Frank, T.D., Isbell, J.L. (Eds.), Resolving the Late Palaeozoic Ice Age in Time and Space. Geological Society of America Special Paper, 441, 71-82.

ISO 7404-5, 2009. Methods for the Petrographic Analysis of Coal, Part 5: Methods of Determining Microscopically the Reflectance of Vitrinite. International Organization for Standardization, Geneva, Switzerland, p. 14.

ISO 11760, 2018. Classification of coals. International Organization for Standardization, Geneva, Switzerland, 2nd ed., p. 9.

Jamal, D.L., 2005. Crustal Studies across Selected Geotransects in NE Mozambique: Differentiating between Mozambican (Kibaran) and Pan African Events, with implications for Gondwana Studies. University of Cape Town, unpublished Ph.D. thesis, Cape Town, South Africa.

Johnson, M.R., van Vuuren, C.J., Hegenberger, W.F., Key, R., Shoko, U., 1996. Stratigraphy of the Karoo Supergroup in Southern Africa: an overview. Journal of African Earth Sciences, 23(1), 3-15.

Kreuser, T. and Woldu, G., 2010. Formation of euxinic lakes during the deglaciation phase in the Early Permian of East Africa. In: Late Paleozoic Glacial Events and Postglacial Transgressions in Gondwana, Oscar R. López-Gamundí (Ed.). Geological Society of America Special Paper, 468, 101-112.

Lächelt, S., 2004. Geology and Mineral Resources of Mozambique. Direcção Nacional de Geologia, Maputo, 515 p.

1008

1009 Lakshminarayana G., 2015. Geology of Barcode type coking coal seams, Mecondezi sub-
1010 basin, Moatize Coalfield, Mozambique. International Journal of Coal Geology, 146, 1-13.

1011

1012 Lopes, G., Pereira, Z., Fernandes, P., Marques, J., 2014. Datação palinológica dos sedimentos
1013 glaciogénicos da Formação Tilítica de Vúzi, sondagem ETA 65, Bacia Carbonífera de
1014 Moatize-Minjova, Moçambique: resultados preliminares. Comunicações Geológicas, 101,
1015 Especial I, 481-484

1016

1017 Mariño, J, Marshak, S., Mastalerz M., 2015. Evidence for stratigraphically controlled
1018 paleogeotherms in the Illinois Basin based on vitrinite-reflectance analysis: Implications for
1019 interpreting coal-rank anomalies**.** Amer. Assoc. Petrol. Geol. Bulletin, 99(10), 1803-1825.

1020

1021 McPhilemy, B., 1988. The value of fluorescence microscopy in routine palynofacies
1022 analysis: Lower Carboniferous successions from Counties Armagh and
1023 Roscommon, Ireland. Review of Palaeobotany and Palynology, 56, 345-359.

1024

1025 Mendonça Filho, J.G., Araujo, C.V., Borrego, A.G., Cook, A., Flores, D., Hackley, P., Hower,
1026 J.C., Kern, M.L., Kommeren, K., Kus, J., Mastalerz, M., Mendonça, J.O., Menezes, T.R.,
1027 Newman, J., Ranasinghe, P., Souza, I.V.A.F., Suarez-Ruiz, I., Ujiié. Y., 2010. Effect of
1028 concentration of dispersed organic matter on optical maturity parameters: Interlaboratory
1029 results of the organic matter concentration working group of the ICCP. International Journal
1030 of Coal Geology, 84, 154-165.

1031

1032

1033 Middleton, M.F., 1982.Tectonic history from Vitrinite Reflectance. Geophysical Journal of
1034 Royal Astronomical Society, 68, 121-132.

1035

1036 Montesi, G., 2016. Palynology and Organic Maturation studies of Permian Succession in the
1037 Moatize - Minjova Basin (N'Condédzi sub-basin, Karoo Supergroup, Mozambique) and the
1038 Zagros Basin (Iran). University of Perugia, unpublished MSc thesis, 123 p.

1039

1040 Mugabe, J.A., 1999. Karoo Deposits of Zambezi Graben - Moatize e Tete City Mozambique;
1041 Sedimentary Facies Distribution and Palynological Approach. Univ. Utrecht, unpublished
1042 Ph.D. thesis. 297 p.

1043

1044 Norconsult Consortium, 2007. Notícia Explicativa: Folhas 1039 Muidine, 1040 Palma, 1134
1045 Ponta Messuli, 1135 Lupilichi, 1136 Milepa, 1137 Macalange, 1138, Negomano, 1139 Mueda,
1046 1140 Mocímboa da Praia, 1234 Metangula, 1235 Macaloge-Chiconono, 1236 Mavago, 1237
1047 Mecula, 1238 Xixano, 1239 Meluco, 1240 Quissanga-Pemba, 1334 Meponda, 1335 Lichinga,
1048 1336 Majune, 1337 Marrupa, 1338 Namuno, 1339 Montepuez, 1340 Mecúfi, 1435 Mandimba,
1049 1436 Cuamba, 1437 Malema, 1438 Ribáuè-Mecubúri, 1535 Insaca, 1536 Gúruè, 1635
1050 Milange e 1636 Lugela-Mocuba, Moçambique. Direcção Nacional de Geologia, Ministério
1051 dos Recursos Minerais, Maputo.

1052

1053 Paterson, N.W.; Mangerud, G., Holen, L. H., Landa, J., Lundschien, B. A., Eide, F.,
1054 2018. Late Triassic (early Carnian–Norian) palynology of the Sentralbanken High, Norwegian
1055 Barents Sea. Palynology. doi: https://doi.org/10.1080/01916122.2017.1413018

Pearson, D. L., 1984. Pollen/Spore Color Standard, version No.2 Phillips Petroleum, Exploration Project Section. Bartelsville, Oklahoma.

Pereira, Z., Lopes, G., Fernandes, P., Marques, J., 2014. Estudo palinoestratigráfico da sondagem ETA 72 do Karoo Inferior da Bacia de Moatize, Moçambique - Resultados Preliminares. Actas do IX Congresso Nacional de Geologia/2º Congresso de Geologia dos Países de Língua Portuguesa, Porto, Portugal, 6 p..

Pereira, Z., Fernandes, P., Lopes, G., Marques, J., Vasconcelos, L. 2016. The Permian-Triassic transition in the Moatize-Minjova Basin, Karoo Supergroup, Mozambique: a Palynological Perspective. Review of Palaeobotany and Palynology, 226, 1-19.

Pinna, P., Jourde, G., Calvez, J.Y., Mroz, J.P., Marques, J.M., 1993. The Mozambique Belt in northern Mozambique: Neoproterozoic (1100-850 Ma) crustal growth and tectogenesis, and superimposed Pan-African (800-550 Ma) tectonism. Precambrian Research, 62, 1-59.

Price, L., 1983. Geological time as a parameter in organic methamorphism and vitrinite reflectance as an absolute paleogeothermomether. Journal of Petroleum Geology, 6, 5-38.

Real, F., 1966. Geologia da Bacia do Rio Zambeze (Moçambique). Características geológico-mineiras da Bacia do Rio Zambeze em território moçambicano. 183 p., 57 Plates; 2 Maps. Junta de Investigações do Ultramar. Lisboa.

1080 Robert, P., 1988. Organic Metamorphism and Geothermal History. Elf-Aquitane and Reidel
1081 Publishing, Dordrecht, 311 p.
1082
1083 Silva, G.H., Barreto, L.S., Carvalho, L.H.B., 1967. *Dadoxylon nicoli* (Seward) do Karoo
1084 de Tete. Revista Est. Ger. Univ. Moçambique, 4. Série VI, Ciências Geológicas,
1085 156pp., Lourenço Marques, Moçambique.
1086
1087 Staplin, F.L., 1982. How to assess maturation and palaeotemperatures: Introduction. In:
1088 Staplin, F.L., *et al*. (Eds.), How to Assess Maturation and Palaeotemperatures, pp. 1 and 5.
1089 Society of Economic Paleontologists and Mineralogists, Short Course No.7.
1090
1091 Suárez-Ruiz, I., Flores, D., Mendonça Filho, J.G., Hackley, P.C., 2012. Review and
1092 update of the applications of organic petrology: Part 1, geological applications.
1093 International Journal of Coal Geology, 99, 54-112.
1094
1095 Taylor, G.H., Teichmuller, M., Davis, A., Diessel, C.F.K., Littke, R., Robert, P., 1998.
1096 Organic Petrology. Gebruder Borntraeger, Berlin, p. 704.
1097
1098 Thonnard, R., 1971/1972. Le graben de Moatize au Mozambique. Bulletin Séances,
1099 Académie Royale Sciences Outre-Mer, Bruxelles, 2.
1100
1101 Tissot, B. and Welte, D. H.,1978. Petroleum Formation and Occurrence: A new approach to
1102 oil and gas exploration. Springer-Velag Berlin.
1103
1104 Van Gijzel, P., 1979. Manual of the Techniques and Some Geological Applications of

1105 Fluorescence Microscopy. American Association of Stratigraphical Palynologists Foundation,
1106 Dallas.
1107
1108 Vasconcelos, L., 1995. Contribuição para o conhecimento dos carvões da Bacia Carbonífera
1109 de Moatize, Província de Tete, República de Moçambique. Tese de Doutoramento. Texto
1110 (Volume I), Tabelas, Figuras, Estampas (Volume II). Faculdade de Ciências, Universidade do
1111 Porto, Porto, Portugal.
1112
1113 Vasconcelos, L., 2000. Overview of the Moatize coal basin geology, Tete Province, Republic
1114 of Mozambique. Chron. Rech. Minière, Orléans, 538, 47-58.
1115
1116 Vasconcelos, L., 2013. Coal deposits in Mozambique an overview. Presentation at FFF
1117 Mozambique coal conference, October 2013 - Johannesburg, South Africa.
1118
1119 Viola, G., Henderson, I.H.C., Bingen, B., Thomas, R.J., Smethurst, M.A., Azevedo, S.,
1120 2008. Growth and collapse of a deeply eroded orogen: Insights from structural and
1121 geochronological constraints on the Pan-African evolution of NE
1122 Mozambique. Tectonics 27, TC5009.
1123
1124 Visser, J.N.J., 1989, The Permo-Carboniferous Dwyka Formation of Southern Africa;
1125 deposition by a predominantly subpolar marine ice sheet: Palaeogeography,
1126 Palaeoclimatology, Palaeoecology, v. 70, p. 377–391.
1127
1128
1129

Figure Captions

Figure 1. Simplified geology of the Tete Province, Mozambique, with the location of Karoo basins of the Zambezi River valley and the N'Condédzi, Moatize and Muarádzì sub-basins. Adapted from Geological Map of Mozambique, Direcção Nacional de Geologia, Maputo (2006).

Figure 2. Simplified geology of N'Condédzi sub-basin showing the location of the studied boreholes. Map adapted from Geological Map of Mozambique, sheet no. 1533/1534, Cazula / Zóbuè, Geological Series 1/250000, Direcção Nacional de Geologia, Maputo, 2006.

Figure 3. Lithological log and vitrinite reflectance profile of borehole ZSA-32. The key to lithologies is the same as used in figures 3 to 9.

Figure 4. Lithological log, vitrinite reflectance profile and selected palynomorphs illustrating the variation of TAI of borehole A1TR-018.

Figure 5. Lithological log and vitrinite reflectance profile of borehole TGDH(C)005.

Figure 6. Lithological log, vitrinite reflectance profile and selected palynomorphs showing the range of TAI values and spore/pollen fluorescence of borehole A1TM-085.

Figure 7. Lithological log, vitrinite reflectance results and selected palynomorphs showing the range of TAI values and spore/pollen fluorescence of borehole CIMT-014.

Figure 8. Lithological log and vitrinite reflectance results and selected palynomorphs showing the range of TAI values and spore/pollen fluorescence of borehole A1TM-039.

Figure 9. Lithological log and vitrinite reflectance profile of borehole A1TM-058.

Figure 10. Selected palynomorphs showing the range of TAI values and spore/pollen fluorescence of boreholes A1TM-058 and TDGH(C)005.

Figure 11. Some examples of vitrinite particles found and measured in this study. Above each photograph of vitrinite particles is indicated the borehole, sample reference and the %Ro measured for that particular vitrinite particles, (vitrinite particles were chosen to illustrate grains with %*Ro* values close to the mean %*Ro* value of the sample).

Figure 12. Differences observed in transmitted and fluorescent light between the indigenous and recycled palynomorphs assemblages in borehole CIMT-014: a.) sp. reworked Permian spore (*Leiotriletes directus*) showing no fluorescence (a.1) and pl. Upper Triassic pollen (*Platysaccus queenslandi*) showing yellow fluorescence colour (a.1), sample MQ115; b.) sp. reworked Permian spore (*Polycingulatisporites* sp.) showing no fluorescence (b.1) and pl. unidentified pollen grain, possible Upper Triassic age, showing yellow fluorescence colour (b.2), sample MQ115; c.) sp. Upper Triassic spore (*Rogalskaisporites cicatricosus*) showing strong yellor fluorescence colour (c.1) and sp.1, sp.2, sp.3 reworked Permian spores showing weak fluorescence or no fluorescence (c.1), sample MQ111; d.) sp. reworked Permian spore

(*Densoisporites* sp.) showing no fluorescence (d.1) and pl. two unidentified pollen grains, possible Upper Triassic age, showing strong yellow fluorescence colour (d.1), sample MQ111.

Figure 13. Calculated palaeogeothermal gradients for the boreholes studied. For boreholes A1TM-039 and CIMT-014 due to the reduced number of samples with VR results palaeogeothermal gradients were not calculated.

Figure 14. Schematic cross-sections illustrating the tectonic and thermal evolution of the Permian - Triassic Karoo rocks of the N'Condédzi sub-basin. Figures not to scale. (**a**) Late Guadalupian: extensional basin initiation by the tectonic reactivation of Precambrian shear zones, forming half-graben sedimentary basins. (**b**) Late Lopingian to Lower Triassic: fault-induced subsidence and deposition of very thick sequences (>1000 m). Beginning of hot diagenetic fluid flow driven only by lithostatic pressure. **(c)** Upper Triassic: after a phase of non-deposition during the Middle Triassic, deposition of Upper Triassic red beds together with reworked Permian palynomorphs from the neighbouring Karoo basins, re-burial of the Permian – Lower Triassic sequences. (**d**) Schematic cross-section of the N'Condédzi region showing the position of some of the boreholes studied.

Table 1. Organic maturation results and palaeotemperatures (^{o}C) calculated using method described by Barker (1988) for the boreholes of the N'Condédzi sub-basin. All samples are black carbonaceous mudstones or black/grey mudstones. R_O (%) - vitrinite reflectance values, SD - standard deviation, Fluo. - spore fluorescence colours (Y – yellow, DY – dark yellow, DO - dark orange, R - red), spore colour TAI - Thermal Alteration Index, * - samples with vitrinite reflectance values due to heating effects of dolerite intrusions (details in Table 2), and TAI Reworked / Fluo. Reworked, refers to the reworked palynomorph population of

boreholes CIMT-014 and A1TM-039.

Table 2. Vitrinite reflectance values of the dolerite heat affected samples, showing also its relations to the dolerite sills, namely the distance of the samples to the nearest intrusion wall and the thickness of the nearest intrusion (distance in metres).

Table

Click here to download Table: Table 1 3rd revision.pdf

Sample (Ref.)	Lithology	Depth (m)	%Ro	SD	Palaeotemp. (ºC)	Fluo.	TAI	Fluo. Reworked	TAI Reworked
Borehole ZSA-32									
MZ227	Black mudstone	20.26	1.21	0.14	167.8	O	3		
MZ226*	B. carb. mudstone	44.7	3.83	0.15	-	-	5		
MZ225*	Black mudstone	47.83	1.88	0.17	-	-	4-/4		
MZ224	Black mudstone	78.52	1.16	0.09	163.4	O	3		
MZ222	Black mudstone	84.42	1.22	0.08	168.7	DO	3/3+		
MZ221	Black mudstone	90.2	1.24	0.1	170.4	-	3+/4-		
MZ220*	Black mudstone	103.38	4.88	0.17	-	-	5		
MZ218*	Black mudstone	125.75	3.83	0.16	-	-	5		
MZ217*	B. carb. mudstone	136.75	4.72	0.17	-	-	5		
MZ216*	Black mudstone	140.52	1.94	0.14	-	-	4-/4		
MZ215	Black mudstone	153.91	1.24	0.08	170.4	DO	3/3+		
MZ212	Black mudstone	196.9	1.32	0.11	176.9	DO	3/3+		
MZ207	Black mudstone	203.93	1.31	0.11	176.1	DO	3/3+		
Borehole A1TR-018									
MQ183	B. carb. mudstone	11.26	1.51	0.12	190.9	-	3+/4-		
MQ186	Black mudstone	21.13	1.53	0.07	192.2	-	3+/4-		
MQ200	Black mudstone	29.37	1.59	0.09	196.2	-	3+/4-		
MQ204	Black mudstone	37.58	1.61	0.06	197.5	-	3+/4-		
MQ207	Black mudstone	48.4	1.62	0.07	198.2	-	3+/4-		
MQ212	Black mudstone	69.2	1.72	0.15	204.4	-	3+/4-		
Borehole TGDH(C)005									
MZ232	B. carb. mudstone	19.7	0.97	0.1	144.8	Y	2		
MZ236	B. carb. mudstone	35.9	0.96	0.08	143.8	Y	2		
MZ239	Black mudstone	53.8	0.97	0.07	144.8	Y	2		
MZ244	Black mudstone	81.05	0.99	0.1	147	Y	2		
MZ246	Black mudstone	90.41	1.05	0.11	153.1	Y	2		
MZ248	Black mudstone	105.7	1.08	0.07	155	Y	2		
MZ251	Black mudstone	132.55	1.07	0.05	155	Y	2		
MZ254	Black mudstone	152.73	1.07	0.06	155	Y	2		
MZ256	Black mudstone	165.05	1.08	0.08	156	Y	2		
MZ258	Black mudstone	182.83	1.1	0.07	157.9	Y	2		
MZ260	Black mudstone	192.71	1.16	0.08	163.4	Y	2		
MZ265	Black mudstone	206	1.15	0.05	162.5	DY	2+		
Borehole A1TM-085									
MQ157	B. carb. mudstone	138	1.43	0.08	185.2	-	3+/4-		
MQ158*	B. carb. mudstone	187.74	2.57	0.14	-	-	5		
MQ160	B. carb. mudstone	222.64	1.37	0.1	180.7	DO	3/3+		
MQ162	Black mudstone	394.84	1.48	0.09	188.8	DO	3/3+		
MQ166	B. carb. mudstone	454.64	1.49	0.08	189.5	DO	3/3+		
MQ167	B. carb. mudstone	515.15	1.51	0.07	190.9	-	3+/4-		
MQ170	Black mudstone	547.64	1.5	0.07	190.2	-	3+/4-		
MQ174	B. carb. mudstone	608.6	1.53	0.09	192.2	-	3+/4-		
MQ177	Black mudstone	660	1.52	0.07	191.5	-	3+/4-		
MQ182	Black mudstone	731	1.56	0.1	194.2	-	3+/4-		
Borehole CIMT-014									
MQ111	Grey mudstone	132.12	1.11	0.09	158.9	Y	2+	O/DO	3/4-
MQ115	Grey mudstone	148.8	1.14	0.07	161.6	Y	2+	O/DO	3/4-
MQ127	Grey mudstone	323	1.24	0.06	170.4	DY	3	O/DO	3/4-
MQ147	Black mudstone	489	1.5	0.1	190.2	DO/R	3+/4-		
Borehole A1TM-039									
MQ231	Grey mudstone	554.59	1.15	0.06	162.5	Y	2+	DO	3+/4-
MQ233	Grey mudstone	562.44	1.17	0.07	164.3	Y	2+	DO	3+/4-
Borehole A1TM-058									
MQ44	Black mudstone	23.52	1.19	0.04	166.1	DO	3/3+		
MQ45	Black mudstone	26.62	1.2	0.11	167	DO	3/3+		
MQ48*	Black mudstone	67.3	1.83	0.13	-	-	4-/4		
MQ50*	Black mudstone	76.22	1.36	0.09	-	DO	4-/4		
MQ52*	B. carb. mudstone	89	1.34	0.08	-	DO	4-/4		
MQ54*	Black mudstone	104.1	1.38	0.09	-	DO	4-/4		
MQ56*	Black mudstone	111.42	1.36	0.1	-	-	4-/4		
MQ59*	B. carb. mudstone	144.65	1.33	0.08	-	-	4-/4		
MQ60*	Black mudstone	180.59	1.78	0.1	-	-	4-/4		
MQ63	B. carb. mudstone	379.2	1.28	0.08	173.7	DO	3/3+		
MQ64	B. carb. mudstone	409.4	1.29	0.09	174.5	DO	3/3+		
MQ68	B. carb. mudstone	490.2	1.31	0.07	176.1	DO	3/3+		
MQ70	Black mudstone	514	1.33	0.1	177.7	-	3+/4-		
MQ71	B. carb. mudstone	537.2	1.33	0.08	177.7	-	3+/4-		
MQ73	Black mudstone	567.2	1.35	0.12	179.2	-	3+/4-		
MQ75	Black mudstone	577.3	1.36	0.09	180	-	4-/4		
MQ77*	Black mudstone	609.47	1.69	0.1	-	-	4-/4		
MQ79*	B. carb. mudstone	624.45	1.68	0.07	-	-	3+/4-		
MQ81	B. carb. mudstone	663,0	1.4	0.1	183	-	3+/4-		
MQ83	B. carb. mudstone	743.2	1.4	0.07	183	-	3+/4-		
MQ84	Black mudstone	753.2	1.42	0.08	184.5	-	3+/4-		
MQ88	Black mudstone	837.8	1.39	0.08	182.2	-	3+/4-		
MQ90	B. carb. mudstone	844.55	1.41	0.08	183.7	-	3+/4-		
MQ92	B. carb. mudstone	861.2	1.42	0.06	184.5	-	3+/4-		
MQ95	B. carb. mudstone	923.2	1.45	0.07	186.6	-	3+/4-		
MQ98	B. carb. mudstone	944.4	1.5	0.13	190.2	-	3+/4-		
MQ100	B. carb. mudstone	957	1.46	0.11	187.4	-	3+/4-		
MQ101	B. carb. mudstone	960.8	1.53	0.13	192.2	-	3+/4-		
MQ102	Black mudstone	970	1.51	0.12	190.9	-	3+/4-		

Table

Click here to download Table: Table 2 heat affected values.pdf

	Sample (ref.)	%Ro	SD	Distance from the nearest intrusion wall (m)	Thickness of the nearest intrusion (m)
Borehole ZSA-32	MZ226	3.83	0.15	0.7	6
	MZ225	1.88	0.17	0.5	1
	MZ220	4.88	0.17	0.5	1.5
	MZ219	2.3	0.14	1	1.5
	MZ217	4.72	0.17	0.3	2
	MZ216	1.94	0.14	5	2
Borehole A1TM-085	MQ158	2.57	0.14	13.4	17.5
Borehole A1TM-058	MQ48	1.83	0.13	1	3.8
	MQ50	1.36	0.09	10	3.8
	MQ52	1.34	0.08	17	11
	MQ54	1.38	0.09	14	11
	MQ56	1.36	0.1	6	11
	MQ59	1.33	0.08	16	11
	MQ60	1.78	0.1	7	6
	MQ77	1.69	0.1	3	4
	MQ79	1.68	0.09	9	7.5

Figure

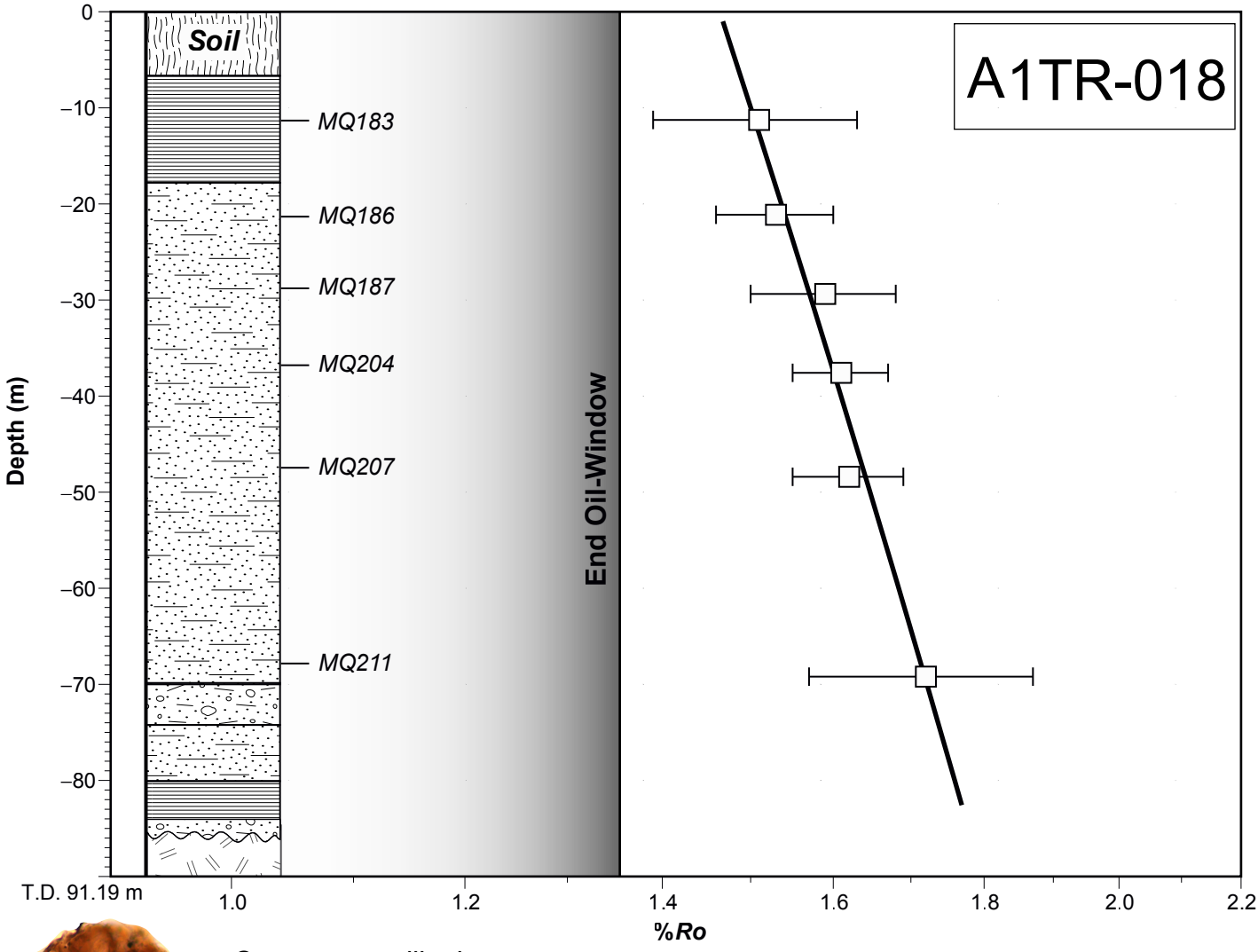

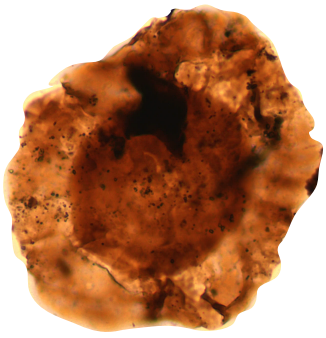

Cannanoropollis densus
(Lele) Bose & Maheshwari 1968
sample MQ182
TAI:3+/4-

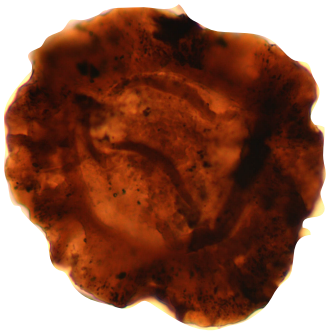

Plicatipollenites gondwanensis
(Balme & Hennelly) Lele 1964
sample MQ185
TAI:3+/4-

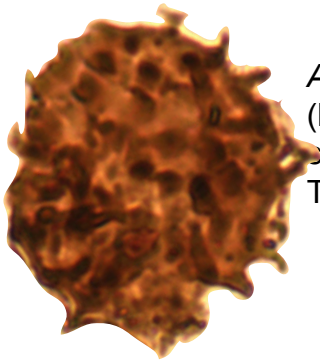

Apiculatisporites cornutus
(Balme & Hennelly) Hoeng & Bose 1960
sample MQ190
TAI:3+/4-

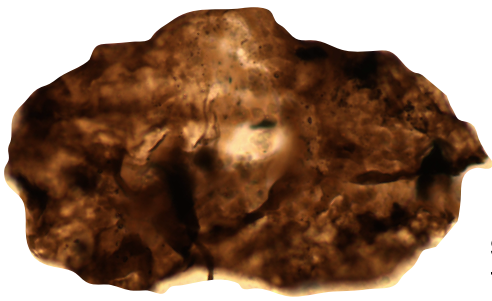

Striatopodocarpites fusus
(Balme & Hennelly) Potonié 1958
sample MQ210
TAI:3+/4-

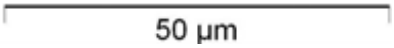

Figure

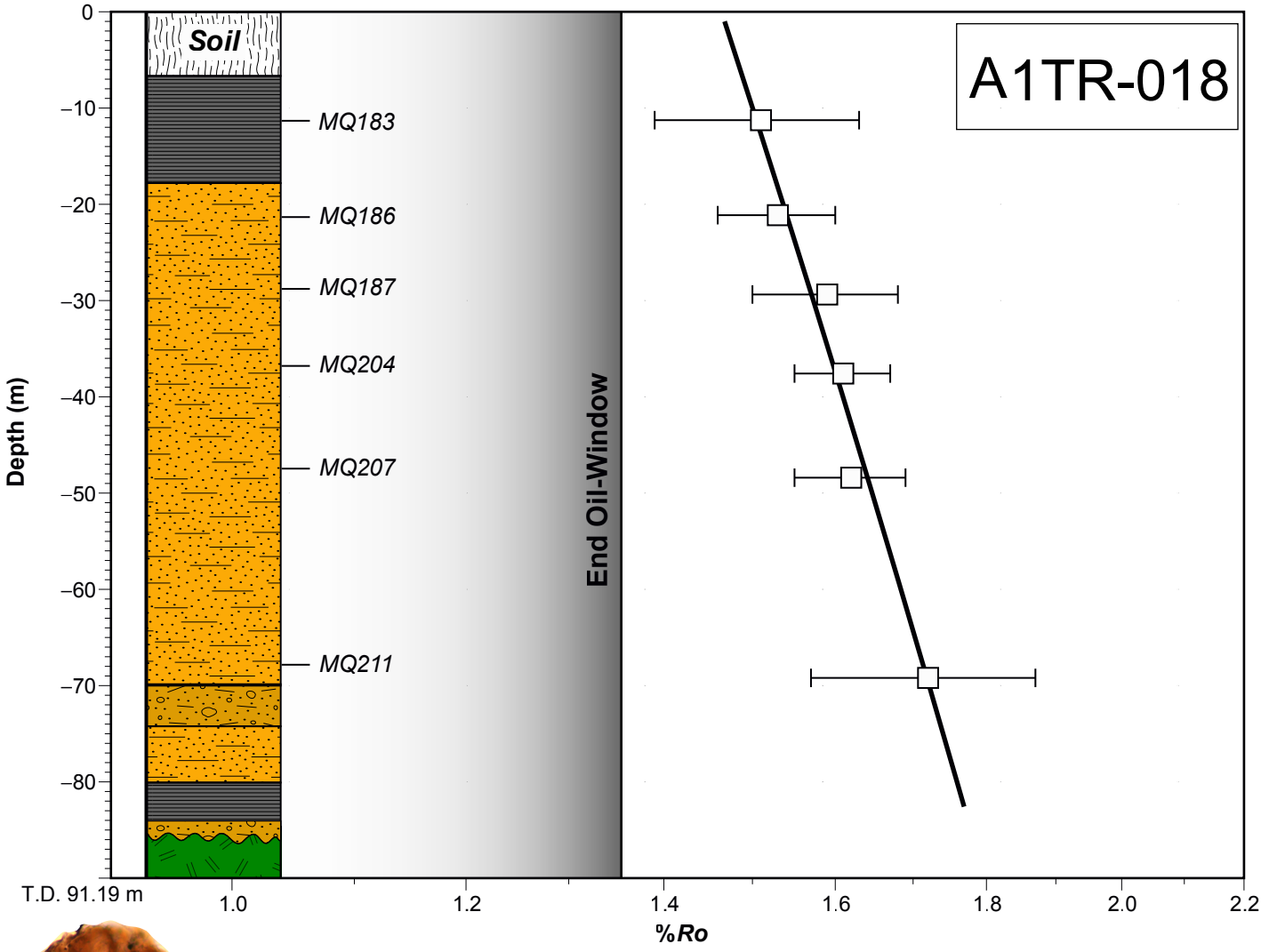

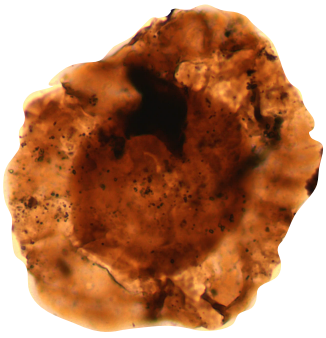

Cannanoropollis densus
(Lele) Bose & Maheshwari 1968
sample MQ182
TAI:3+/4-

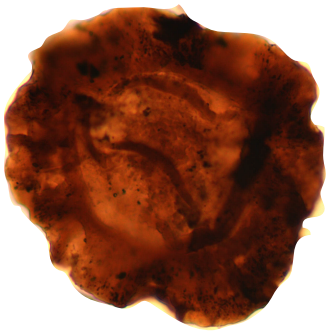

Plicatipollenites gondwanensis
(Balme & Hennelly) Lele 1964
sample MQ185
TAI:3+/4-

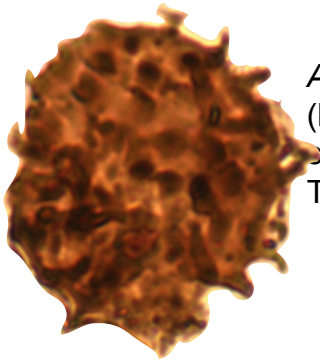

Apiculatisporites cornutus
(Balme & Hennelly) Hoeng & Bose 1960
sample MQ190
TAI:3+/4-

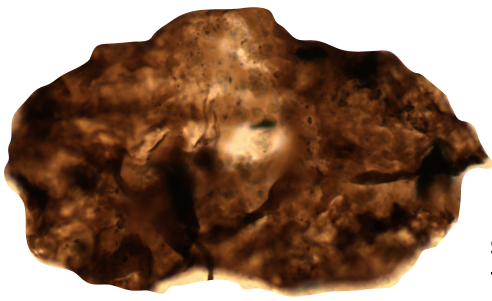

Striatopodocarpites fusus
(Balme & Hennelly) Potonié 1958
sample MQ210
TAI:3+/4-

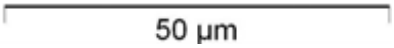

Figure

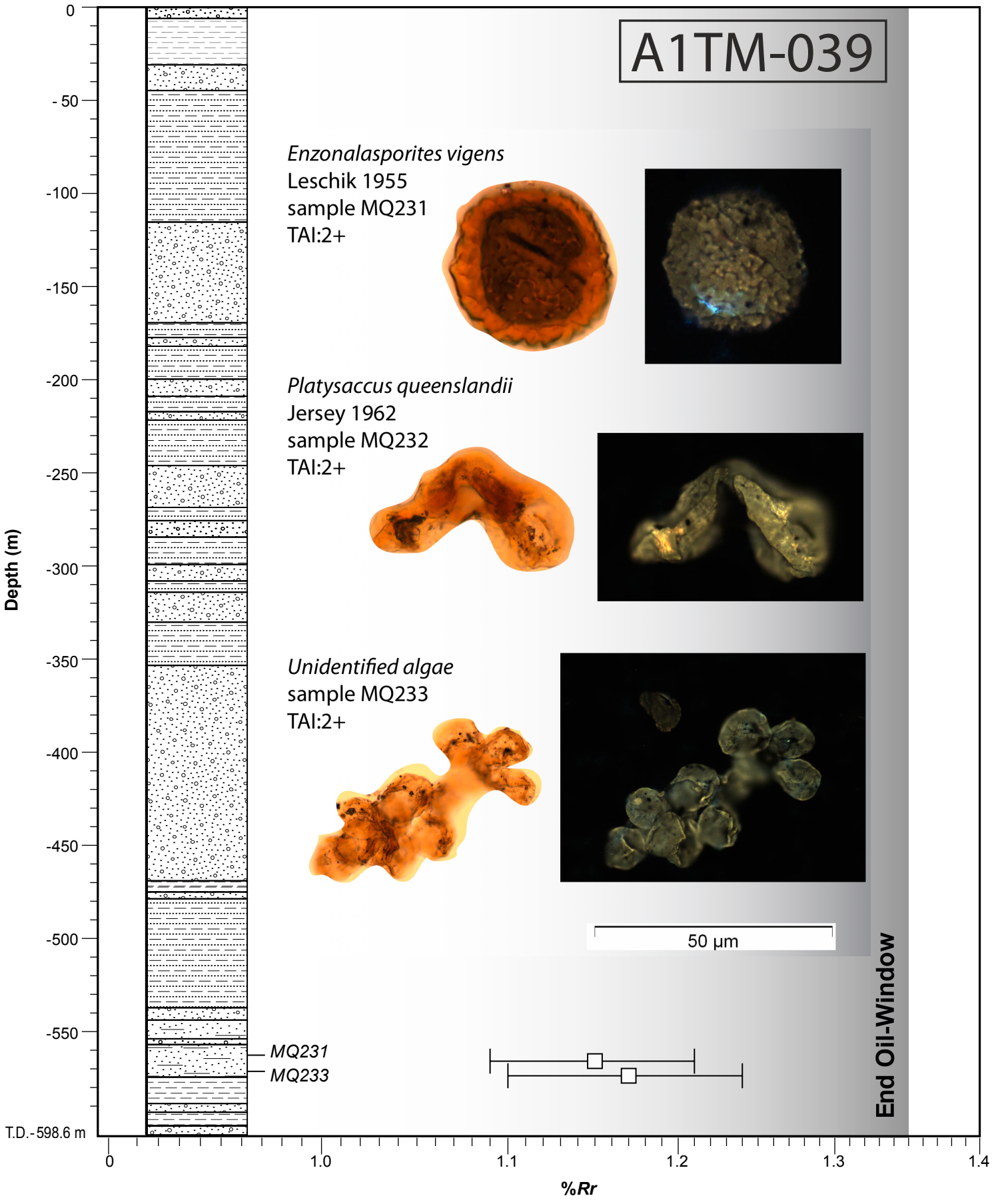
A1TM-039
Enzonalasporites vigens
Leschik 1955
sample MQ231
TAI:2+
Platysaccus queenslandii
Jersey 1962
sample MQ232
TAI:2+
Unidentified algae
sample MQ233
TAI:2+
50 µm
End Oil-Window
MQ231
MQ233
Depth (m)
0
- 50
-100
-150
-200
-250
-300
-350
-400
-450
-500
-550
T.D.- 598.6 m
0
1.0
1.1
1.2
1.3
1.4
%Rr

Figure

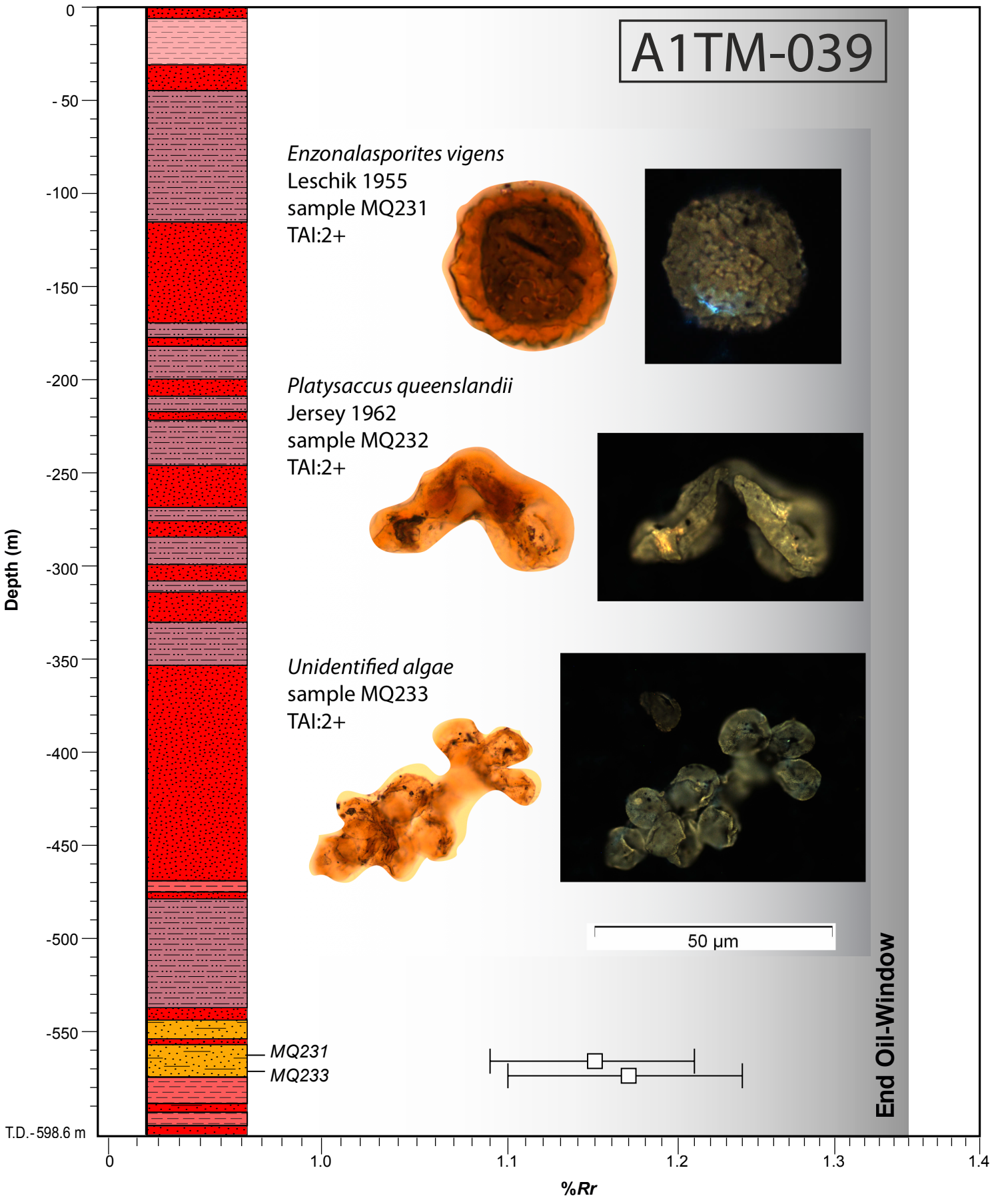
A1TM-039
Enzonalasporites vigens
Leschik 1955
sample MQ231
TAI:2+
Platysaccus queenslandii
Jersey 1962
sample MQ232
TAI:2+
Unidentified algae
sample MQ233
TAI:2+
50 µm
End Oil-Window
MQ231
MQ233
Depth (m)
0
- 50
-100
-150
-200
-250
-300
-350
-400
-450
-500
-550
T.D.- 598.6 m
0
1.0
1.1
1.2
1.3
1.4
%Rr

Figure

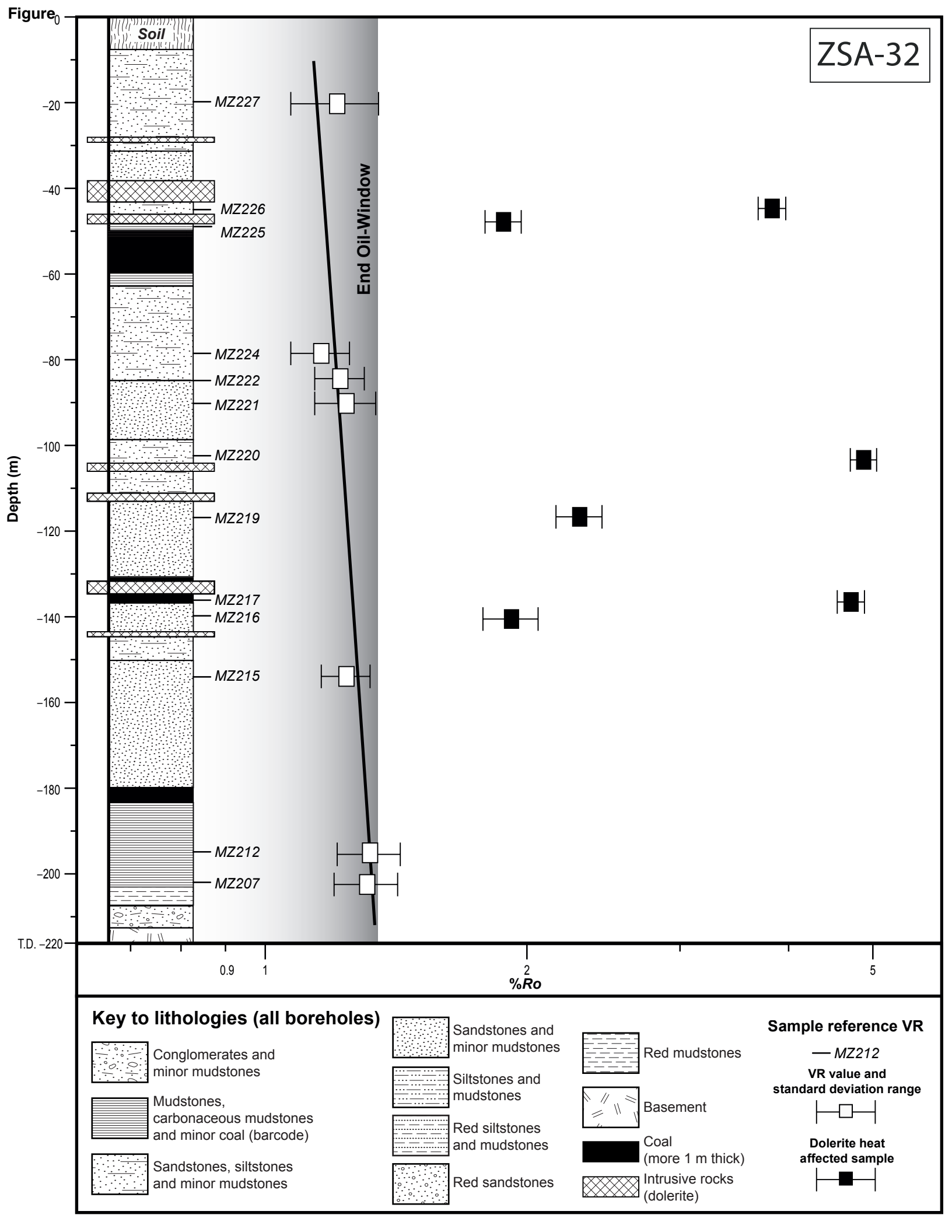
ZSA-32
Soil
MZ227
MZ226
MZ225
MZ224
MZ222
MZ221
MZ220
MZ219
MZ217
MZ216
MZ215
MZ212
MZ207
End Oil-Window
Depth (m)
0
−20
−40
−60
−80
−100
−120
−140
−160
−180
−200
T.D. −220
0.9
1
2
5
%Ro
Key to lithologies (all boreholes)
Conglomerates and minor mudstones
Mudstones, carbonaceous mudstones and minor coal (barcode)
Sandstones, siltstones and minor mudstones
Sandstones and minor mudstones
Siltstones and mudstones
Red siltstones and mudstones
Red sandstones
Red mudstones
Basement
Coal (more 1 m thick)
Intrusive rocks (dolerite)
Sample reference VR
MZ212
VR value and standard deviation range
Dolerite heat affected sample

Figure

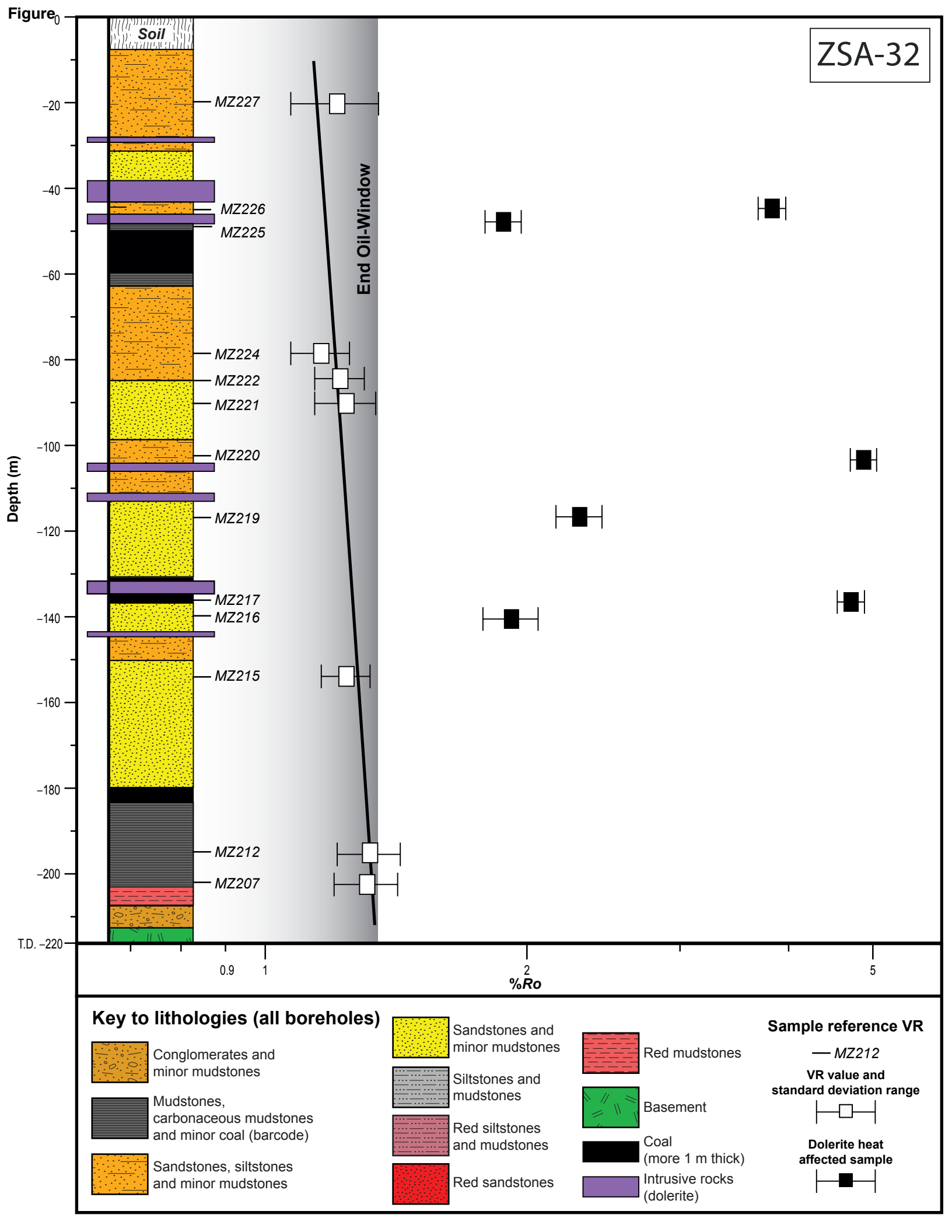
ZSA-32
Soil
MZ227
MZ226
MZ225
MZ224
MZ222
MZ221
MZ220
MZ219
MZ217
MZ216
MZ215
MZ212
MZ207
End Oil-Window
Depth (m)
0
−20
−40
−60
−80
−100
−120
−140
−160
−180
−200
T.D. −220
0.9
1
2
5
%Ro
Key to lithologies (all boreholes)
Conglomerates and minor mudstones
Mudstones, carbonaceous mudstones and minor coal (barcode)
Sandstones, siltstones and minor mudstones
Sandstones and minor mudstones
Siltstones and mudstones
Red siltstones and mudstones
Red sandstones
Red mudstones
Basement
Coal (more 1 m thick)
Intrusive rocks (dolerite)
Sample reference VR
MZ212
VR value and standard deviation range
Dolerite heat affected sample

Figure

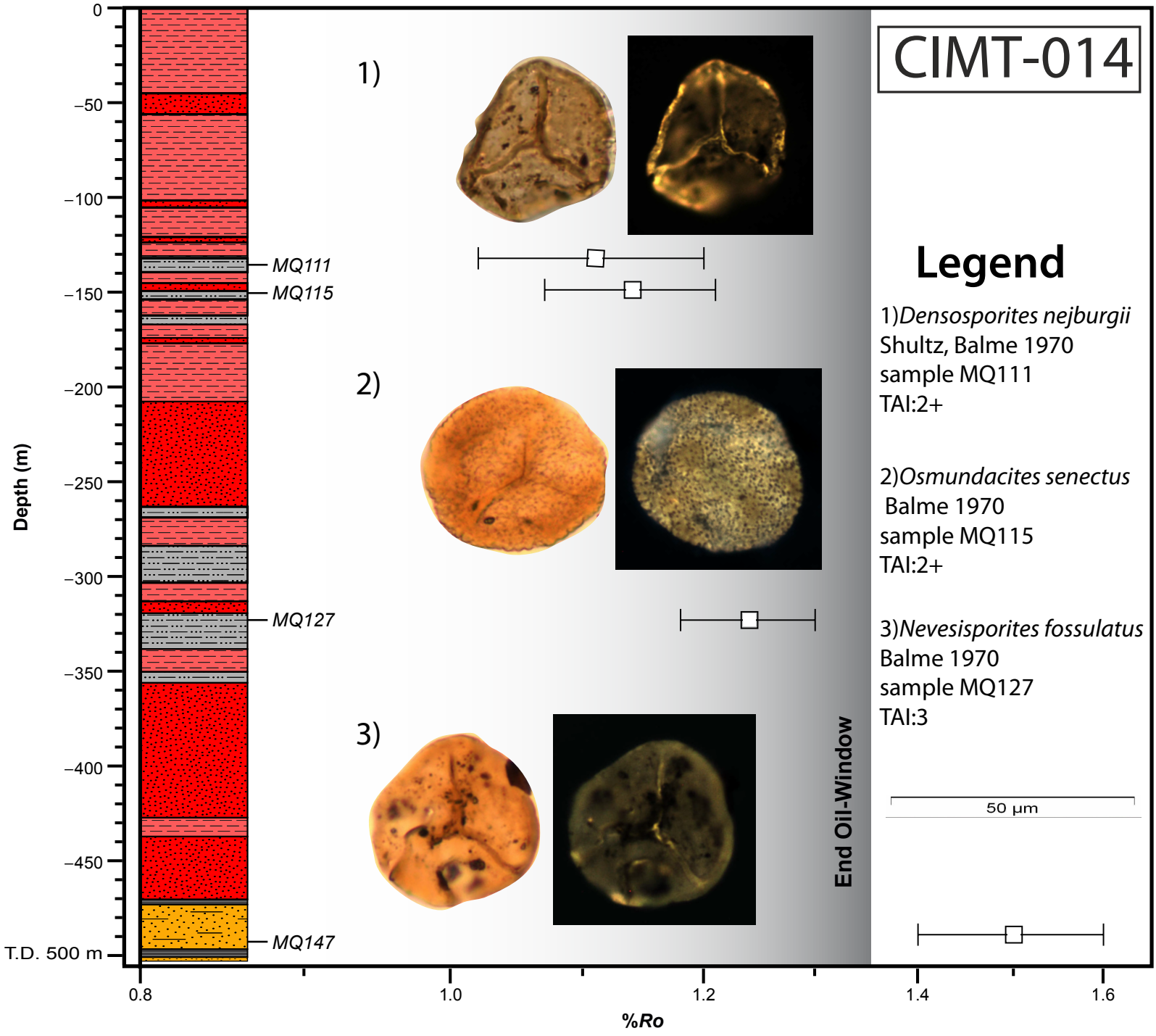
CIMT-014
Legend
1)Densosporites nejburgii
Shultz, Balme 1970
sample MQ111
TAI:2+
2)Osmundacites senectus
Balme 1970
sample MQ115
TAI:2+
3)Nevesisporites fossulatus
Balme 1970
sample MQ127
TAI:3
50 µm
End Oil-Window
Depth (m)
0
-50
-100
-150
-200
-250
-300
-350
-400
-450
T.D. 500 m
MQ111
MQ115
MQ127
MQ147
0.8
1.0
1.2
1.4
1.6
%Ro

Figure

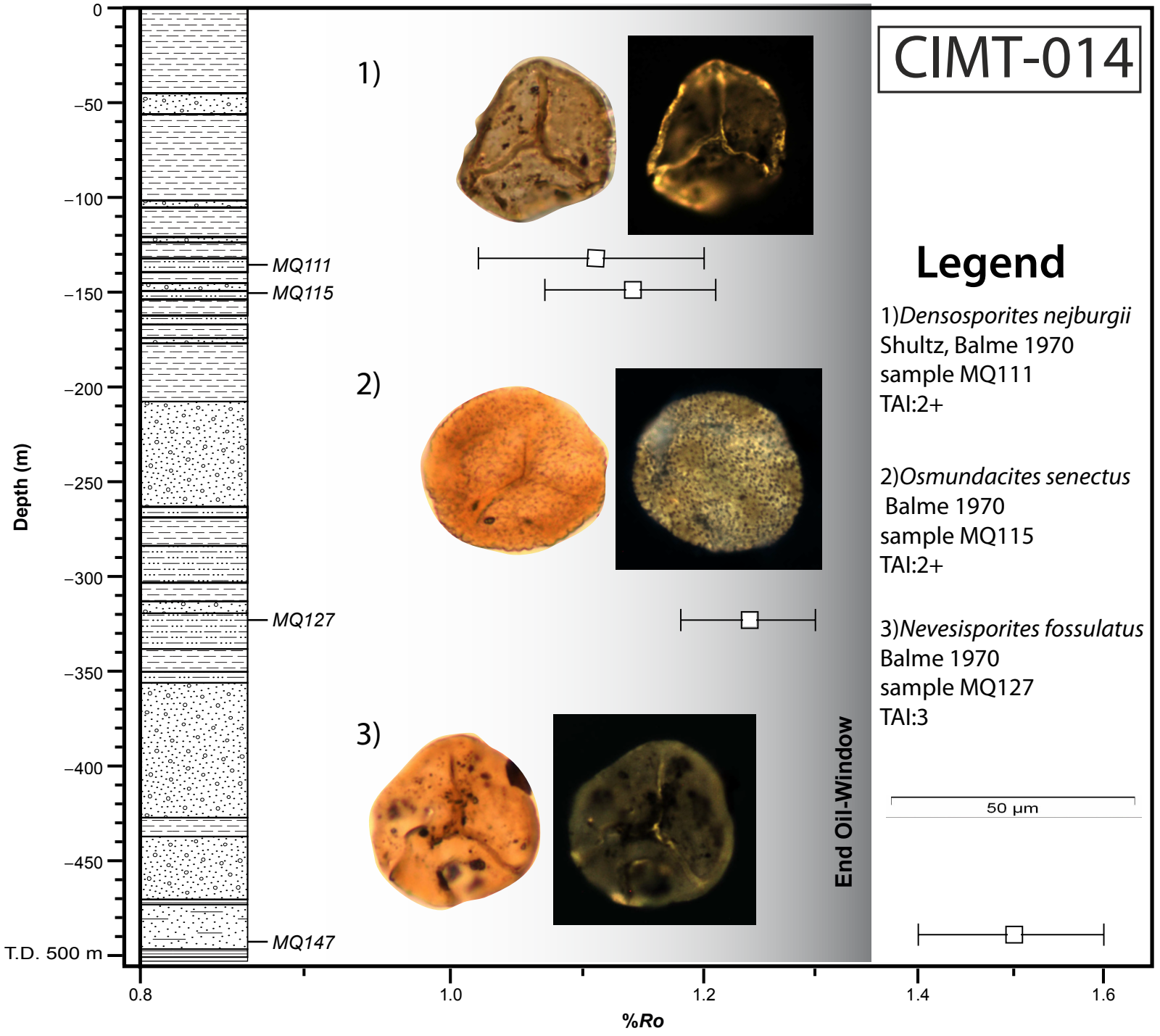
CIMT-014
Legend
1)Densosporites nejburgii
Shultz, Balme 1970
sample MQ111
TAI:2+
2)Osmundacites senectus
Balme 1970
sample MQ115
TAI:2+
3)Nevesisporites fossulatus
Balme 1970
sample MQ127
TAI:3
50 µm
End Oil-Window
Depth (m)
0
-50
-100
-150
-200
-250
-300
-350
-400
-450
T.D. 500 m
MQ111
MQ115
MQ127
MQ147
0.8
1.0
1.2
1.4
1.6
%Ro

Figure

A1TM-058

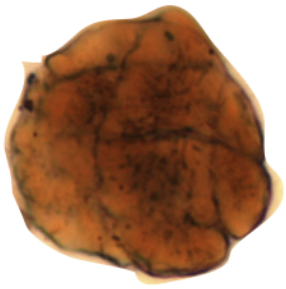

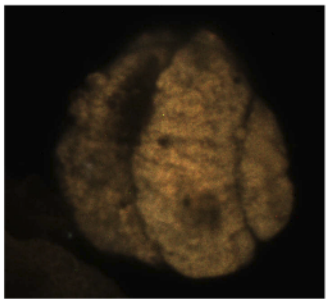

Guttullapollenites hannonicus
(Goubin 1965)
sample MQ45
TAI:3/3+

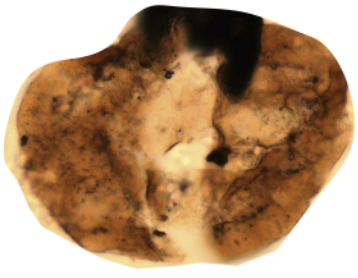

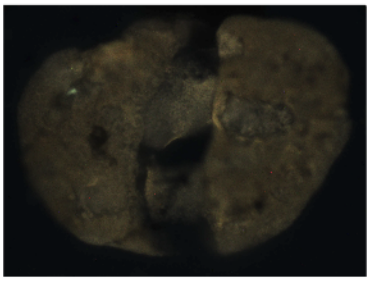

Lueckisporites virkkiae
(Potonié & Klaus, Goubin 1965)
sample MQ63
TAI:3/3+

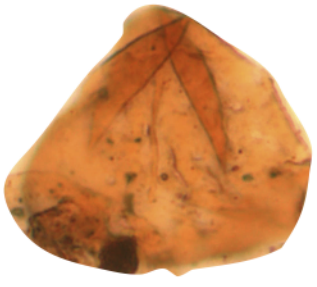

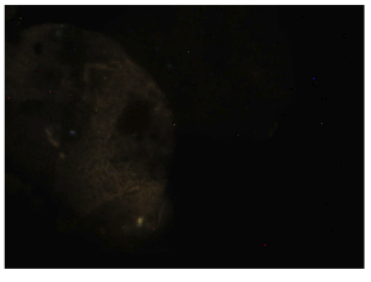

Leiotriletes sp.
sample MQ68
TAI:3/3+

50 µm

TGDH(C)005

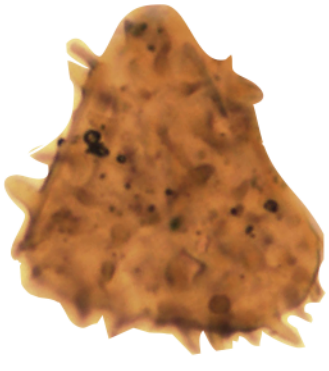

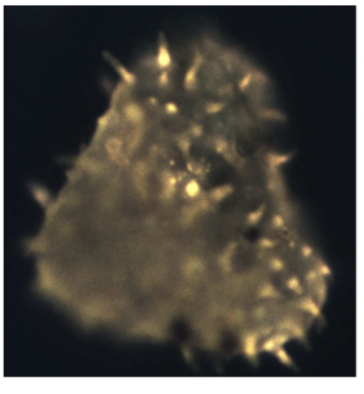

Horriditriletes tereteangulatus
(Balme & Hennelly,
Backhouse 1991)
sample MZ248
TAI:2

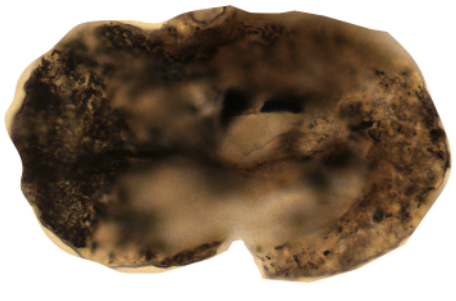

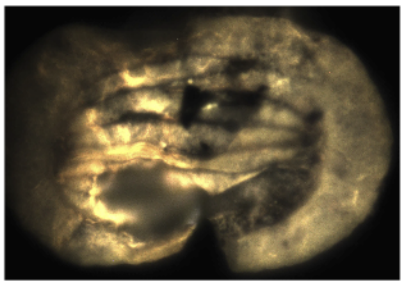

Protohaploxypinus limpidus
(Balme & Hennelly,
Balme & Playford 1968)
sample MZ256
TAI:2

Figure

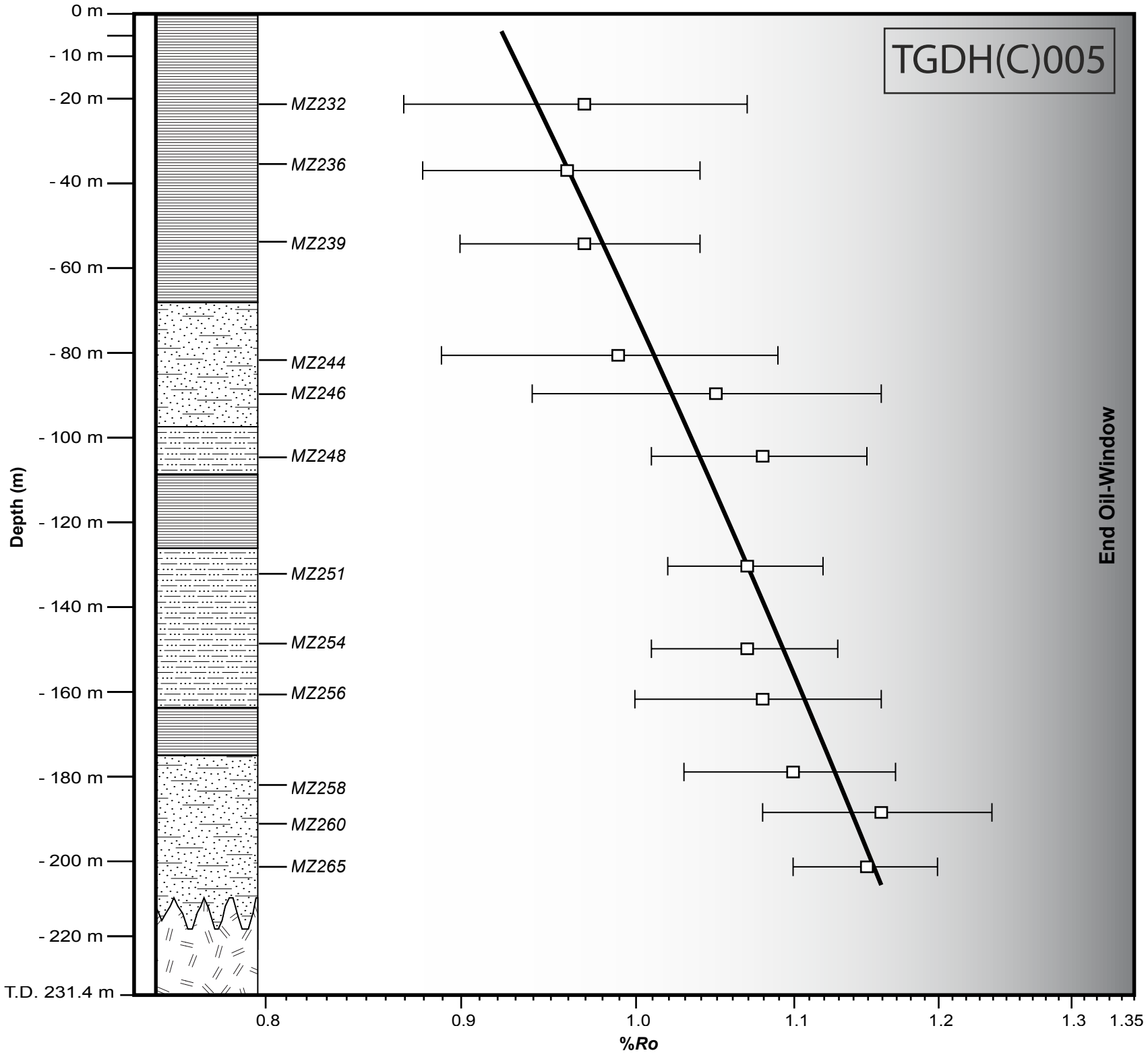
TGDH(C)005
0 m
- 10 m
- 20 m
- 40 m
- 60 m
- 80 m
- 100 m
- 120 m
- 140 m
- 160 m
- 180 m
- 200 m
- 220 m
T.D. 231.4 m
Depth (m)
MZ232
MZ236
MZ239
MZ244
MZ246
MZ248
MZ251
MZ254
MZ256
MZ258
MZ260
MZ265
End Oil-Window
0.8
0.9
1.0
1.1
1.2
1.3
1.35
%Ro

Figure

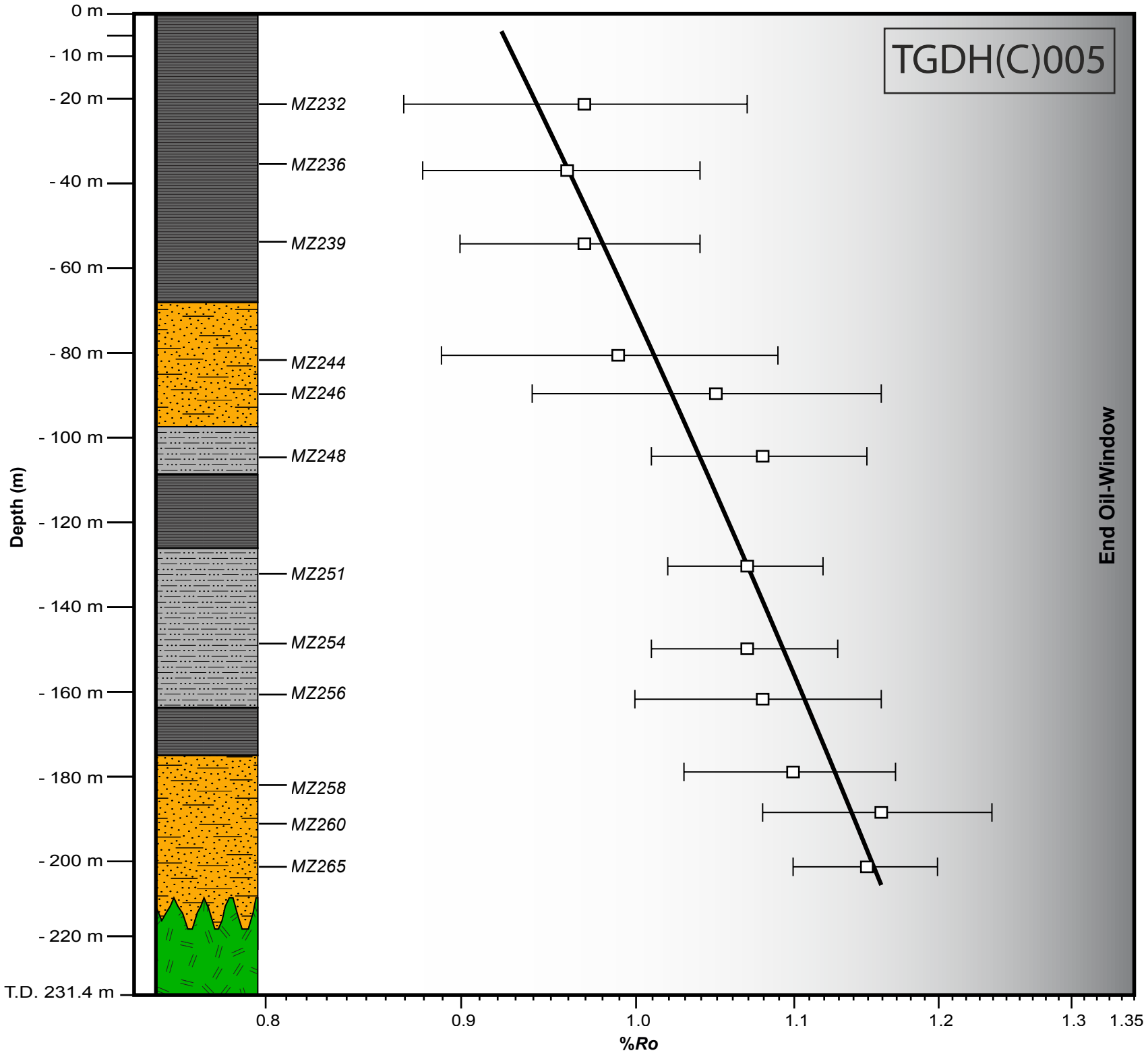
TGDH(C)005
0 m
- 10 m
- 20 m
- 40 m
- 60 m
- 80 m
- 100 m
- 120 m
- 140 m
- 160 m
- 180 m
- 200 m
- 220 m
T.D. 231.4 m
Depth (m)
MZ232
MZ236
MZ239
MZ244
MZ246
MZ248
MZ251
MZ254
MZ256
MZ258
MZ260
MZ265
End Oil-Window
0.8
0.9
1.0
1.1
1.2
1.3
1.35
%Ro

Figure

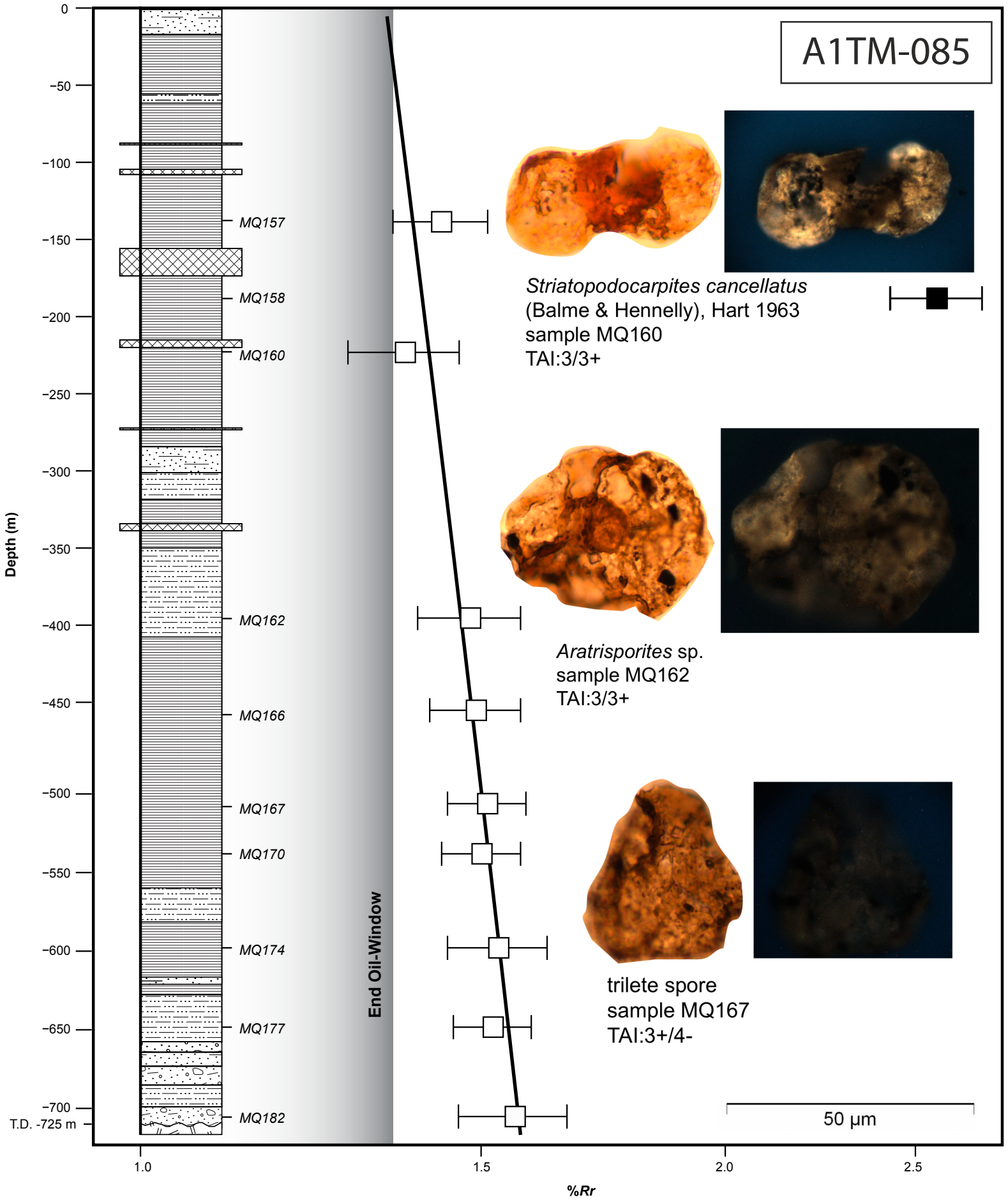
A1TM-085
Depth (m)
0
-50
-100
-150
-200
-250
-300
-350
-400
-450
-500
-550
-600
-650
-700
T.D. -725 m
MQ157
MQ158
MQ160
MQ162
MQ166
MQ167
MQ170
MQ174
MQ177
MQ182
End Oil-Window
1.0
1.5
2.0
2.5
%Rr
Striatopodocarpites cancellatus
(Balme & Hennelly), Hart 1963
sample MQ160
TAI:3/3+
Aratrisporites sp.
sample MQ162
TAI:3/3+
trilete spore
sample MQ167
TAI:3+/4-
50 µm

Figure

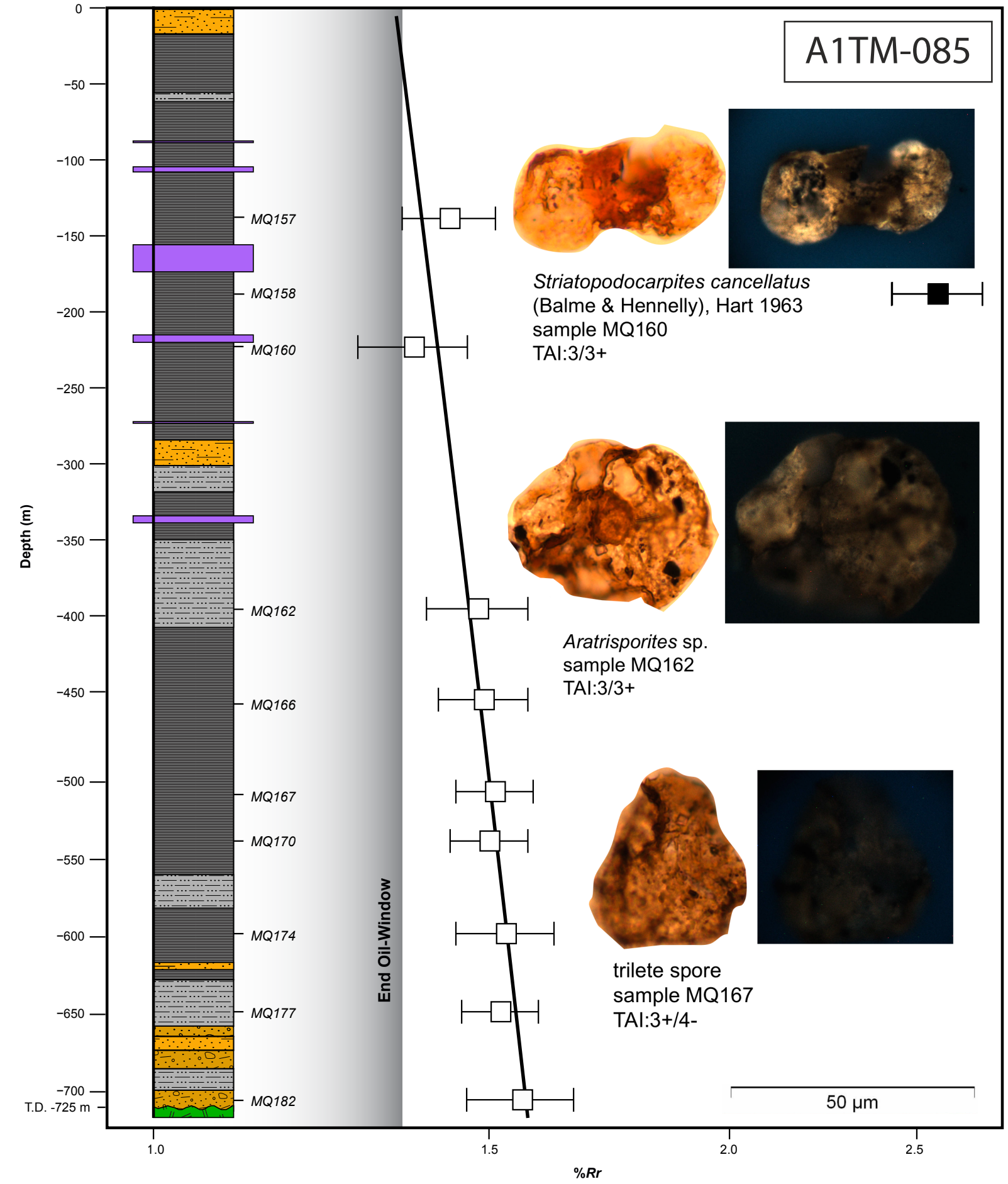
A1TM-085
Depth (m)
0
-50
-100
-150
-200
-250
-300
-350
-400
-450
-500
-550
-600
-650
-700
T.D. -725 m
MQ157
MQ158
MQ160
MQ162
MQ166
MQ167
MQ170
MQ174
MQ177
MQ182
End Oil-Window
1.0
1.5
2.0
2.5
%Rr
Striatopodocarpites cancellatus
(Balme & Hennelly), Hart 1963
sample MQ160
TAI:3/3+
Aratrisporites sp.
sample MQ162
TAI:3/3+
trilete spore
sample MQ167
TAI:3+/4-
50 µm

Figure

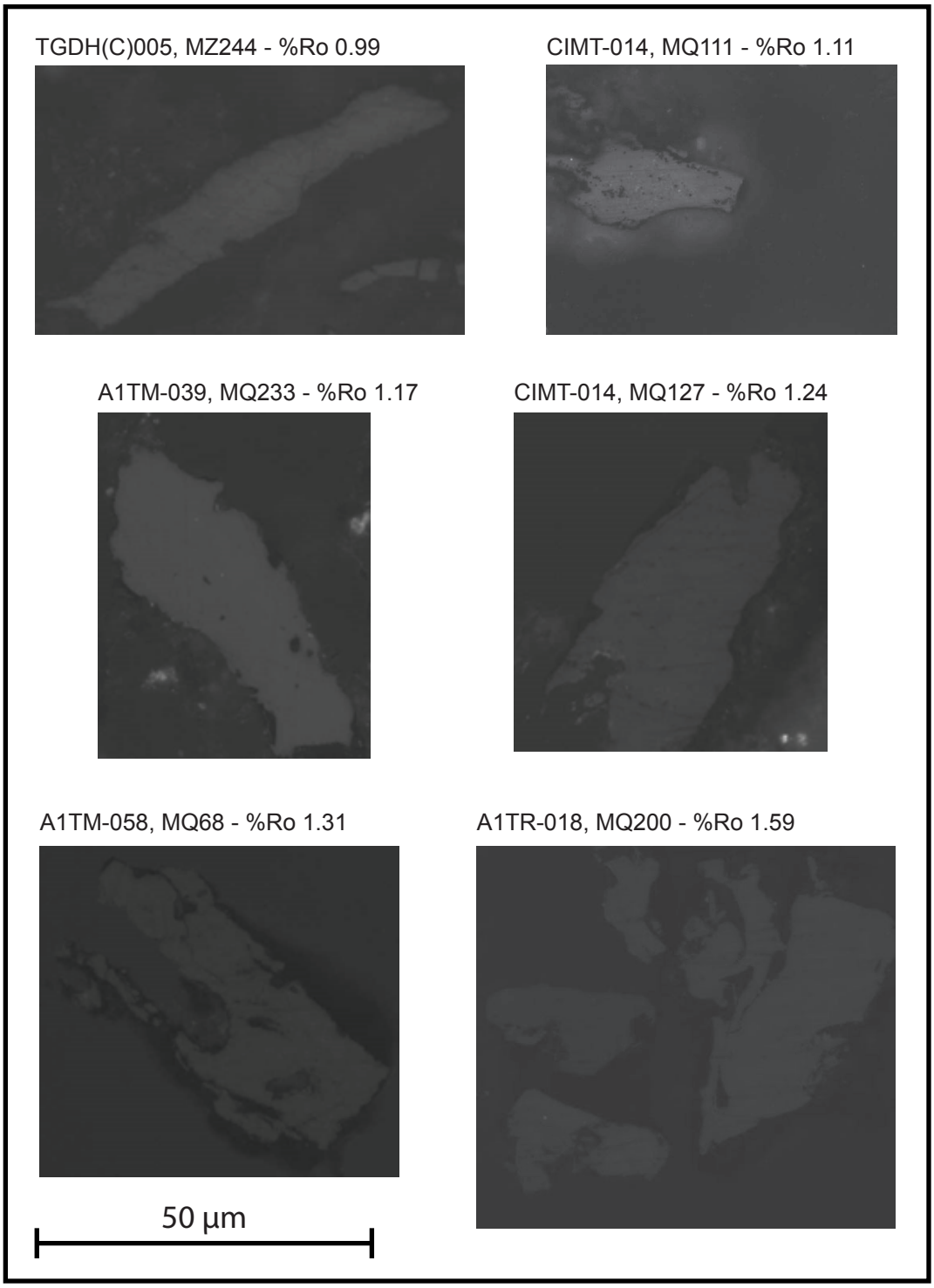
TGDH(C)005, MZ244 - %Ro 0.99
CIMT-014, MQ111 - %Ro 1.11
A1TM-039, MQ233 - %Ro 1.17
CIMT-014, MQ127 - %Ro 1.24
A1TM-058, MQ68 - %Ro 1.31
A1TR-018, MQ200 - %Ro 1.59
50 µm

Figure

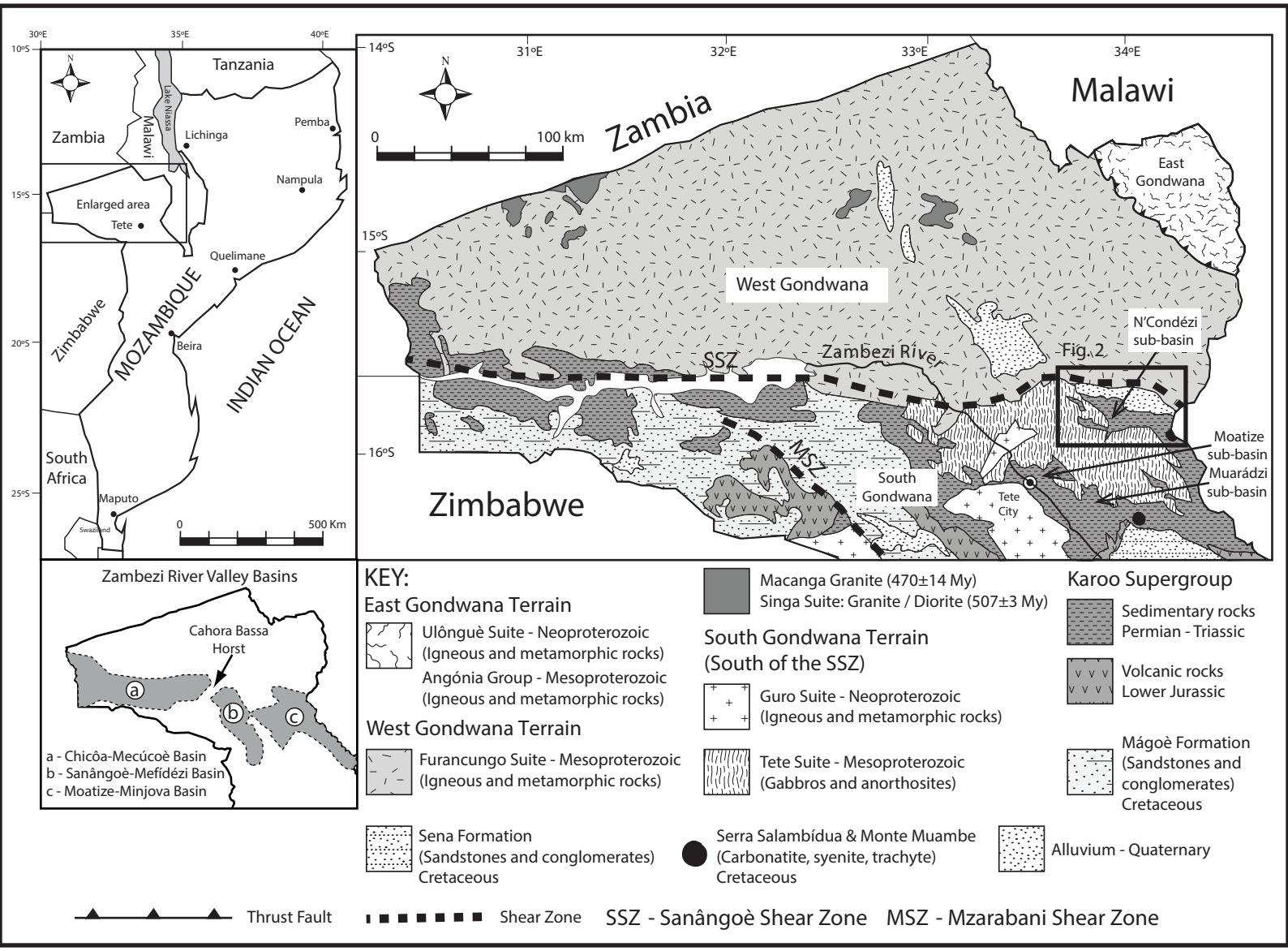
30ºE
35ºE
40ºE
10ºS
15ºS
20ºS
25ºS
N
Tanzania
Zambia
Malawi
Lake Niassa
Lichinga
Pemba
Nampula
Enlarged area
Tete
Quelimane
Zimbabwe
MOZAMBIQUE
INDIAN OCEAN
Beira
South Africa
Maputo
Swaziland
0
500 Km
14ºS
31ºE
32ºE
33ºE
34ºE
0
100 km
Zambia
Malawi
East Gondwana
West Gondwana
N'Condézi sub-basin
Fig. 2
SSZ
Zambezi River
MSZ
Moatize sub-basin
Muarádzi sub-basin
South Gondwana
Tete City
Zimbabwe
Zambezi River Valley Basins
Cahora Bassa Horst
a
b
c
a - Chicôa-Mecúcoè Basin
b - Sanângoè-Mefídézi Basin
c - Moatize-Minjova Basin
KEY:
East Gondwana Terrain
Ulônguè Suite - Neoproterozoic
(Igneous and metamorphic rocks)
Angónia Group - Mesoproterozoic
(Igneous and metamorphic rocks)
West Gondwana Terrain
Furancungo Suite - Mesoproterozoic
(Igneous and metamorphic rocks)
Sena Formation
(Sandstones and conglomerates)
Cretaceous
Macanga Granite (470±14 My)
Singa Suite: Granite / Diorite (507±3 My)
South Gondwana Terrain
(South of the SSZ)
Guro Suite - Neoproterozoic
(Igneous and metamorphic rocks)
Tete Suite - Mesoproterozoic
(Gabbros and anorthosites)
Serra Salambídua & Monte Muambe
(Carbonatite, syenite, trachyte)
Cretaceous
Karoo Supergroup
Sedimentary rocks
Permian - Triassic
Volcanic rocks
Lower Jurassic
Mágoè Formation
(Sandstones and conglomerates)
Cretaceous
Alluvium - Quaternary
Thrust Fault
Shear Zone
SSZ - Sanângoè Shear Zone
MSZ - Mzarabani Shear Zone

Figure

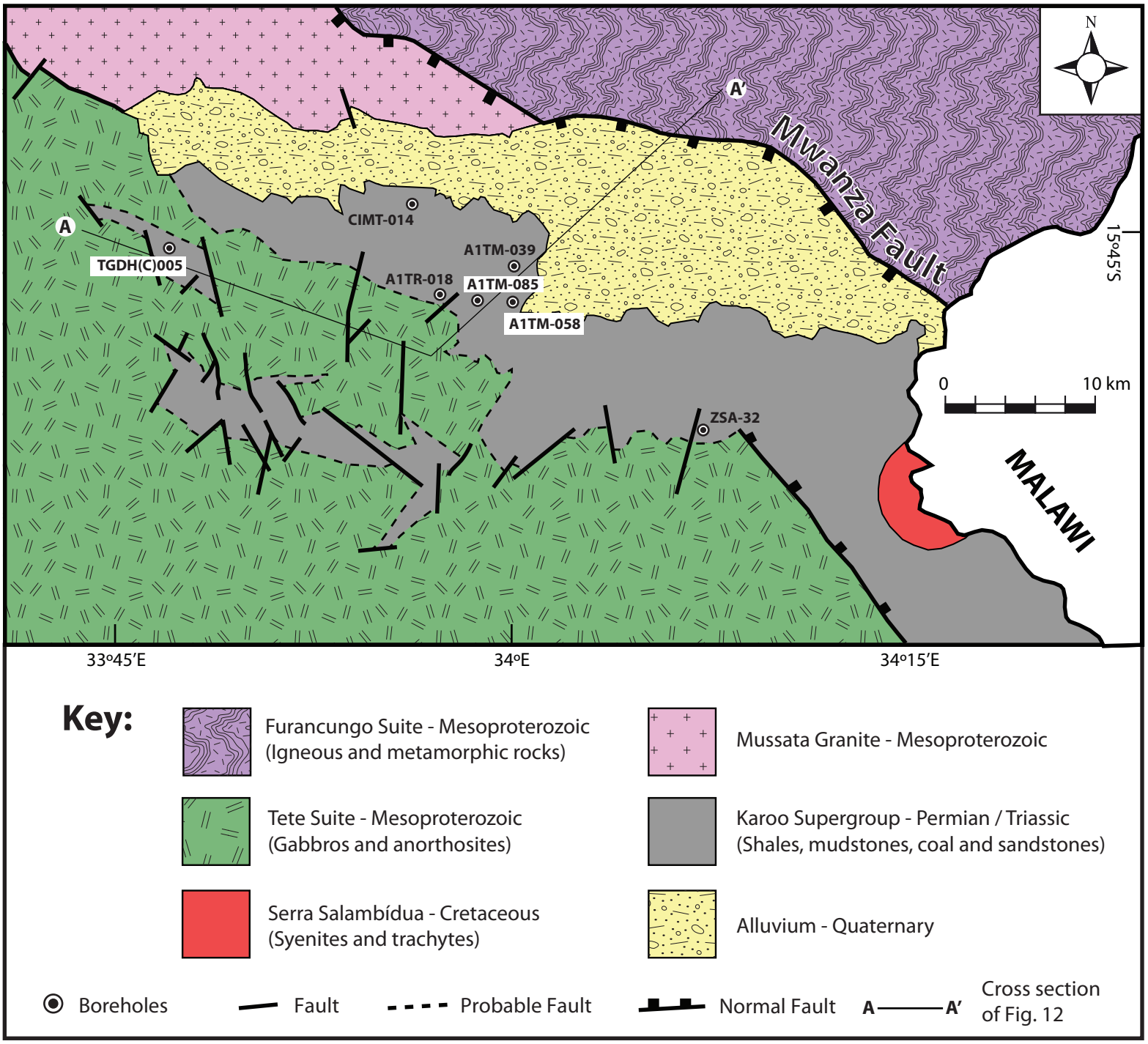
N
A
A'
Mwanza Fault
CIMT-014
TGDH(C)005
A1TM-039
A1TR-018
A1TM-085
A1TM-058
ZSA-32
15°45'S
0
10 km
MALAWI
33°45'E
34°E
34°15'E
Key:
Furancungo Suite - Mesoproterozoic
(Igneous and metamorphic rocks)
Mussata Granite - Mesoproterozoic
Tete Suite - Mesoproterozoic
(Gabbros and anorthosites)
Karoo Supergroup - Permian / Triassic
(Shales, mudstones, coal and sandstones)
Serra Salambídua - Cretaceous
(Syenites and trachytes)
Alluvium - Quaternary
Boreholes
Fault
Probable Fault
Normal Fault
A——A'
Cross section
of Fig. 12

Figure

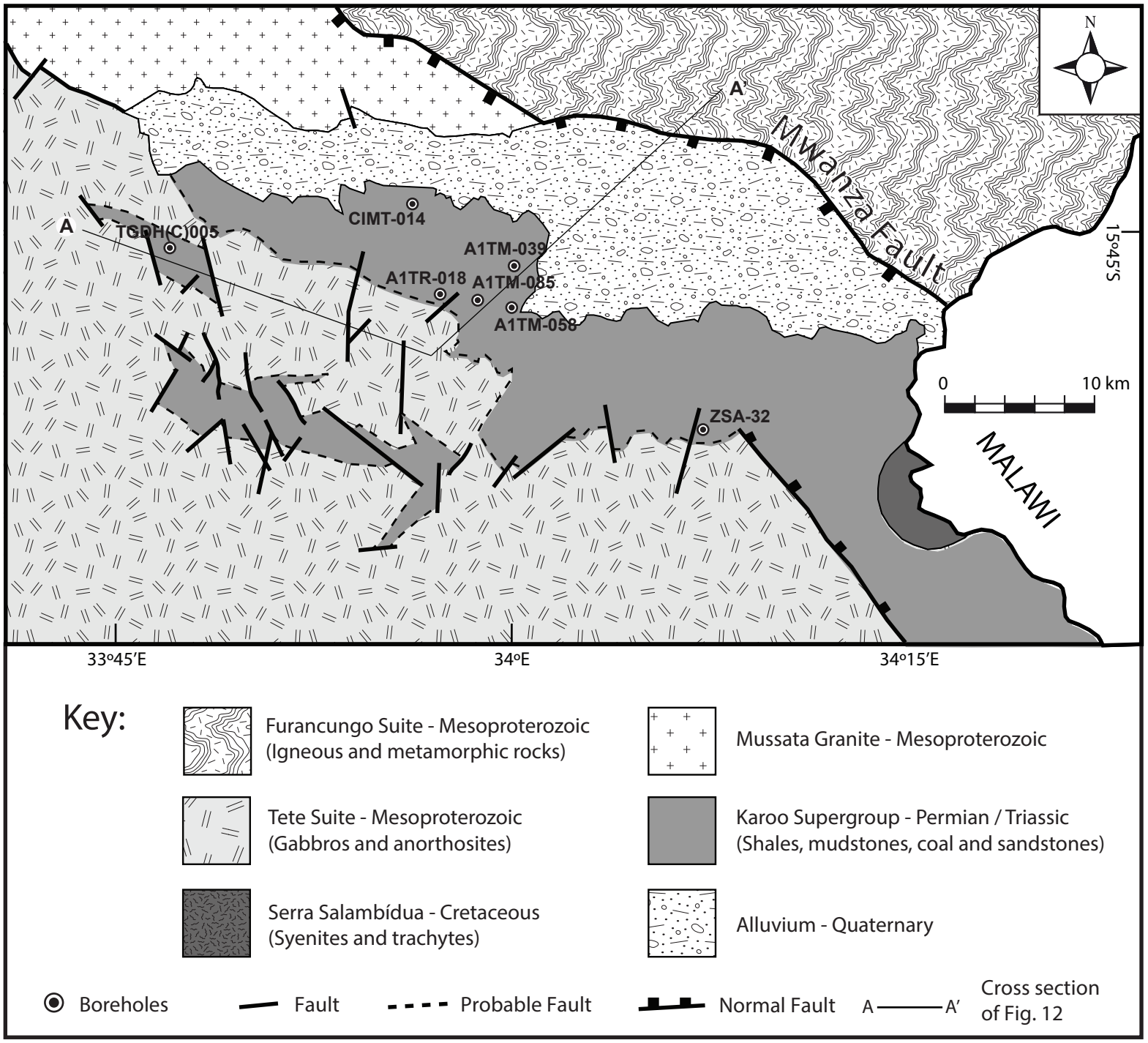
N
A
A'
Mwanza Fault
CIMT-014
TGDH(C)005
A1TM-039
A1TR-018
A1TM-085
A1TM-058
ZSA-32
15°45'S
0
10 km
MALAWI
33°45'E
34°E
34°15'E
Key:
Furancungo Suite - Mesoproterozoic
(Igneous and metamorphic rocks)
Mussata Granite - Mesoproterozoic
Tete Suite - Mesoproterozoic
(Gabbros and anorthosites)
Karoo Supergroup - Permian / Triassic
(Shales, mudstones, coal and sandstones)
Serra Salambídua - Cretaceous
(Syenites and trachytes)
Alluvium - Quaternary
Boreholes
Fault
Probable Fault
Normal Fault
A A'
Cross section
of Fig. 12

Figure

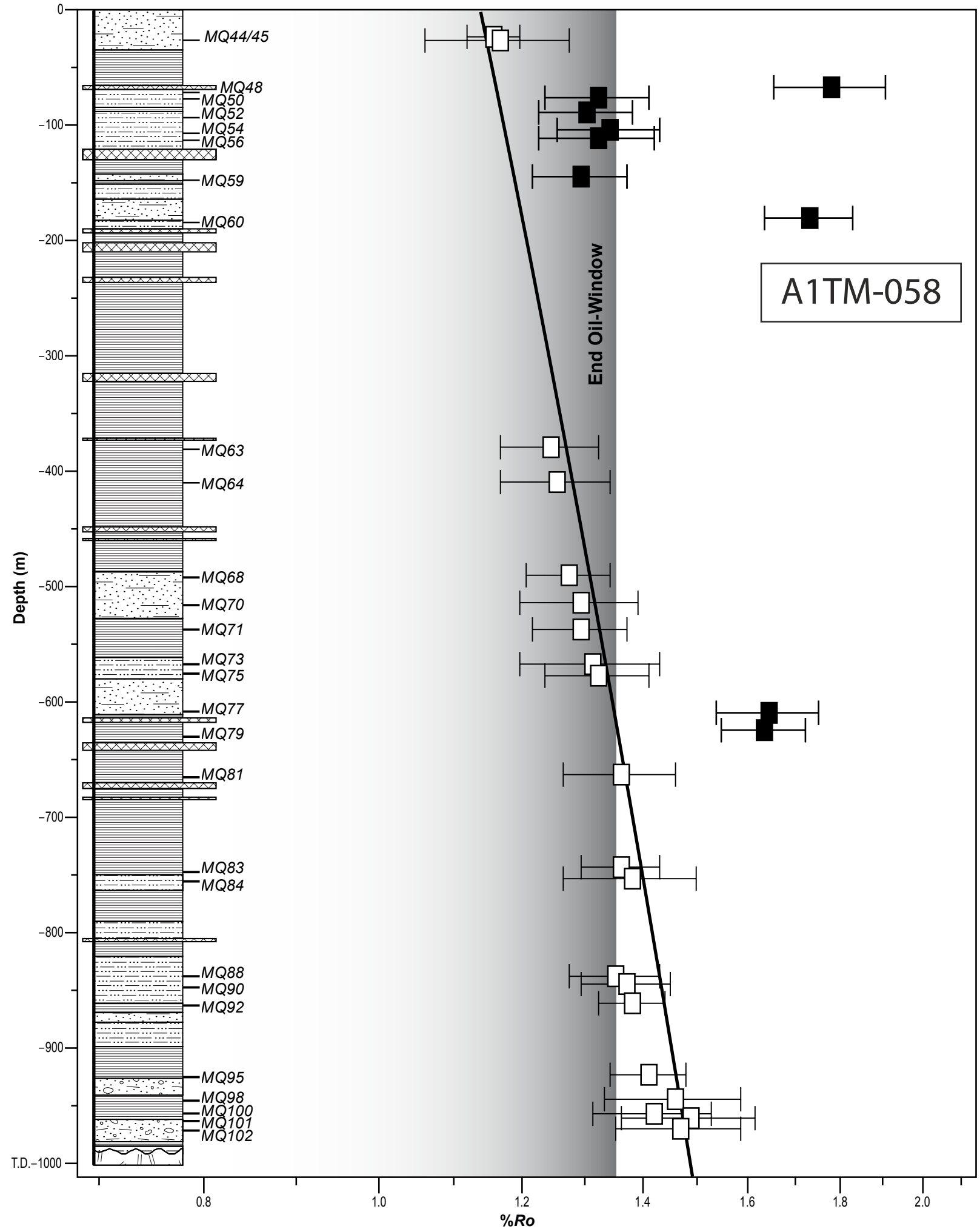
MQ44/45
MQ48
MQ50
MQ52
MQ54
MQ56
MQ59
MQ60
MQ63
MQ64
MQ68
MQ70
MQ71
MQ73
MQ75
MQ77
MQ79
MQ81
MQ83
MQ84
MQ88
MQ90
MQ92
MQ95
MQ98
MQ100
MQ101
MQ102
T.D.
0
−100
−200
−300
−400
−500
−600
−700
−800
−900
−1000
Depth (m)
End Oil-Window
A1TM-058
0.8
1.0
1.2
1.4
1.6
1.8
2.0
%Ro

Figure

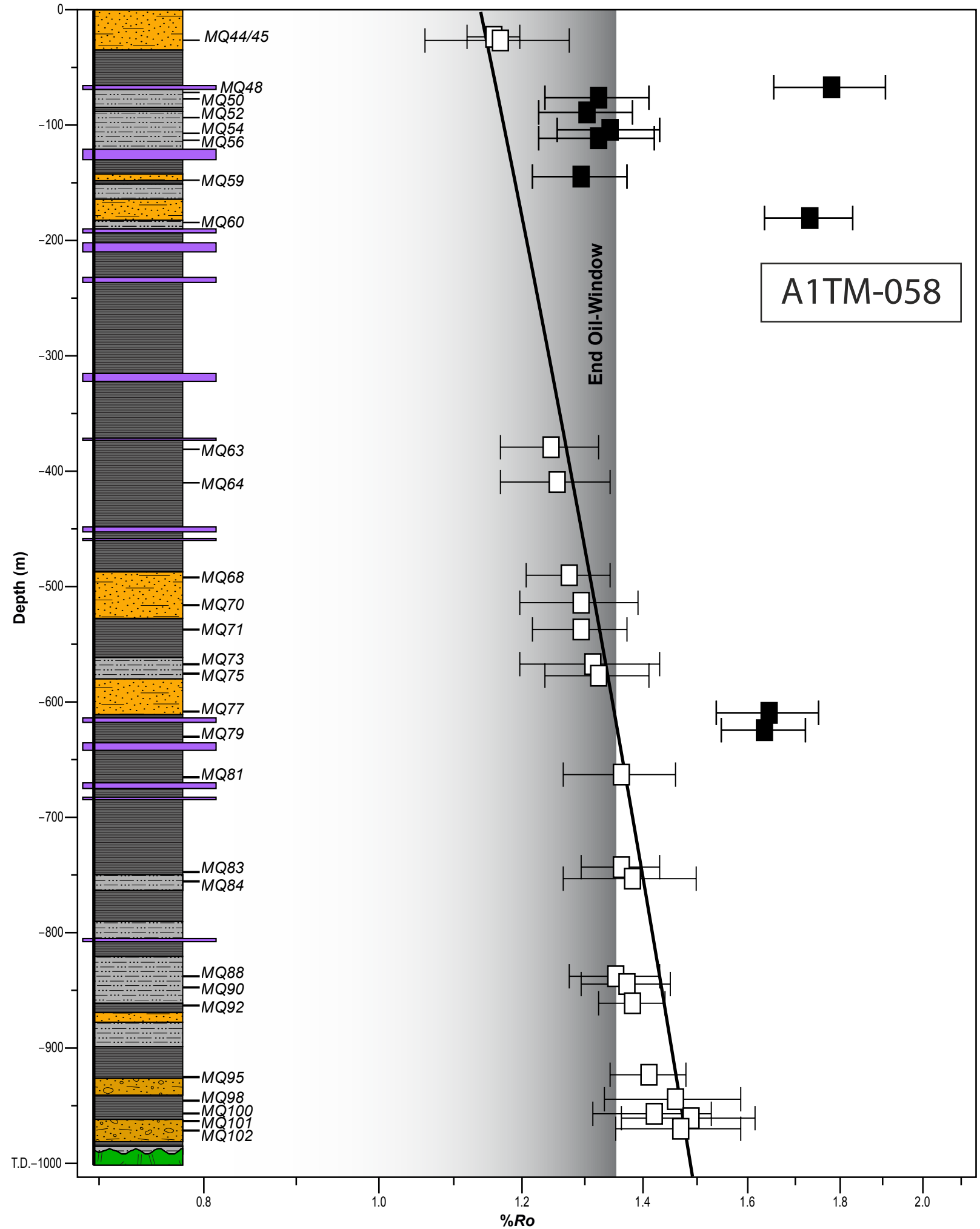
MQ44/45
MQ48
MQ50
MQ52
MQ54
MQ56
MQ59
MQ60
MQ63
MQ64
MQ68
MQ70
MQ71
MQ73
MQ75
MQ77
MQ79
MQ81
MQ83
MQ84
MQ88
MQ90
MQ92
MQ95
MQ98
MQ100
MQ101
MQ102
T.D.
0
−100
−200
−300
−400
−500
−600
−700
−800
−900
−1000
Depth (m)
End Oil-Window
A1TM-058
0.8
1.0
1.2
1.4
1.6
1.8
2.0
%Ro

Figure

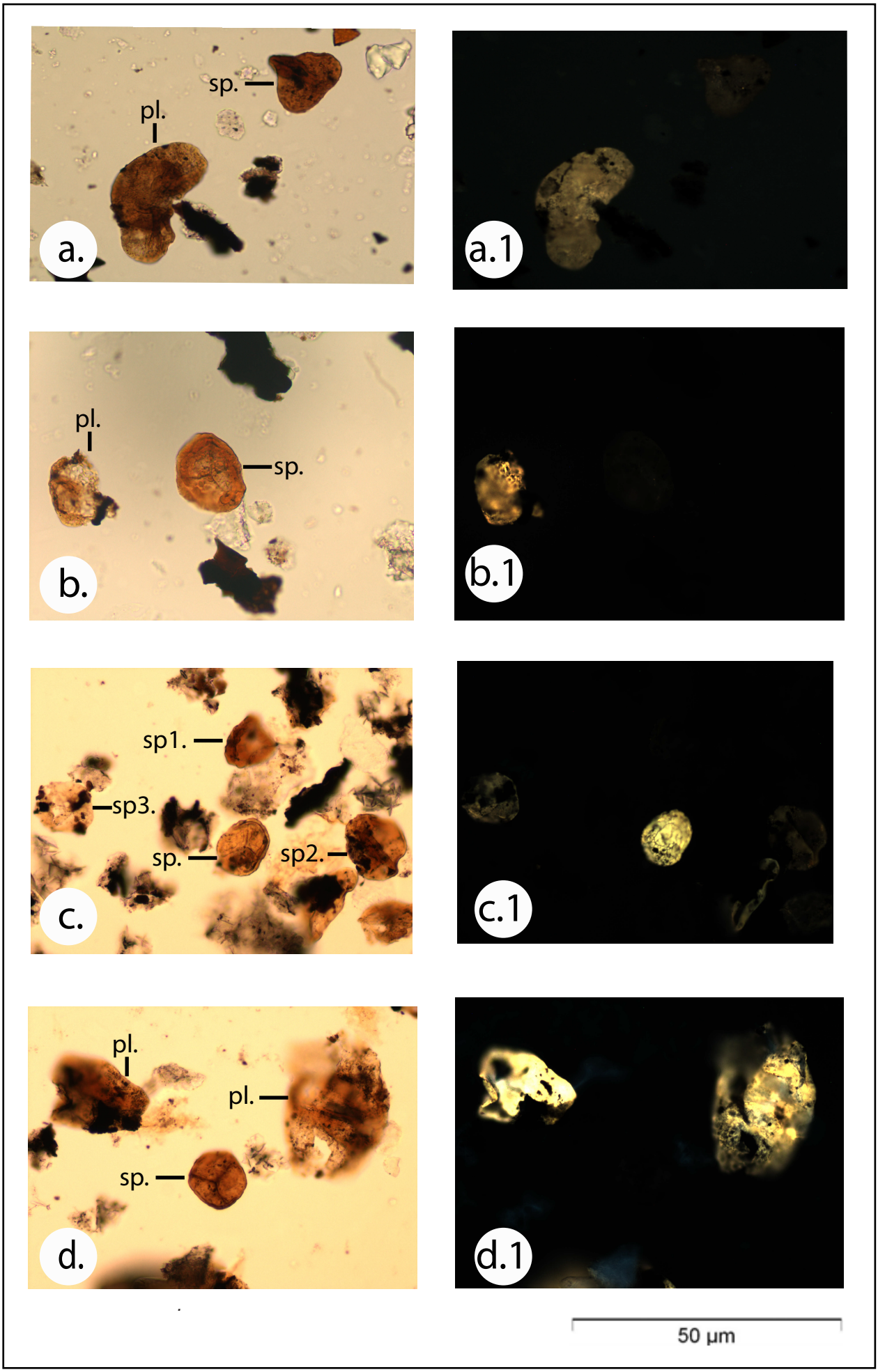

Figure

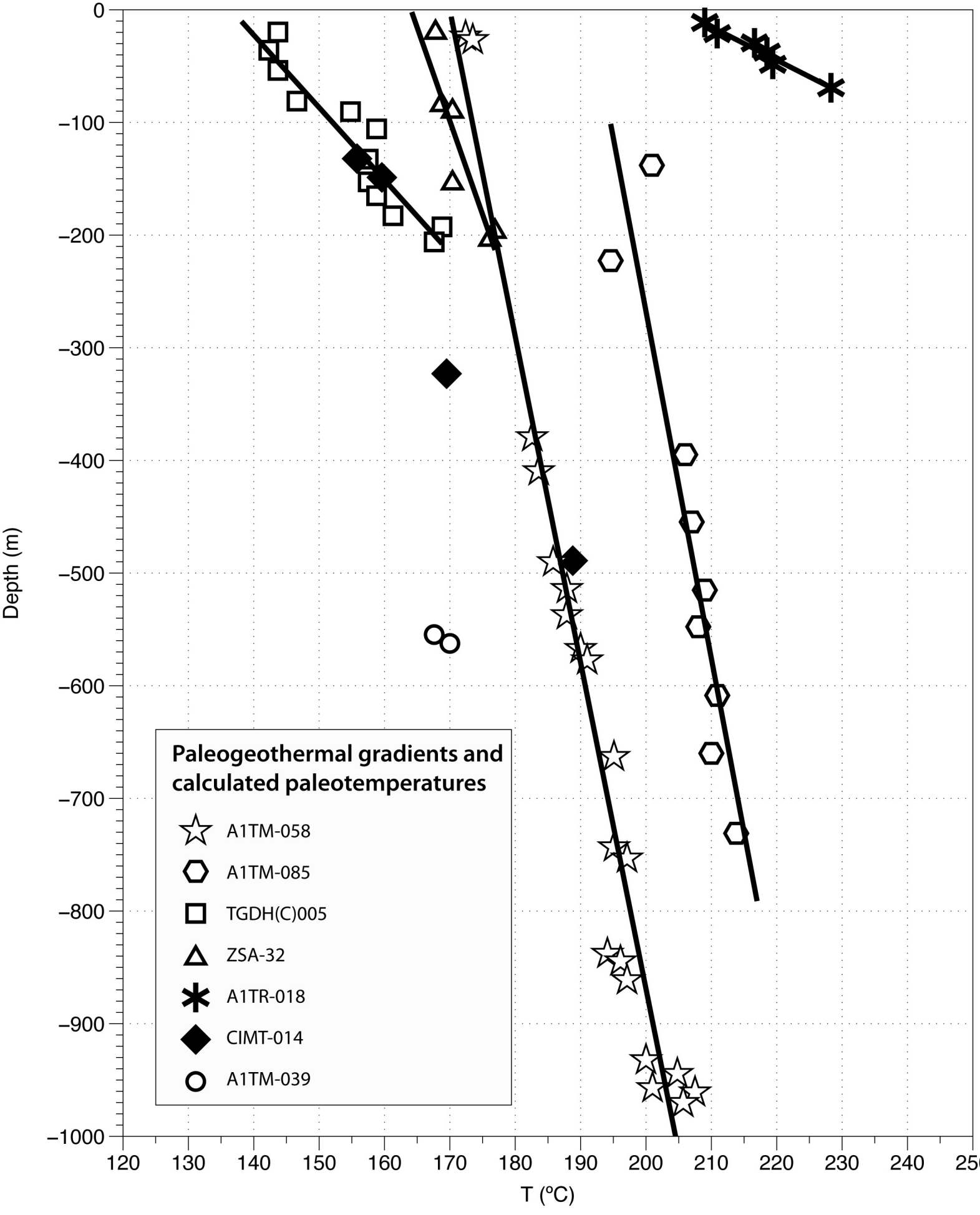
Paleogeothermal gradients and calculated paleotemperatures
A1TM-058
A1TM-085
TGDH(C)005
ZSA-32
A1TR-018
CIMT-014
A1TM-039
Depth (m)
0
−100
−200
−300
−400
−500
−600
−700
−800
−900
−1000
120
130
140
150
160
170
180
190
200
210
220
230
240
250
T (ºC)

Figure

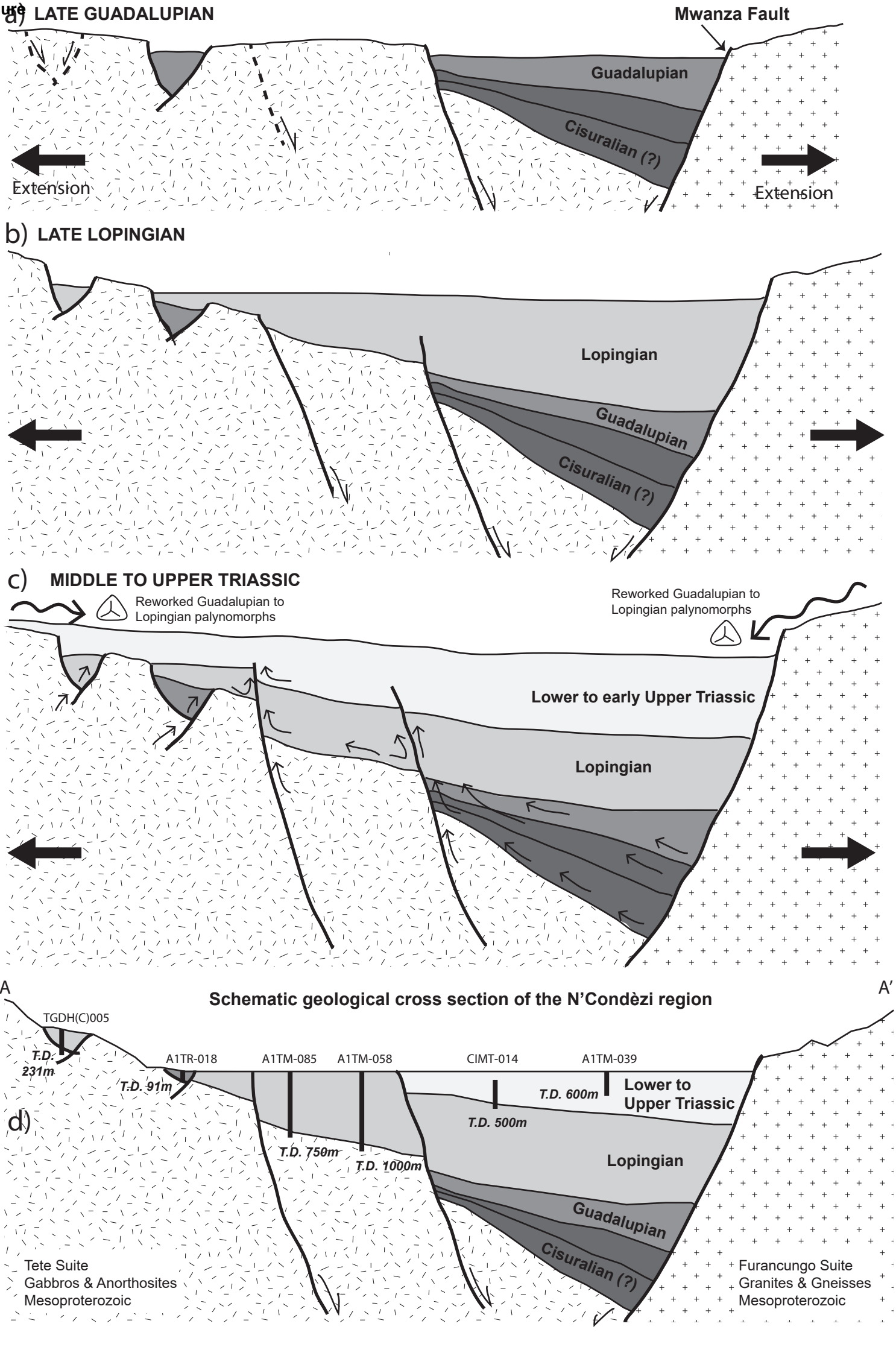
a) LATE GUADALUPIAN
Mwanza Fault
Guadalupian
Cisuralian (?)
Extension
Extension
b) LATE LOPINGIAN
Lopingian
Guadalupian
Cisuralian (?)
c) MIDDLE TO UPPER TRIASSIC
Reworked Guadalupian to Lopingian palynomorphs
Reworked Guadalupian to Lopingian palynomorphs
Lower to early Upper Triassic
Lopingian
A
A′
Schematic geological cross section of the N'Condèzi region
TGDH(C)005
T.D. 231m
A1TR-018
A1TM-085
A1TM-058
CIMT-014
A1TM-039
T.D. 91m
T.D. 600m
Lower to Upper Triassic
T.D. 500m
d)
T.D. 750m
T.D. 1000m
Lopingian
Guadalupian
Cisuralian (?)
Tete Suite
Gabbros & Anorthosites
Mesoproterozoic
Furancungo Suite
Granites & Gneisses
Mesoproterozoic

*Title page

Thermal history and basin evolution of the Moatize - Minjova Coal Basin (N'Condédzi sub-basin, Mozambique) constrained by organic maturation levels

Francesca Galasso[1,2]*¶, Paulo Fernandes[2], Giovanni Montesi[1], João Marques[3], Amalia Spina[1], Zélia Pereira[4]

1. Department of Physics and Geology, University of Perugia.Via Pascoli, 06123 Perugia, Italy

2. Centro de Investigação Marinha e Ambiental (CIMA), Universidade do Algarve, Campus de Gambelas, 8005-139 Faro, Portugal

3. Gondwana Empreendimentos e Consultorias, Limitada, Rua B, no. 233, Bairro da COOP, Caixa Postal 832, Maputo, Mozambique

4. Laboratório Nacional de Energia e Geologia (LNEG), Rua da Amieira, Apartado 1089, 4466-901 S. Mamede Infesta, Portugal